

Elsevier Editorial System(tm) for Science of
the Total Environment
Manuscript Draft

Manuscript Number: STOTEN-D-19-18676R1

Title: Methane and nitrous oxide porewater concentrations and surface fluxes of a regulated river

Article Type: Research Paper

Keywords: hyporheic zone
methane conductance
porewater
methane flux
nitrous oxide flux

Corresponding Author: Dr. Jorge A Villa,

Corresponding Author's Institution: The Ohio State University

First Author: Jorge A Villa

Order of Authors: Jorge A Villa; Garrett J Smith; Yang Ju; Lupita Renteria; Jordan C Angle; Evan Arntzen; Samuel F Harding; Huiying Ren; Xingyuan Chen; Audrey H Sawyer; Emily B Graham; James C Stegen; Kelly C Wrighton; Gil Bohrer

Abstract: Greenhouse gas (GHG) emissions from rivers are a critical missing component of current global GHG models. Their exclusion is mainly due to a lack of in-situ measurements and a poor understanding of the spatiotemporal dynamics of GHG production and emissions, which prevents optimal model parametrization. We combined simultaneous observations of porewater concentrations along different beach positions and depths, and surface fluxes of methane and nitrous oxide at a plot scale in a large regulated river during three water stages: rising, falling, and low. Our goal was to gain insights into the interactions between hydrological exchanges and GHG emissions and elucidate possible hypotheses that could guide future research on the mechanisms of GHG production, consumption, and transport in the hyporheic zone (HZ). Results indicate that the site functioned as a net source of methane. Surface fluxes of methane during river water stages at three beach positions (shallow, intermediate and deep) correlated with porewater concentrations of methane. However, fluxes were significantly higher in the intermediate position during the low water stage, suggesting that low residence time increased methane emissions. Vertical profiles of methane peaked at different depths, indicating an influence of the magnitude and direction of the hyporheic mixing during the different river water stages on methane production and consumption. The site acted as either a sink or a source of nitrous oxide depending on the elevation of the water column. Nitrous oxide porewater concentrations peaked at the upper layers of the sediment throughout the different water stages. River hydrological stages significantly influenced porewater concentrations and fluxes of GHG, probably by influencing heterotrophic respiration (production and consumption processes) and transport to and from the HZ. Our results highlight the importance of including dynamic hydrological exchanges when studying and modeling GHG production and consumption in the HZ of large rivers.

Response to Reviewers: Dear editor,

Thanks for your time and consideration of our paper. We have addressed all comments and suggested revisions from the reviewers. We conducted a thorough grammatical revision of the manuscript that included the reviewer's suggestions.

Below, we list our response to all review comments, with our response in italic font, following each comment.

Reviewers/Editor comments:

Reviewer #1:

Summary

Villa et al. present results of a measurement campaign of porewater concentrations and water-atmosphere fluxes of CH₄ and N₂O from depth transects along the Columbia River during the three river stages of 2018. The results, although presenting only a snapshot, are interesting and merit publication. I recommend that some minor additional discussion and, if possible, references to complementary data be added (as listed under the comments section below) to enhance the background understanding of the site characteristics and put the results into better context.

Response: Thanks for your detailed review of the manuscript. The comments were of great help to improve the quality of the content and the text. We addressed all your comments and suggestions in this revised version. Please see below.

Comments

R1-1 Were the chambers attached or anchored to the peepers or peeper locations in any way? How did you corroborate the location of the peepers when submerged for the chamber placement?

Response: "We used standard 4-inch PCV conduit anchored to the river sediments above the peeper location with rebar to house the peeper tubing, allowing for easy sampling even when water levels were high, and marking the peeper location.". We now explain our approach in L153-155 and L207-211. For your reference please see the figure in attached file.

R1-2 What was the flow rate of the water/river during the chamber flux measurements? Surely, if the water is turbulent, there will be more oxygenation and hence loss of methane in the water column, or can this be assumed to be negligible? I see you discuss the impacts of this later in the results.

Response: Although we did not measure the flow rate directly at the experimental site, we consider the effect of the flow negligible. We intentionally placed our sampling plot in a small cove that isolated the site from the flow of the main channel (white frame in Figure 1A in the manuscript). We are clarifying this point in the manuscript. L119-120.

R1-3 Do you have dissolved oxygen measurements of the water?

Response: Unfortunately, we did not measure dissolved oxygen in the water. However, although we did not measure systematically dissolved oxygen in the sediment-water interface and the water column during our samplings, we conducted a series of surveys before sampling that

indicated that both were consistently supersaturated. We included the clarification in the revised version of the manuscript. L354-359.

R1-4 Looking at the porewater CH₄ concentrations there seems to be a difference in the relative location of the peak of the profile depending on whether the depth level is within the fluctuating water level or permanently inundated, i.e. the peak in the profile is relative to the sediment surface if it is within the fluctuating water level zone, vs. the peak being at the same absolute depth if below the permanent water line (or minimum position of the whole season).

Response: We included this explanation in section 3.3. L426-430.

R1-5 Is there any information on the organic carbon content of the sediments? In Section 3.3. you discuss the effect of organic soils on methane production, but these soils seem to be mostly sand (mentioned in the site introduction).

Response: We did not measure directly organic carbon content in the sediments, but we are supporting our discussion in findings from previous studies conducted in the Handford Reach in nearby sites with similar conditions. We are stressing the location of the referenced studies in the text for a better contextualization L407, L433-434.

R1-6 Comparisons of the porewater analysis with dissolved CH₄ and CO₂ in the river water would be interesting to see what the lateral transport and background values are relative to the sediment porewater. This could help determining the upwelling versus downwelling relationships. It would also be interesting to see what the groundwater CH₄ levels are and how much methane is stored in deep sediment porewater of saturated soils. The same can be said for N₂O. Is there lateral transport (or of nitrate, etc.) during the rising phase? Would this explain the decoupling of porewater CO₂ with N₂O concentrations?

Response: We agree with the reviewer. Unfortunately, we did not measure dissolved CH₄, N₂O or CO₂ in the river water. We include the relevance of these measurements for future studies, including a supporting reference for N₂O transport in groundwater as a possible explanation of the decoupling of N₂O and CO₂ (i.e., Clough et al., 2006). L368-370, L536-537.

R1-7 I would welcome some discussion of the role of water flow rate and residence time in relation to the oxygenation and stratification, which you mention to be important for CH₄ concentrations, but also for the N₂O discussion (Section 3.4).

Response: Lower flow rates are associated with low oxygen concentrations, which may enhance N₂O consumption. We rephrase some sentences in Section 3.4 to explain the connection between low flow and N₂O consumption. L495-498.

Minor comments:

R1-8 Line 12: add comma between "shallow, intermediate ..."

Response: We added the comma. L12.

R1-9 Line 51: either replace previous full stop with a semi colon or add a verb to the sentence, such as "In other words, this is equivalent to ..."

Response: We revised accordingly. L51.

R1-10 Line 58: remove comma before "and"

Response: We removed the comma. L58.

R1-11 Line 60: "...processes that lead to ..."

Response: We revised accordingly. L60.

R1-12 Line 63: "... a 100-year horizon,"

Response: We revised accordingly. L63.

R1-13 Line 68: no comma after "and"

Response: We removed the comma. L68.

R1-14 Line 84: "the main production pathway"

Response: We revised accordingly. L87.

R1-15 Line 96: "to more robustly represent biogeochemical ..." and remove second "aquatic"

Response: We revised accordingly. L99.

R1-16 Line 112: capitalize "Reach"

Response: We revised accordingly here and in other instances of the document. L114, L123, L407, L434, L445, L507.

R1-17 Line 120: rephrase first sentence segment, such as "We sampled on three occasions between 25th April and 25th August in 2018 consisting of (1) ..."

Response: We revised accordingly. L123.

R1-18 Section 2.2: possibly use "level" instead of "elevation" when referring to the height of the river and groundwater.

Response: We re-defined "elevation" as "level" and replace it here (L128), and where appropriate throughout the document, including Figure 1.

R1-19 Figure 1: Is there any meaning of the transect marked in red?

Response: Yes, thank you for noticing our omission. The transect marked in red denotes the transect where sediment temperatures were measured. We included this explanation in L142-143 and the legend of figure 1.

R1-20 Lines 139-140: "in the proximal shore their direction," it's unclear what is meant.

Response: We clarified to "To determine the strength of groundwater flow toward the river, we calculated the hydraulic gradient (HG, m m⁻¹) between the river water and groundwater-well level as..." . L137-138.

R1-21 Line 201: "24-minute periods"

Response: We revised accordingly. L202.

R1-22 Line 271: "fit models for flux calculations, and "

Response: We revised accordingly. L282.

R1-23 Line 292: "after the spring thaw"

Response: We revised accordingly. L303.

R1-24 Line 295: "and remained low during the ..."

Response: We revised accordingly. L306.

R1-25 Line 312: "each sampling stage" and "... of each sampling period."

Response: We meant the sampling conducted during each river stage. We are clarifying now in the Figure 2 legend.

R1-26 Line 316: again "At each sampling stage"

Response: We meant the sampling conducted during each river stage. We are clarifying now in the Figure 2 legend.

R1-27 Line 318: "(which are labeled in (B) for clarification)."

Response: We revised accordingly. Figure 2 legend.

R1-28 Line 345-346: "low concentrations throughout the sediment"

Response: We revised accordingly. L343.

R1-29 Lines 362-366: rephrase or shorten sentence for clarification.

Response: We rephrased the sentence. L363-370.

R1-30 Figure 4 caption: add what the thick brown line represents.

Response: We included what the thick brown represents in the legends of Figure 4 and Figure 8.

R1-31 Line 439: capitalize "Hanford Reach" and again on lines 472, 551

Response: We revised accordingly here and in other instances of the document. L114, L123, L407, L434, L445, L507.

R1-32 Line 492: "when the water level drops"

Response: We revised accordingly. L456.

R1-33 Line 499: "with a shift from"

Response: We revised accordingly. L463.

R1-34 Line 528: "benthic zone water column" and possibly you mean either "system gains size" or "system grain size"?

Response: We rephrase the sentence for more clarity. L483-484.

R1-35 Line 533: remove comma before "and" and again on line 538

Response: We revised accordingly.

R1-36 Line 547: "dynamics" and again on 553

Response: We revised accordingly. L503, L509.

R1-37 Line 550: add "the" to "the nitrification and denitrification functional potential" and again on line 554 "the N-cycling functional potential"

Response: We revised accordingly. L506, L510.

R1-38 Line 557: either "concentrations peak" or "concentration peaks"

Response: It is "concentration peak". We revised accordingly. L513.

R1-39 Line 563: "predominantly released gas"

Response: We revised accordingly. L519.

R1-40 Lines 581-582: rephrase sentence "This would explain the negative ... porewater concentrations, which were also seen in observations of other riverine settings ..."

Response: We revised accordingly. L530-532.

R1-41 Line 585: "water elevation transitions"

Response: We revised as "water level transitions. L536.

R1-42 Line 586: "N-cycling populations vary"

Response: We revised accordingly. L535.

R1-43 Lines 588-592: Replace "different" with explaining what the relationship is and how it changes (positive/negative, becomes stronger/weaker etc.)

Response: We revised accordingly. L540.

R1-44 Line 625: "the influence of river regulation"

Response: This sentence was removed.

R1-45 Line 629: "will therefore be"

Response: We revised accordingly. L589-590.

Reviewer #2:

General Comments:

A very interesting study that has produced a lot of relevant data on the mechanisms that control the greenhouse gas emissions from rivers. This is clearly a research area that needs more focus and this study feels like it could be just the start of larger scale experiments. The authors make several hypotheses on the nature of some mechanisms which will be important in guiding further research to test them. My main criticism would be that some of the figures are very dense with information and could use some improvements with their formatting to improve their clarity. Overall though this study was certainly a worthwhile endeavor that opens up many new lines of questioning and should be accepted with minor revisions.

I think the text overall is a bit dense to read but that is likely just due to the relative complexity of the hyporheic zone dynamics the authors are describing. I would recommend the authors ensure they are organizing some of their more complex sentences in the clearest way possible. I have highlighted some of these instances in my more specific comments below. I have also included below some other specific suggestions on edits to the text and figures. I would also recommend the authors review the text with an eye for grammatical errors as I have found a few, some I have called out below, but I do not intend to correct them all.

Response: Thank you for the positive comments. We have addressed all your comments and suggestions, included a thorough grammatical revision of the document.

More Specific Suggestions/Edits:

R2-1 Page 3 Line 67: "MicClain" should be "McClain", small edit but will cause proofing headaches if left in.

Response: We revised accordingly. L67.

R2-2 Page 5 Line 100-101: "links between fluxes with lateral groundwater fluxes", this statement is unclear, maybe need to add 'GHG' before the first 'fluxes' or change 'groundwater fluxes' to 'groundwater flows' if that makes sense in this context (are we talking about just water flow or also gasses that may be in that water?).

Response: To clarify, we revised to "field studies of GHG fluxes in rivers rarely address small-scale spatial variability across the bank, and temporal variation in relation to the hydrological dynamics between the groundwater and river." L101-103.

R2-3 Page 7 Line 139-140: "To determine the strength of groundwater flows at a given time in the proximal shore their direction,.." It is not clear to me what this sentence is saying, I would consider rewording.

Response: We clarified to "To determine the strength of groundwater flow toward the river, we calculated the hydraulic gradient (HG, m m⁻¹) between the river water and groundwater-well level as..." . L137-138.

R2-4 Page 8 Line 162-165: In this methods paragraph, I would consider briefly explaining why the container is filled with N₂ to avoid oxygen intrusion, and also why the 10-ml containers were pre-acidified.

Response:" The sampling consisted of extracting 10-ml of water from the cells through one of the cell tubings while keeping the other connected to a container filled with N₂ to avoid oxygen intrusion that could

disturb the anaerobic environment within and around the cells. After the extraction, the cell was refilled with deionized water degassed with N2. Samples were placed in 10-ml containers pre-acidified with 0.2 ml HCl 2M to ensure pH levels below 2.0, which prevent the post-sampling biological transformation of the gases dissolved in the sample." Lines 159-166.

R2-5 Page 8 Lines 173-174: This sentence is a bit unclear, I would reword it to say "Helium (25 ml min-1) was used as a carrier gas for methane and CO2 analysis, while ultra-pure N2 (10 ml min-1) was used as a carrier for N2O analysis.

Response: We revised accordingly. L174-176.

R2-6 Page 10 Line 204: check "same quality use control to measure" I think this should read "same quality control used to measure"

Response: We revised accordingly. L205.

R2-7 Page 11 Line 235: again the use of a list and "respectively" in this manner is difficult to parse, I would reword this to be clearer (e.g. 28 for methane and 29 for N2O).

Response: We revised accordingly. L244-246.

R2-8 Page 17 Lines 356-360: very complex sentence, would recommend breaking this up with periods or semicolons at least,

Response: We rewrote the sentence. L359-363.

R2-9 Page 21 Lines 424-425: weird punctuation here, consider revising.

Response: We revised the sentence. L400-402.

R2-10 Page 33 Line 617: what process is using nitrous oxide as a terminal electron acceptor? May be worth mentioning.

Response: We rephrased the sentences expanding on the explanation of the processes and included an additional supporting reference (i.e., Khalil et al., 2004). L560-564.

R2-11 Figure 2: I would add in a legend for the dark blue and light blue lines of graphs B, C, and D. Only having these definitions in the (very long) caption seems less than ideal. The axes labels are color coded to their corresponding line colors, but I am not sure if this is clear enough. I would also recommend repeating the River Elevation axis title on the left side, it might be slightly more cluttered, but would add some clarity. Finally, the last sentence in the caption says 'horizontal gray bars' but should say 'vertical gray bars' an important distinction.

Response: We included the legends for dark and light blue in Figure 2C. We duplicated the left y-label titles as suggested and additionally changed "River elevation" for "River level" in attention to the comment 18 from reviewer 1. We corrected vertical gray bars in the legend as well.

R2-12 Figure 4: I like that the spatial structure of these plots corresponds to real world elevations, but the actual data is largely overlapping and difficult to discern. I am not sure how to best fix this,

but urge the authors try to make the results a bit easier to parse (thinner lines or lines of varying thickness for each color maybe?). There are also the thick colored gradient lines which are only defined in the caption, I would somehow label them in figure if there is room (perhaps up with the legend in the upper left). Finally, in the last sentence of the caption, "Tick" should be "Thick".

Response: We improved the clarity of the figure by reducing the width of the lines and filling the markers of the data for the samplings during the falling and water stages. We included labels for the gradients in the figure and also provided descriptions in the text (L426-430).

R2-13 Figure 8: See the first two sentences of my comments for Figure 4, they also apply to this figure.

Response: We improved the clarity of Figure 8 in the same way as we did for Figure 4.

Reviewer # 3

Thanks for the opportunity to review your very interesting manuscript.

Big Picture comments:

The authors present a unique set of GHG concentration (porewater) and chamber flux measurements at a range of elevations and river stages and comment on potential mechanisms of the patterns observed. The motivation for the work - that dynamic river GHG fluxes are largely missing from models, is valid, although the paper is not able to proscribe specific modeling frameworks that should be implemented - other than pointing out how dynamic and variable river GHG are at various river stages and elevations - which is an important first step.

As discussed, net flux or concentration measurements are the product of consumption and production of CH₄ or N₂O; the methods used here are able only to speculate about the reasons for the small scale spatio-temporal variability (e.g. Line 398, Line 575). The authors are up front with this limitation (repeatedly mention that they don't measure oxidation or reduction directly, or different CH₄ or N₂O-producing pathways).

Despite these limitations, the measurement 'snapshots' (Line 621) are novel and the dataset is worthy of this standalone reporting. While the discussion/conclusions are well written, the paper may benefit from:

Response: Thank you for the positive comment. We addressed all of your comments and incorporated your suggestions. Please see below.

R3-1 Clearer descriptions of how the findings of this paper could lead to improved biogeochemical river submodels (Line 95). It would be useful in the conclusion or late discussion to revisit this intention, and describe what parameters or mechanisms would be most important to model to get GHG fluxes from river sediment right.

Response: We included specific mentions in the conclusion section regarding the processes that could help improve model representation of GHG fluxes in the Hyporheic Zone. L555-557, L566-569.

R3-2 More discussion of how the management of the river impacts the GHG flux. This issue is eluded to in line 635 ('...assess the influence river regulation on GHG production and consumption processes...'). You also mention a 'regulated river' in the title. It would be interesting for the reader to understand how a managed river compares to an unmanaged river... I wonder if the authors could speculate as to how an unregulated river would compare, to draw out the human impact on this system of management?

Response: We rephrased and expanded the second paragraph of the conclusions to include a clearer picture of river regulation in GHG dynamics, including a contrast with non-regulated systems. L570-585.

R3-3 A more general recognition that GHG production and consumption is a result of a constellation of aspects: microbial population, temperature, nutrient content, and redox conditions. The paper seems to mostly emphasize the redox controls, but the production and consumption is driven by all of these aspects - which would need to be dealt with in a modeling framework.

Response: We have included explicit allusions to these aspects in the introduction (L68-70) and in the conclusions (L580-581).

Overall, the paper is well-written and clear, with good figures and a novel dataset. I recommend acceptance with minor revisions.

Response: Thank you for recognizing the novelty character of our dataset.

Detailed comments:

R3-4 Line 60: 'lead' not 'leads'

Response: We revised accordingly. L60.

R3-5 Line 79: 'mediated' not 'meditated'

Response: We revised accordingly. L82.

R3-6 Line 96: 'aquatic' doubled

Response: We removed the additional 'aquatic'. L99.

R3-7 Line 139: please revise 'in the proximal shore their direction' for clarity

Response: We clarified to "To determine the strength of groundwater flow toward the river, we calculated the hydraulic gradient (HG, m m⁻¹) between the river water and groundwater-well level as..." . L137-138.

R3-8 Line 236: please say more about the decision to remove $r^2 < 0.8$. How was this cutoff established? What is the impact of keeping this data?

Response: We expanded the explanation regarding the cutoff on the r^2 of the linear and non-linear regressions (L241-246). The use of the r^2 threshold to determine the goodness of fit in linear and non-linear regressions is a common practice in the measurement of greenhouse gas fluxes using static chambers. There is not a standard procedure or an established criterion to determine the cutoff value (Hüppi et al., 2018). Usually, r^2 values are set by researchers between 0.7 (e.g. Pihlatie et al., 2007) and 0.9 (e.g. Veber et al., 2018) based on expert knowledge. After reviewing our chamber runs, we opted for the 0.8 value as an acceptable compromise between the number of points measured and the uncertainty in the assumptions of the linear (N₂O) and non-linear regressions (CH₄) (Pedersen et al., 2010; Hüppi et al., 2018). We further decided to use the same cutoff for methane and N₂O chambers for consistency. We deemed measurements with r^2 values below the threshold ($r^2 < 0.8$) as measurements of poor quality and excluded them from the analyses to avoid error.

R3-9 Line 246: The first five concentrations - is this deemed to be before the chamber space is influenced by soil and water efflux? Please explain.

Response: This is correct. We re-wrote the sentence explaining what the first five measurements represent. L256-260.

R3-7 Line 256: Is this a theoretically valid assumption? Are there citations that support this?

Response: We rephrased and provided a reference: "We followed the approach by Bastviken et al., (2004) to independently determine the conductance to methane in the water column K_w for each flux chamber, by solving the following equation". L267-268.

References included in document:

Bastviken, D., Cole, J., Pace, M., Tranvik, L., 2004. Methane emissions from lakes: Dependence of lake characteristics, two regional assessments, and a global estimate. *Global Biogeochemical Cycles* 18, GB4009.
<https://doi.org/10.1029/2004GB002238>

Clough, T.J., Bertram, J.E., Sherlock, R.R., Leonard, R.L., Nowicki, B.L., 2006. Comparison of measured and EF5-r-derived N₂O fluxes from a spring-fed river. *Global Change Biology* 12, 477-488.
<https://doi.org/10.1111/j.1365-2486.2005.01092.x>

Khalil, K., Mary, B., Renault, P., 2004. Nitrous oxide production by nitrification and denitrification in soil aggregates as affected by O₂ concentration. *Soil Biology and Biochemistry* 36, 687-699.
<https://doi.org/10.1016/j.soilbio.2004.01.004>

References used in support of reviewers' replies:

Hüppi, R., Felber, R., Krauss, M., Six, J., Leifeld, J., Fuß, R., 2018. Restricting the nonlinearity parameter in soil greenhouse gas flux

calculation for more reliable flux estimates. PLOS ONE 13, e0200876.
<https://doi.org/10.1371/journal.pone.0200876>

Pedersen, A.R., Petersen, S.O., Schelde, K., 2010. A comprehensive approach to soil-atmosphere trace-gas flux estimation with static chambers. European Journal of Soil Science 61, 888-902.

<https://doi.org/10.1111/j.1365-2389.2010.01291.x>

Pihlatie, M., Pumpanen, J., Rinne, J., Ilvesniemi, H., Simojoki, A., Hari, P., Vesala, T., 2007. Gas concentration driven fluxes of nitrous oxide and carbon dioxide in boreal forest soil. Tellus B: Chemical and Physical Meteorology 59, 458-469.

Veber, G., Kull, A., Villa, J.A., Maddison, M., Paal, J., Oja, T., Iturraspe, R., Pärn, J., Teemusk, A., Mander, Ü., 2018. Greenhouse gas emissions in natural and managed peatlands of America: Case studies along a latitudinal gradient. Ecological Engineering 114, 34-45.

<https://doi.org/10.1016/j.ecoleng.2017.06.068>

Jorge A. Villa

Department of Civil, Environmental and Geodetic Engineering
The Ohio State University
416 Bolz Hall
2036 Neil Ave
Columbus, OH 43210

November 21, 2019

Dr. Damià Barceló & Dr. Jay Gan
Co-Editors-in Chief
Science of the Total Environment

We wish to submit the research article entitled "*Methane and nitrous oxide porewater concentration and surface fluxes of a regulated river*" for consideration by Science of the Total Environment.

In this paper, we investigated the interaction between hydrological exchanges and greenhouse gas emissions in a large regulated river. We aimed to understand the spatio-temporal heterogeneity of greenhouse gas emissions of a river beach section and elucidate possible hypotheses that could guide future research of greenhouse gas production, consumption, and transport in the hyporheic zone. Our measurements of greenhouse gases, conducted in the sediment porewater and water/air interface, and hydrological measurements of river and groundwater elevations of a dam-regulated river lay on the intersection of the biosphere, atmosphere, hydrosphere, and anthroposphere.

Our manuscript features results of methane, nitrous oxide, and carbon dioxide porewater concentrations in horizontal and vertical resolutions along an elevation gradient, coupled with co-located methane and nitrous oxide chamber measurements during three river stages characteristic of the hydrological dynamic of the Columbia River. Results indicate that the beach section we evaluated acted as a net sink of methane and as either a sink or source of nitrous oxide depending on the elevation of the water column. The difference in the hydrological mixing during the three different river stages drove different methane and nitrous oxide porewater concentrations, their distribution in the vertical profile, and their correlation with the carbon dioxide porewater concentrations. Altogether, results indicate the relative importance of river downwelling and groundwater upwelling in the conditions leading to methane and nitrous oxide production and consumption and provide evidence supporting previous studies in the same river reach highlighting changes in microbial processes driven by hydrological mixing.

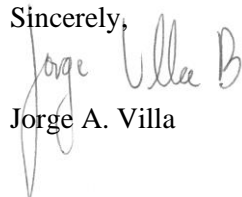
In this first submission, we have placed the figures accompanying the text to facilitate the work of the reviewers. For the revised version, we will place the figures at the end of the manuscript.

We confirm that this manuscript has not been published elsewhere and is not under consideration by another journal. All authors have approved the manuscript and agreed with its submission Science of the Total Environment, and we have no conflicts of interest to declare.

Please address all correspondence concerning this manuscript to me at villa-betancur.1@osu.edu.

Thank you for your consideration of this manuscript.

Sincerely,



Jorge A. Villa

1
2
3
4 **Methane and nitrous oxide porewater concentrations and surface fluxes of a regulated**
5
6 **river**
7
8
9
10

11 Jorge A. Villa^{1,2*}, Garrett J. Smith³, Yang Ju¹, Lupita Renteria⁴, Jordan C. Angle³, Evan
12 Arntzen⁴, Samuel F. Harding⁴, Huiying Ren⁴, Xingyuan Chen⁴, Audrey H. Sawyer⁵, Emily B.
13
14 Graham⁴, James C. Stegen⁴, Kelly C. Wrighton⁶, and Gil Bohrer¹.
15
16

17
18
19
20
21 ¹ Department of Civil, Environmental and Geodetic Engineering, Ohio State University, 470
22
23 Hitchcock Hall, 2070 Neil Avenue, Columbus, OH 43210, USA
24
25

26 ² Now at: School of Geosciences, University of Louisiana at Lafayette, 323 Hamilton Hall, 611
27
28 McKinley Street, Lafayette, LA 70504.
29
30

31 ³ Department of Microbiology, Ohio State University, 105 Biological Sciences Building
32
33 484 W. 12 Ave., Columbus, OH 43210, USA
34
35

36 ⁴ Pacific Northwest National Laboratory, 902 Battelle Blvd, Richland, WA 99354, USA
37
38

39 ⁵ School of Earth Sciences, Ohio State University, 125 Oval Dr S, Columbus, OH 43210, USA
40
41 ⁶ Department of Soil and Crop Sciences, Colorado State University, 307 University Ave, Fort
42
43 Collins, CO 80521, USA
44
45

46 * Corresponding author: jorge.villa@louisiana.edu
47
48
49
50
51
52
53
54
55
56
57
58
59
60
61
62
63
64
65

Dear editor,

Thanks for your time and consideration of our paper. We have addressed all comments and suggested revisions from the reviewers. We conducted a thorough grammatical revision of the manuscript that included the reviewer's suggestions.

Below, we list our response to all review comments, with our response in italic font, following each comment.

Reviewers/Editor comments:

Reviewer #1:

Summary

Villa et al. present results of a measurement campaign of porewater concentrations and water-atmosphere fluxes of CH₄ and N₂O from depth transects along the Columbia River during the three river stages of 2018. The results, although presenting only a snapshot, are interesting and merit publication. I recommend that some minor additional discussion and, if possible, references to complementary data be added (as listed under the comments section below) to enhance the background understanding of the site characteristics and put the results into better context.

Response: Thanks for your detailed review of the manuscript. The comments were of great help to improve the quality of the content and the text. We addressed all your comments and suggestions in this revised version. Please see below.

Comments

R1-1 Were the chambers attached or anchored to the peepers or peeper locations in any way? How did you corroborate the location of the peepers when submerged for the chamber placement?

Response: "We used standard 4-inch PCV conduit anchored to the river sediments above the peeper location with rebar to house the peeper tubing, allowing for easy sampling even when water levels were high, and marking the peeper location.". We now explain our approach in L153-155 and L207-211. For your reference please see the figure below.



Figure 1. Chamber positioning approach. (A) installed peeper (below ground) with white PVC conduit extending above the peeper location held up by 3 rebar rods (inside the conduit, not visible in picture). The PVC conduit houses the sampling tubing (in the picture, the tubing is extended to full length beyond the top end of the PVC tube and held by Dr. Villa's hand). (B) positioning and securing of the methane sampling chamber above the peeper location as marked by the PVC conduit. (C) positioning and anchoring of the N₂O sampling chambers, surrounding the PVC conduit around the peeper location.

R1-2 What was the flow rate of the water/river during the chamber flux measurements? Surely, if the water is turbulent, there will be more oxygenation and hence loss of methane in the water column, or can this be assumed to be negligible? I see you discuss the impacts of this later in the results.

Response: Although we did not measure the flow rate directly at the experimental site, we consider the effect of the flow negligible. We intentionally placed our sampling plot in a small cove that isolated the site from the flow of the main channel (white frame in Figure 1A in the manuscript). We are clarifying this point in the manuscript. L119-120.

R1-3 Do you have dissolved oxygen measurements of the water?

Response: Unfortunately, we did not measure dissolved oxygen in the water. However, although we did not measure systematically dissolved oxygen in the sediment-water interface and the water column during our samplings, we conducted a series of surveys before sampling that indicated that both were consistently supersaturated. We included the clarification in the revised version of the manuscript. L354-359.

R1-4 Looking at the porewater CH₄ concentrations there seems to be a difference in the relative location of the peak of the profile depending on whether the depth level is within the fluctuating water level or permanently inundated, i.e. the peak in the profile is relative to the sediment surface if it is within the fluctuating water level zone, vs. the peak being at the same absolute depth if below the permanent water line (or minimum position of the whole season).

Response: We included this explanation in section 3.3. L426-430.

R1-5 Is there any information on the organic carbon content of the sediments? In Section 3.3. you discuss the effect of organic soils on methane production, but these soils seem to be mostly

sand (mentioned in the site introduction).

Response: We did not measure directly organic carbon content in the sediments, but we are supporting our discussion in findings from previous studies conducted in the Hanford Reach in nearby sites with similar conditions. We are stressing the location of the referenced studies in the text for a better contextualization L407, L433-434.

R1-6 Comparisons of the porewater analysis with dissolved CH₄ and CO₂ in the river water would be interesting to see what the lateral transport and background values are relative to the sediment porewater. This could help determining the upwelling versus downwelling relationships. It would also be interesting to see what the groundwater CH₄ levels are and how much methane is stored in deep sediment porewater of saturated soils. The same can be said for N₂O. Is there lateral transport (or of nitrate, etc.) during the rising phase? Would this explain the decoupling of porewater CO₂ with N₂O concentrations?

Response: We agree with the reviewer. Unfortunately, we did not measure dissolved CH₄, N₂O or CO₂ in the river water. We include the relevance of these measurements for future studies, including a supporting reference for N₂O transport in groundwater as a possible explanation of the decoupling of N₂O and CO₂ (i.e, Clough et al., 2006). L368-370, L536-537.

R1-7 I would welcome some discussion of the role of water flow rate and residence time in relation to the oxygenation and stratification, which you mention to be important for CH₄ concentrations, but also for the N₂O discussion (Section 3.4).

Response: Lower flow rates are associated with low oxygen concentrations, which may enhance N₂O consumption. We rephrase some sentences in Section 3.4 to explain the connection between low flow and N₂O consumption. L495-498.

Minor comments:

R1-8 Line 12: add comma between "shallow, intermediate ..."

Response: We added the comma. L12.

R1-9 Line 51: either replace previous full stop with a semi colon or add a verb to the sentence, such as "In other words, this is equivalent to ..."

Response: We revised accordingly. L51.

R1-10 Line 58: remove comma before "and"

Response: We removed the comma. L58.

R1-11 Line 60: "...processes that lead to ..."

Response: We revised accordingly. L60.

R1-12 Line 63: "... a 100-year horizon,"

Response: We revised accordingly. L63.

R1-13 Line 68: no comma after "and"

Response: We removed the comma. L68.

R1-14 Line 84: "the main production pathway"

Response: We revised accordingly. L87.

R1-15 Line 96: "to more robustly represent biogeochemical ..." and remove second "aquatic"

Response: We revised accordingly. L99.

R1-16 Line 112: capitalize "Reach"

Response: We revised accordingly here and in other instances of the document. L114, L123, L407, L434, L445, L507.

R1-17 Line 120: rephrase first sentence segment, such as "We sampled on three occasions between 25th April and 25th August in 2018 consisting of (1) ..."

Response: We revised accordingly. L123.

R1-18 Section 2.2: possibly use "level" instead of "elevation" when referring to the height of the river and groundwater.

Response: We re-defined "elevation" as "level" and replace it here (L128), and where appropriate throughout the document, including Figure 1.

R1-19 Figure 1: Is there any meaning of the transect marked in red?

Response: Yes, thank you for noticing our omission. The transect marked in red denotes the transect where sediment temperatures were measured. We included this explanation in L142-143 and the legend of figure 1.

R1-20 Lines 139-140: "in the proximal shore their direction," it's unclear what is meant.

Response: We clarified to "To determine the strength of groundwater flow toward the river, we calculated the hydraulic gradient (HG, $m m^{-1}$) between the river water and groundwater-well level as..." . L137-138.

R1-21 Line 201: "24-minute periods"

Response: We revised accordingly. L202.

R1-22 Line 271: "fit models for flux calculations, and "

Response: We revised accordingly. L282.

R1-23 Line 292: "after the spring thaw"

Response: We revised accordingly. L303.

R1-24 Line 295: "and remained low during the ..."

Response: We revised accordingly. L306.

R1-25 Line 312: "each sampling stage" and "... of each sampling period."

Response: We meant the sampling conducted during each river stage. We are clarifying now in the Figure 2 legend.

R1-26 Line 316: again "At each sampling stage"

Response: We meant the sampling conducted during each river stage. We are clarifying now in the Figure 2 legend.

R1-27 Line 318: "(which are labeled in (B) for clarification)."

Response: We revised accordingly. Figure 2 legend.

R1-28 Line 345-346: "low concentrations throughout the sediment"

Response: We revised accordingly. L343.

R1-29 Lines 362-366: rephrase or shorten sentence for clarification.

Response: We rephrased the sentence. L363-370.

R1-30 Figure 4 caption: add what the thick brown line represents.

Response: We included what the thick brown represents in the legends of Figure 4 and Figure 8.

R1-31 Line 439: capitalize "Hanford Reach" and again on lines 472, 551

Response: We revised accordingly here and in other instances of the document. L114, L123, L407, L434, L445, L507.

R1-32 Line 492: "when the water level drops"

Response: We revised accordingly. L456.

R1-33 Line 499: "with a shift from"

Response: We revised accordingly. L463.

R1-34 Line 528: "benthic zone water column" and possibly you mean either "system gains size" or "system grain size"?

Response: We rephrase the sentence for more clarity. L483-484.

R1-35 Line 533: remove comma before "and" and again on line 538

Response: We revised accordingly.

R1-36 Line 547: "dynamics" and again on 553

Response: We revised accordingly. L503, L509.

R1-37 Line 550: add "the" to "the nitrification and denitrification functional potential" and again on line 554 "the N-cycling functional potential"

Response: We revised accordingly. L506, L510.

R1-38 Line 557: either "concentrations peak" or "concentration peaks"

Response: It is "concentration peak". We revised accordingly. L513.

R1-39 Line 563: "predominantly released gas"

Response: We revised accordingly. L519.

R1-40 Lines 581-582: rephrase sentence "This would explain the negative ... porewater concentrations, which were also seen in observations of other riverine settings ..."

Response: We revised accordingly. L530-532.

R1-41 Line 585: "water elevation transitions"

Response: We revised as "water level transitions. L536.

R1-42 Line 586: "N-cycling populations vary"

Response: We revised accordingly. L535.

R1-43 Lines 588-592: Replace "different" with explaining what the relationship is and how it changes (positive/negative, becomes stronger/weaker etc.)

Response: We revised accordingly. L540.

R1-44 Line 625: "the influence of river regulation"

Response: This sentence was removed.

R1-45 Line 629: "will therefore be"

Response: We revised accordingly. L589-590.

Reviewer #2:

General Comments:

A very interesting study that has produced a lot of relevant data on the mechanisms that control the greenhouse gas emissions from rivers. This is clearly a research area that needs more focus and this study feels like it could be just the start of larger scale experiments. The authors make several hypotheses on the nature of some mechanisms which will be important in guiding further research to test them. My main criticism would be that some of the figures are very dense with information and could use some improvements with their formatting to improve their clarity. Overall though this study was certainly a worthwhile endeavor that opens up many new lines of questioning and should be accepted with minor revisions.

I think the text overall is a bit dense to read but that is likely just due to the relative complexity of the hyporheic zone dynamics the authors are describing. I would recommend the authors ensure they are organizing some of their more complex sentences in the clearest way possible. I have highlighted some of these instances in my more specific comments below. I have also included below some other specific suggestions on edits to the text and figures. I would also recommend the authors review the text with an eye for grammatical errors as I have found a few, some I have called out below, but I do not intend to correct them all.

Response: Thank you for the positive comments. We have addressed all your comments and suggestions, included a thorough grammatical revision of the document.

More Specific Suggestions/Edits:

R2-1 Page 3 Line 67: "MicClain" should be "McClain", small edit but will cause proofing headaches if left in.

Response: We revised accordingly. L67.

R2-2 Page 5 Line 100-101: "links between fluxes with lateral groundwater fluxes", this statement is unclear, maybe need to add 'GHG' before the first 'fluxes' or change 'groundwater

fluxes' to 'groundwater flows' if that makes sense in this context (are we talking about just water flow or also gasses that may be in that water?).

Response: To clarify, we revised to "field studies of GHG fluxes in rivers rarely address small-scale spatial variability across the bank, and temporal variation in relation to the hydrological dynamics between the groundwater and river." L101-103.

R2-3 Page 7 Line 139-140: "To determine the strength of groundwater flows at a given time in the proximal shore their direction,.." It is not clear to me what this sentence is saying, I would consider rewording.

Response: We clarified to "To determine the strength of groundwater flow toward the river, we calculated the hydraulic gradient (HG, $m m^{-1}$) between the river water and groundwater-well level as... ". L137-138.

R2-4 Page 8 Line 162-165: In this methods paragraph, I would consider briefly explaining why the container is filled with N2 to avoid oxygen intrusion, and also why the 10-ml containers were pre-acidified.

Response: "The sampling consisted of extracting 10-ml of water from the cells through one of the cell tubings while keeping the other connected to a container filled with N2 to avoid oxygen intrusion that could disturb the anaerobic environment within and around the cells. After the extraction, the cell was refilled with deionized water degassed with N2. Samples were placed in 10-ml containers pre-acidified with 0.2 ml HCl 2M to ensure pH levels below 2.0, which prevent the post-sampling biological transformation of the gases dissolved in the sample. " Lines 159-166.

R2-5 Page 8 Lines 173-174: This sentence is a bit unclear, I would reword it to say "Helium (25 ml min-1) was used as a carrier gas for methane and CO₂ analysis, while ultra-pure N2 (10 ml min-1) was used as a carrier for N₂O analysis.

Response: We revised accordingly. L174-176.

R2-6 Page 10 Line 204: check "same quality use control to measure" I think this should read "same quality control used to measure"

Response: We revised accordingly. L205.

R2-7 Page 11 Line 235: again the use of a list and "respectively" in this manner is difficult to parse, I would reword this to be clearer (e.g. 28 for methane and 29 for N₂O).

Response: We revised accordingly. L244-246.

R2-8 Page 17 Lines 356-360: very complex sentence, would recommend breaking this up with periods or semicolons at least,

Response: We rewrote the sentence. L359-363.

R2-9 Page 21 Lines 424-425: weird punctuation here, consider revising.

Response: We revised the sentence. L400-402.

R2-10 Page 33 Line 617: what process is using nitrous oxide as a terminal electron acceptor? May be worth mentioning.

Response: We rephrased the sentences expanding on the explanation of the processes and included an additional supporting reference (i.e., Khalil et al., 2004). L560-564.

R2-11 Figure 2: I would add in a legend for the dark blue and light blue lines of graphs B, C, and D. Only having these definitions in the (very long) caption seems less than ideal. The axes labels are color coded to their corresponding line colors, but I am not sure if this is clear enough. I would also recommend repeating the River Elevation axis title on the left side, it might be slightly more cluttered, but would add some clarity. Finally, the last sentence in the caption says 'horizontal gray bars' but should say 'vertical gray bars' an important distinction.

Response: We included the legends for dark and light blue in Figure 2C. We duplicated the left y-label titles as suggested and additionally changed "River elevation" for "River level" in attention to the comment 18 from reviewer 1. We corrected vertical gray bars in the legend as well.

R2-12 Figure 4: I like that the spatial structure of these plots corresponds to real world elevations, but the actual data is largely overlapping and difficult to discern. I am not sure how to best fix this, but urge the authors try to make the results a bit easier to parse (thinner lines or lines of varying thickness for each color maybe?). There are also the thick colored gradient lines which are only defined in the caption, I would somehow label them in figure if there is room (perhaps up with the legend in the upper left). Finally, in the last sentence of the caption, "Tick" should be "Thick".

Response: We improved the clarity of the figure by reducing the width of the lines and filling the markers of the data for the samplings during the falling and water stages. We included labels for the gradients in the figure and also provided descriptions in the text (L426-430).

R2-13 Figure 8: See the first two sentences of my comments for Figure 4, they also apply to this figure.

Response: We improved the clarity of Figure 8 in the same way as we did for Figure 4.

Reviewer # 3

Thanks for the opportunity to review your very interesting manuscript.

Big Picture comments:

The authors present a unique set of GHG concentration (porewater) and chamber flux

measurements at a range of elevations and river stages and comment on potential mechanisms of the patterns observed. The motivation for the work – that dynamic river GHG fluxes are largely missing from models, is valid, although the paper is not able to proscribe specific modeling frameworks that should be implemented – other than pointing out how dynamic and variable river GHG are at various river stages and elevations – which is an important first step.

As discussed, net flux or concentration measurements are the product of consumption and production of CH₄ or N₂O; the methods used here are able only to speculate about the reasons for the small scale spatio-temporal variability (e.g. Line 398, Line 575). The authors are up front with this limitation (repeatedly mention that they don't measure oxidation or reduction directly, or different CH₄ or N₂O-producing pathways).

Despite these limitations, the measurement 'snapshots' (Line 621) are novel and the dataset is worthy of this standalone reporting. While the discussion/conclusions are well written, the paper may benefit from:

Response: Thank you for the positive comment. We addressed all of your comments and incorporated your suggestions. Please see below.

R3-1 Clearer descriptions of how the findings of this paper could lead to improved biogeochemical river submodels (Line 95). It would be useful in the conclusion or late discussion to revisit this intention, and describe what parameters or mechanisms would be most important to model to get GHG fluxes from river sediment right.

Response: We included specific mentions in the conclusion section regarding the processes that could help improve model representation of GHG fluxes in the Hyporheic Zone. L555-557, L566-569.

R3-2 More discussion of how the management of the river impacts the GHG flux. This issue is eluded to in line 635 ('...assess the influence river regulation on GHG production and consumption processes...'). You also mention a 'regulated river' in the title. It would be interesting for the reader to understand how a managed river compares to an unmanaged river... I wonder if the authors could speculate as to how an unregulated river would compare, to draw out the human impact on this system of management?

Response: We rephrased and expanded the second paragraph of the conclusions to include a clearer picture of river regulation in GHG dynamics, including a contrast with non-regulated systems. L570-585.

R3-3 A more general recognition that GHG production and consumption is a result of a constellation of aspects: microbial population, temperature, nutrient content, and redox conditions. The paper seems to mostly emphasize the redox controls, but the production and consumption is driven by all of these aspects – which would need to be dealt with in a modeling framework.

Response: We have included explicit allusions to these aspects in the introduction (L68-70) and in the conclusions (L580-581).

Overall, the paper is well-written and clear, with good figures and a novel dataset. I recommend acceptance with minor revisions.

Response: Thank you for recognizing the novelty character of our dataset.

Detailed comments:

R3-4 Line 60: 'lead' not 'leads'

Response: We revised accordingly. L60.

R3-5 Line 79: 'mediated' not 'meditated'

Response: We revised accordingly. L82.

R3-6 Line 96: 'aquatic' doubled

Response: We removed the additional 'aquatic'. L99.

R3-7 Line 139: please revise 'in the proximal shore their direction' for clarity

Response: We clarified to "To determine the strength of groundwater flow toward the river, we calculated the hydraulic gradient (HG, $m m^{-1}$) between the river water and groundwater-well level as... ". L137-138.

R3-8 Line 236: please say more about the decision to remove $r^2 < 0.8$. How was this cutoff established? What is the impact of keeping this data?

Response: We expanded the explanation regarding the cutoff on the r^2 of the linear and non-linear regressions (L241-246). The use of the r^2 threshold to determine the goodness of fit in linear and non-linear regressions is a common practice in the measurement of greenhouse gas fluxes using static chambers. There is not a standard procedure or an established criterion to determine the cutoff value (Hüppi et al., 2018). Usually, r^2 values are set by researchers between 0.7 (e.g. Pihlatie et al., 2007) and 0.9 (e.g. Veber et al., 2018) based on expert knowledge. After reviewing our chamber runs, we opted for the 0.8 value as an acceptable compromise between the number of points measured and the uncertainty in the assumptions of the linear (N_2O) and non-linear regressions (CH_4) (Pedersen et al., 2010; Hüppi et al., 2018). We further decided to use the same cutoff for methane and N_2O chambers for consistency. We deemed measurements with r^2 values below the threshold ($r^2 < 0.8$) as measurements of poor quality and excluded them from the analyses to avoid error.

R3-9 Line 246: The first five concentrations – is this deemed to be before the chamber space is influenced by soil and water efflux? Please explain.

Response: This is correct. We re-wrote the sentence explaining what the first five measurements represent. L256-260.

R3-7 Line 256: Is this a theoretically valid assumption? Are there citations that support this?

Response: We rephrased and provided a reference: "We followed the approach by Bastviken et al., (2004) to independently determine the conductance to methane in the water column K_w for each flux chamber, by solving the following equation". L267-268.

References included in document:

Bastviken, D., Cole, J., Pace, M., Tranvik, L., 2004. Methane emissions from lakes: Dependence of lake characteristics, two regional assessments, and a global estimate. *Global Biogeochemical Cycles* 18, GB4009. <https://doi.org/10.1029/2004GB002238>

Clough, T.J., Bertram, J.E., Sherlock, R.R., Leonard, R.L., Nowicki, B.L., 2006. Comparison of measured and EF5-r-derived N_2O fluxes from a spring-fed river. *Global Change Biology* 12, 477–488. <https://doi.org/10.1111/j.1365-2486.2005.01092.x>

Khalil, K., Mary, B., Renault, P., 2004. Nitrous oxide production by nitrification and denitrification in soil aggregates as affected by O_2 concentration. *Soil Biology and Biochemistry* 36, 687–699. <https://doi.org/10.1016/j.soilbio.2004.01.004>

References used in support of reviewers' replies:

Hüppi, R., Felber, R., Krauss, M., Six, J., Leifeld, J., Fuß, R., 2018. Restricting the nonlinearity parameter in soil greenhouse gas flux calculation for more reliable flux estimates. *PLOS ONE* 13, e0200876. <https://doi.org/10.1371/journal.pone.0200876>

Pedersen, A.R., Petersen, S.O., Schelde, K., 2010. A comprehensive approach to soil-atmosphere trace-gas flux estimation with static chambers. *European Journal of Soil Science* 61, 888–902. <https://doi.org/10.1111/j.1365-2389.2010.01291.x>

Pihlatie, M., Pumpanen, J., Rinne, J., Ilvesniemi, H., Simojoki, A., Hari, P., Vesala, T., 2007. Gas concentration driven fluxes of nitrous oxide and carbon dioxide in boreal forest soil. *Tellus B: Chemical and Physical Meteorology* 59, 458–469.

Veber, G., Kull, A., Villa, J.A., Maddison, M., Paal, J., Oja, T., Iturraspe, R., Pärn, J., Teemusk, A., Mander, Ü., 2018. Greenhouse gas emissions in natural and managed peatlands of America: Case studies along a latitudinal gradient. *Ecological Engineering* 114, 34–45. <https://doi.org/10.1016/j.ecoleng.2017.06.068>

1 **Abstract**

2 Greenhouse gas (GHG) emissions from rivers are a critical missing component of current global
3 GHG models. Their exclusion is mainly due to a lack of in-situ measurements and a poor
4 understanding of the spatiotemporal dynamics of GHG production and emissions, which
5 prevents optimal model parametrization. We combined simultaneous observations of porewater
6 concentrations along different beach positions and depths, and surface fluxes of methane and
7 nitrous oxide at a plot scale in a large regulated river during three water stages: rising, falling,
8 and low. Our goal was to gain insights into the interactions between hydrological exchanges and
9 GHG emissions and elucidate possible hypotheses that could guide future research on the
10 mechanisms of GHG production, consumption, and transport in the hyporheic zone (HZ).
11 Results indicate that the site functioned as a net source of methane. Surface fluxes of methane
12 during river water stages at three beach positions (shallow, intermediate and deep) correlated
13 with porewater concentrations of methane. However, fluxes were significantly higher in the
14 intermediate position during the low water stage, suggesting that low residence time increased
15 methane emissions. Vertical profiles of methane peaked at different depths, indicating an
16 influence of the magnitude and direction of the hyporheic mixing during the different river water
17 stages on methane production and consumption. The site acted as either a sink or a source of
18 nitrous oxide depending on the elevation of the water column. Nitrous oxide porewater
19 concentrations peaked at the upper layers of the sediment throughout the different water stages.
20 River hydrological stages significantly influenced porewater concentrations and fluxes of GHG,
21 probably by influencing heterotrophic respiration (production and consumption processes) and
22 transport to and from the HZ. Our results highlight the importance of including dynamic

23 hydrological exchanges when studying and modeling GHG production and consumption in the
24 HZ of large rivers.

25 **Keywords:** hyporheic zone, methane conductance, porewater, methane flux, nitrous oxide flux

26

27

28

29

30

31

32

33

34

35

36

37

38

39

40

41

42

43

44

45

46 **1. Introduction**

47 Rivers and streams cover a relatively small area of the planet's terrestrial phase (0.47%).
48 Nonetheless, they play a pivotal role in greenhouse gas (GHG) emissions (Raymond et al.,
49 2013). It is estimated that they emit annually 6.6 Pg of carbon dioxide (CO₂) (Raymond et al.,
50 2013), 26.8 Tg of methane (CH₄) (Stanley et al., 2016) and 1.1 Tg of nitrous oxide (N₂O)
51 (Beaulieu et al., 2011). In other words, this is the equivalent to ~12% of CO₂ emissions from
52 fossil fuels and industry (Jackson et al., 2017), and ~5% and ~10% of global methane and N₂O
53 emissions, respectively (Beaulieu et al., 2011; Saunois et al., 2016). The disproportionate
54 contributions from rivers to GHG budgets have challenged the early assumption of rivers as
55 "passive" or "neutral" pipes in global and regional GHG budgets (Cole et al., 2007;
56 Aufdenkampe et al., 2011), placing them as active hotspots for GHG exchange.

57 Whereas the biogeochemical processes that lead to CO₂ emissions from rivers have
58 traditionally received more attention (Raymond et al., 2013; Hotchkiss et al., 2015) and are
59 relatively better represented in current models (e.g., E3SM, Golaz et al., 2019), the processes that
60 lead to methane and N₂O emissions remain poorly constrained in space and time (Bridgman et
61 al., 2013; Quick et al., 2019). Methane and N₂O emissions are low compared with those of CO₂,
62 yet on an equal mass basis, they have 45 and 270 times the potential of CO₂ to warm the
63 atmosphere over a 100-year horizon, respectively (Neubauer and Megonigal, 2015). Most of the
64 biogeochemical activity that leads to methane and N₂O production and consequent emission in
65 rivers occurs within the hyporheic zone (HZ), a transition zone in the saturated sediments
66 adjacent to the streamflow where surface water and subsurface waters are permanently mixing
67 (McClain et al., 2003; Krause et al., 2011). The mixing of downwelling oxidized surface water,
68 and upwelling of reduced subsurface water provides a unique environment of enhanced nutrient

69 and light availability, gradients of temperature and redox potentials, pH, organic matter content,
70 and microbial numbers and activity (Woessner, 2017). This environment represent
71 biogeochemical hotspots for microbial activity where aerobic and anaerobic microbial
72 metabolisms co-occur (Boulton et al., 1998). In general, the HZ is a net source of methane and
73 N₂O (Reeder et al., 2018).

74 Hydrologic exchange strongly affects the flow of organic dissolved carbon, an essential
75 microbial substrate for GHG production processes, as well as the transport of GHG themselves.
76 Methane can be produced in the anaerobic environment within the HZ from CO₂ and H₂ or
77 acetate during the degradation of organic matter (Lyu et al., 2018). Methane may also be
78 transported from the surrounding upland areas dissolved in groundwater (Jones and Mulholland,
79 1998). Once in the HZ, methane can be oxidized and transformed back into CO₂ with sufficient
80 electron acceptors, particularly oxygen, by methanotrophic microorganisms (Chistoserdova et
81 al., 2009). The remaining portion of methane that is not oxidized can be emitted via diffusion,
82 ebullition, or plant-mediated transport (Bridgman et al., 2013).

83 N₂O production in the HZ is mainly the result of four distinct processes: (1) denitrification or
84 reduction of nitrate or nitrite to dinitrogen with nitrous oxide as an intermediate, (2) by-products
85 of oxidation of ammonia to nitrate or nitrite, (3) dissimilatory reduction of nitrate to ammonia,
86 and (4) chemo-denitrification involving the abiotic reaction of nitrite with iron(II) (Quick et al.
87 2019), of which denitrification is thought as the main production pathway in lotic systems
88 (Baulch et al., 2011a; Beaulieu et al., 2011). N₂O transport from the HZ to the atmosphere occurs
89 primarily via diffusion (Baulch et al., 2011a).

90 A better understanding of the dynamics and interactions of different processes throughout the
91 HZ is needed in order to resolve the role of rivers in global GHG emissions correctly. There is a

92 need for an improved mechanistic understanding of the biogeochemical processes involved in the
93 production, consumption, and transformation of carbon and nitrogen species leading to riverine
94 GHG emissions. However, river systems are spatially complex and temporally dynamic, making
95 predictions of GHG emissions, especially challenging. The lack of observations for evaluating
96 specific parameters that describe each process often leads to simplistic representation in models,
97 and consequently, high sensitivity and uncertainty in the model results. The inclusion of sub-
98 models that can resolve transient hydrological exchanges in land-surface models is paramount to
99 more robustly represent biogeochemical processes in the terrestrial-aquatic interphases
100 (Buchkowski et al., 2017; Graham et al., 2019). With very few exceptions (e.g., Rulík et al.,
101 2000; Bednářík et al., 2015; Comer-Warner et al., 2018), field studies of GHG fluxes in rivers
102 rarely address small-scale spatial variability across the bank, and temporal variation in relation to
103 the hydrological dynamics between the groundwater and river. In addition, very few have
104 considered simultaneously methane and N₂O and how they may be linked at the site scale.

105 Here we present results from methane and N₂O porewater concentrations and chamber flux
106 measurements conducted at different river stages at a plot of the Columbia River, a large
107 regulated river. Our goal was to assess the spatio-temporal variability in porewater
108 concentrations and surface fluxes. We further utilize the results to identify the relationships
109 between HZ hydrological processes and the sources or sinks of methane and N₂O.

110

111 **2. Methods**

112 **2.1 Study site and sampling approach**

113 This study was conducted in the experimental ‘Genome to Greenhouse Gas (3G) observatory’
114 at the Columbia River on the Hanford Reach (Hanford 300 Area), Washington State, USA

115 (Figure 1). The observatory consists of an array of 3 triplicate porewater samplers (peepers)
116 deployed at a sandy beach on bank-to-river transects (6 m long) along a microtopographic
117 gradient representing three nominal beach positions: shallow, intermediate and deep (Figure 1B).
118 The sampling array encompasses a small, 11 m-long plot. The plot is located in a small cove that
119 isolates the site from the flow influences of the main river channel. Concurrent measurements of
120 methane, CO₂ and N₂O porewater concentrations and surface fluxes of methane and N₂O were
121 conducted during three distinct river stages representing the main phases of a typical
122 hydrological year at the study site, ~80 km downstream of the Priest Rapids Dam at the Hanford
123 Reach. We sampled on three occasions between 25th April and 25th August in 2018 consisting of
124 (1) a rising water stage during spring snowmelt, (2) a falling water stage during summer after the
125 annual peak in early June, and (3) a highly regulated low water stage starting late in the summer
126 that typically extends to the onset of the next spring snowmelt.

127

128 **2.2 River levels and hydraulic gradient**

129 River water and groundwater levels were recorded using pressure transducers. We conducted
130 river water measurements at the 3G observatory during August 2018 (5 min resolution) and river
131 water and groundwater measurements in a transect perpendicular to the river, 410 m downstream
132 of the 3G observatory during 2018 (15 min resolution) (Figure 1A). We generated a time series
133 for the 3G observatory during 2018 using water levels from the point of measurement
134 downstream ($r^2 = 0.99, p < 0,001$, 27 days in August), and a known discrete level at the 3G site.
135 We used as a zero-reference location for the water level the sediment surface of the shallow
136 position (Figure 1C).

137 To determine the strength of groundwater flow toward the river, we calculated the hydraulic
138 gradient (HG , m m^{-1}) between the river water and groundwater-well level as:

139
$$HG = \Delta h L^{-1} \quad (1)$$

140 Where Δh is the head difference between the river water level (m) and the groundwater level of
141 the well (m) at a given time, and L is the distance between their two points of measurement (114
142 m). Sediment temperatures (at 10 cm sediment depth) were measured at each position along one
143 transect during the study period using thermistors (marked in red in Figure 1A).

144

145 **2.3 Porewater sampling and processing**

146 Vertical profiles of methane, N_2O , and CO_2 concentration of sediment porewater were
147 determined at each gradient's position using the peepers described by MacDonald et al. (2013).
148 The peepers allowed for non-destructive consecutive sampling of the sediment profile at the
149 same depth and beach positions. The peepers feature 20 stacked cells (61.4 ml) at a 2.8 cm
150 vertical resolution. Each cell has 22.5 cm^2 windows covered with a $0.22\text{-}\mu\text{m}$ pore size
151 polyethersulfon membrane that allows water inside the cell to equilibrate with dissolved gas
152 concentrations in the sediments. Cells were fitted with two sampling ports consisting of plastic
153 tubing that allowed water extraction and refill. We used standard 4-inch PCV conduit anchored
154 to the river sediments above the peeper location with rebar to house the peeper tubing, allowing
155 for easy sampling even when water levels were high, and marking the peeper location. Peepers
156 were deployed two months before our first sampling to ensure equilibration, which usually could
157 take between 4 days and up to three weeks (MacDonald et al. 2013).

158 We sampled ten cells, starting at the top cell (at zero sediment depth) and every other after that,
159 until reaching the bottom-most cell at 50-cm sediment depth. The sampling consisted of

160 extracting 10-ml of water from the cells through one of the cell tubings while keeping the other
161 connected to a container filled with N₂ to avoid oxygen intrusion **that could disturb the anaerobic**
162 **environment within and around the cells.** After the extraction, the cell was refilled with deionized
163 water degassed with N₂. Samples were placed in 10-ml containers pre-acidified with 0.2 ml HCl
164 **2M to ensure pH levels below 2.0, which prevent the post-sampling biological transformation of**
165 **the gases dissolved in the sample. Then, samples were refrigerated and transported to the**
166 laboratory for further processing.

167

168 **2.4 Porewater concentrations**

169 Gas concentrations in porewater were determined using the gas chromatograph headspace
170 equilibration technique described by (Kampbell et al., 1989). We used a 5-ml subsample of each
171 vial to equilibrate with a 15-ml N₂ headspace. Upon equilibration, we injected 10 ml of
172 headspace into 10-ml pre-evacuated vials and analyzed them in a gas chromatograph equipped
173 with a flame ionization detector fitted with a 1.8 Poropack Q column **and an electron capture Ni-**
174 **63 detector** (Shimadzu GC-2014, Shimadzu Scientific Instruments, Kyoto, Japan). **Helium (25**
175 **ml min⁻¹) was used as the carrier gas for methane and CO₂ analysis and ultra-pure N₂ (10 ml min⁻¹**
176 **) was used as the carrier gas for N₂O analysis.** We included methane, CO₂, and N₂O check
177 standards every 20 samples to ensure that the chromatograph maintained the calibration
178 throughout the analysis. If the deviation between the measured value and the value of the check
179 standard was greater than 10%, we recalibrated the chromatograph and re-ran the samples.

180 Molar concentrations of methane, CO₂, and N₂O (C_{molar_pore}) were calculated from the
181 measured gas concentrations as:

$$182 C_{molar_pore} = \frac{\frac{p_i}{RT} Vh + \frac{p_i}{HCP} Vl}{Vl} \quad (2)$$

183 Where p_i is the partial pressure of methane, CO₂ or N₂O, R is the universal gas constant (m³ Pa
184 mol⁻¹ K⁻¹), T is the room temperature (K), Vh is the volume of the headspace (ml), H^{cp} is
185 Henry's volatility constant (m³ Pa mol⁻¹) for methane, CO₂, and N₂O, respectively, and Vl the
186 volume of the liquid subsample used to create the headspace (ml).

187

188 **2.5 Surface flux measurements**

189 Flux measurements were conducted using non-steady-state chambers. At each sampling, we
190 conducted triplicate chamber measurements at the water surface right above the peepers when
191 they were submerged or around it when the water table was below the sediments, and the peepers
192 were surfacing. We used transparent polypropylene dome-shaped chambers (7.3×10^{-2} m²
193 surface area, 7.7×10^{-3} m³ volume), equipped with a digital thermometer to record inner
194 temperatures and a 12v fan to mix air within the chamber and polyethylene foam in the bottom
195 rim for flotation. For methane flux measurements, we used a single chamber connected to a
196 cavity ring-down spectroscopy methane analyzer (Gas Scouter G4301, Picarro, Santa Clara, CA)
197 that recirculated the air at a rate of 1L min⁻¹. The analyzer recorded methane concentrations in
198 the chamber at a 1-Hz frequency. Each chamber deployment lasted for three minutes, and
199 measurements were consecutive at each peeper location.

200 For N₂O flux measurements, the chambers included a 30-cm long, 1.6 mm ID tube for pressure
201 relief and a gray butyl rubber stopper as a sampling port as well. At each sampling, we deployed
202 three chambers simultaneously for 24-minute periods at each peeper location. Six 10-ml samples
203 were collected at 4-min frequency during each deployment, placed in pre-evacuated vials and
204 transported for chromatography analysis in the laboratory. The concentrations of the gas samples

205 were analyzed in the same chromatograph, and under the same quality control used to measure
206 N₂O concentrations in porewater.

207 Methane and N₂O chambers positioning during sampling followed an equilateral triangular
208 arrangement with two chambers positioned parallel to the shore. For methane sampling, we
209 ensured the position of the single manually during the sampling period. For the N₂O sampling,
210 we attached the chambers with polyethylene foam and then the chamber array was anchored
211 above the peeper location by surrounding the PVC conduit used to house the peeper tubing.

212

213 **2.6 Surface flux calculations**

214 For each methane chamber measurement, we fitted a 2 minute, 1-Hz time series of methane
215 concentrations, C_{HM} ($\mu\text{mol mol}^{-1}$), to the non-linear Hutchinson and Moiser one-dimension
216 diffusion model (Hutchinson and Mosier, 1981; Kutzbach et al., 2007; Pedersen et al., 2010):

$$217 \quad C_{HM} = C_s + (C_0 - C_s) e^{-kt} \quad (3)$$

218 Where C_0 is the pre-deployment concentration of methane ($\mu\text{mol mol}^{-1}$), C_s is the constant
219 source or sink concentration ($\mu\text{mol mol}^{-1}$), and k is a curve shape parameter (h^{-1}). C_0 , C_s , and k
220 are parameters determined by fitting the observed gas concentrations in the chamber over time, t
221 (h). We then calculated the flux of methane (F_{CH_4} , $\mu\text{mol m}^{-2} \text{h}^{-1}$) at the water or sediment
222 surface as:

$$223 \quad F_{CH_4} = k (C_0 - C_s) \frac{PV}{RTA}, \quad (4)$$

224 where P (Pa) is the atmospheric pressure, measured with a digital barometer at the site; V the
225 volume of the chamber (m^3), R the universal gas constant ($\text{m}^3 \text{Pa mol}^{-1} \text{K}^{-1}$), T the temperature
226 inside the chamber (K), and A the surface area of the chamber (m^2).

227 For N₂O chamber measurements, we calculated the molar concentrations of N₂O (C_{molar_Ch} ,
228 $\mu\text{mol m}^{-3}$), in each sample using a modified gas law, following the procedure described by
229 (Holland et al., 1999):

$$230 \quad C_{molar_Ch} = \frac{Cv \cdot P}{R \cdot T} \quad (5)$$

231 where Cv is the concentration (nmol mol⁻¹) of N₂O in the sample, P is atmospheric pressure (Pa),
232 R is the universal gas constant (m³ Pa mol⁻¹ K⁻¹), and T is the air temperature (K) of the chamber.
233 Then, the accumulation rate, C_{rate} (nmol m⁻³ h⁻¹), was determined using the slope of the linear
234 regression fitted to the time points (t , h) collected for each chamber after rejecting outliers in the
235 regressions following the procedure described by (Rey-Sanchez et al., 2018):

$$236 \quad C_{molar_Ch}(t) = C_{molar_Ch}(0) + C_{rate} \times t \quad (6)$$

237 and with the C_{rate} , we calculated the flux rate (F_{N_2O} , nmol m⁻² h⁻¹) as:

$$238 \quad F_{N_2O} = \frac{V \cdot C_{rate}}{A}, \quad (7)$$

239 where V is the volume of the chamber (m³), and A the area of the water/sediment surface covered
240 by the chamber (m²).

241 We used the coefficient of determination (r^2) of the fit between the model (linear in the case of
242 N₂O or non-linear in the case of CH₄) and concentration observations in the chamber and a
243 quality control criterion. Flux measurements with $r^2 < 0.8$ were considered of poor quality and
244 were discarded from our analyses to avoid error. Out of the 81 flux measurements for methane
245 and N₂O, 28 for methane and 29 for N₂O, were discarded due to this criterion of poor
246 observation quality.

247

248 **2.7 Methane conductance and conductivity**

249 We used the following general expression to solve for the bulk transfer velocity of methane, or
250 methane conductance (K), at the different beach positions and river water stages assuming that
251 methane is not being produced in the water column:

252 $F_CH_{4d} = K (C_{sed} - C_{air} P H^{cp})$, for $F > 0$ (8)

253 where F_CH_{4d} is methane the flux measured at each flux chamber but in units of $\mu\text{mol m}^{-2} \text{d}^{-1}$ to
254 correspond with the unit convention of conductance. C_{sed} ($\mu\text{mol m}^{-3}$) is the concentration of
255 methane in the sediments **porewater** at a given depth and C_{air} ($\mu\text{mol m}^{-3}$) is the aqueous
256 equivalent of the concentration of methane in the air, **calculated as the product of the initial**
257 **concentration in the chamber ($\mu\text{mol mol}^{-1}$), P the atmospheric pressure at the moment of**
258 **sampling (Pa), and H^{cp} the Henry's solubility constant for methane ($\text{mol Pa}^{-1} \text{m}^{-3}$)**. The initial
259 **concentration in the chamber, representing the concentration before enclosure, was calculated as**
260 **the average of the first five measurements of each chamber run.**

261 We assume that the overall conductance, K , is the combined result of two transport processes –
262 K_w , the conductance to methane transport in the water from the soil surface to the air, and K_s , the
263 conductance for methane diffusion/transport in the soil from the peak concentration depth to the
264 soil surface. Adding the **resistance** to methane flux in a sequential process, we obtain the term
265 for the combined conductance K :

266
$$K = \frac{K_w K_s}{K_w + K_s}$$
 (9)

267 We followed the approach by Bastviken et al., (2004) to independently determine the
268 **conductance to methane in the water column K_w for each flux chamber, by solving the equation:**

269 $F_CH_4 = K_w (C_{ss} - C_{air})$ (10)

270 where C_{ss} ($\mu\text{mol m}^{-3}$) is the concentration of methane at the surface of the sediments assumed
271 as the concentration in the first peeper cell.

272 Substituting eq 9 into eq 8, and using the porewater concentration at the depth of peak
273 concentration in the soil, C_{ps} we obtain an equation for K_s :

274
$$F_CH_{4d} = \frac{K_w K_s}{K_w + K_s} (C_{ps} - C_{air}) \quad (11)$$

275 Equation 11 can be solved using the value we obtained for K_w , from equation (10).

276 Then we calculated the conductivity (i.e., conductance per unit length) to methane
277 transport/diffusion in the soil (k_s) as:

278
$$k_s = \frac{K_s}{D_p} \quad (12)$$

279 Where D_p (m) is the depth at which concentration peaks in the sediment profile.

280

281 **2.8 Data analysis**

282 We processed data, fit models for flux calculations, and conducted regression tests of
283 porewater concentrations using MATLAB ® 2018b. We used JMP Pro 14.0.0 for all other
284 statistical tests. All the statistical tests were conducted at a 0.05 significance level.

285 We used Spearman rank correlation to infer the significance of the relationship between
286 average porewater concentrations in the sediment profile and fluxes. We tested the significance
287 of the difference of fluxes and porewater concentrations between water stages for each beach
288 position using paired nonparametric comparisons with the Wilcoxon method. For testing the
289 significance of the differences of water and sediment conductance and sediment conductivity
290 between water stages and within beach positions, we used an ordinal logistic model with the
291 conductances or the conductivity as the response variable, position as a fixed effect and water
292 stage nested by position.

293

294 **2.9 Data availability**

295 All porewater concentrations and fluxes data will be made available through ESS-DiVE
296 (<https://ess-dive.lbl.gov/>), DOI pending. Additional ancillary data for the Hanford site is
297 available through the Phoenix – PNNL Environmental Information Exchange
298 (<https://www.hanford.gov/page.cfm/PHOENIX>).

299

300 **3. Results and discussion**

301 **3.1 Water level and sediment temperature**

302 The water level at the shallow bank position was low (near the sediment surface) during the
303 first part of the year until April when water levels started rising after the spring thaw (Figure
304 2A). The maximum water levels (> 3 m above the reference elevation, set at the shallow peeper
305 position) were observed in mid-May and were followed by a steadily falling water stage until the
306 beginning of July and remained low during the rest of the year. A brief rising limb in the second
307 half of June was driven by dam water release during the falling stage and coincided with the
308 moment we conducted our sampling. Water levels below the reference elevation were observed
309 during the low stages before the rising stage and after the falling stage. The water level during
310 the low water stage was more variable than during previous stages. The operation of the dam
311 upstream can cause up to 0.5 m variations in water levels within a daily period (Zhou et al.,
312 2018).

313 Positive hydraulic gradients (downwelling) occurred through the hydrological year, including
314 the time during the rising and falling water stages (Figure 2B, C). However, reversals to the
315 negative hydraulic gradient (upwelling) were frequent during the low water stage. Hydraulic
316 gradient reversal represents groundwater upwelling or moments when the river receives water

317 from the aquifer. Reversals were also frequent on the days preceding the low water stage
318 sampling (Figure 2D).

319 Sediment temperature increased throughout the sampling period. In general, mean positions'
320 temperatures had a 10 °C increase between the beginning of the study during the rising water
321 stage in April and the study end in August (Figure 2). Temperatures were similar throughout the
322 different beach positions during the rising and falling stages but differed and were more variable
323 at the low water stage when the water level dropped below the soil surface at the reference level.

324

325 **3.2 Methane porewater concentration and fluxes respond similarly to river stage variation**

326 Methane flux to the atmosphere is the result of a balance between methane production and
327 consumption and is influenced by the relative importance of the transport pathways, including
328 diffusion, bubbling, and plant transport (Bridgham et al. 2013). At our site, we regard diffusion
329 as the main transport pathway. We did not observe evidence of bubbling in our peeper chamber
330 measurements (i.e., sudden spikes in methane concentration in the time series during chamber
331 deployments). We also neglected the influence of plant transport because macrophyte vegetation
332 was not present near the sampling locations, although a negligible fraction could have been
333 transported from the shallow bank position through the vascular system of some shrubs present
334 on the riverbank. Methane porewater concentrations and fluxes at the 3G site were negligible
335 during the rising water stage when the sediment temperatures were low (~10 °C, Figure 3A),
336 which is not surprising given the high sensitivity of methane production to temperature (Yvon-
337 Durocher et al., 2014). Methane flux was low at the shallow position during the low water stage
338 as well, when the water level was below the sediment surface (Table 1). Despite relatively higher
339 concentrations in the sediment profile (Figure 3B), the water level dropdown during the low

340 water stage may have resulted in unsaturated or oxygenated sediments and as a result, a
341 predominantly aerobic environment that would have increased methane oxidation above the
342 water table in the sediment column (Segers, 1998). Indeed, the porewater concentration profile at
343 the shallow position during the low water stage showed very low concentrations throughout the
344 sediment above the water table (Figure 4), consistent with increased methane oxidation coupled
345 to aerobic respiration (Conrad and Rothfuss, 1991) or low methane production due to
346 thermodynamic exclusion (Bethke et al., 2011).

347 Both methane production and consumption can co-occur in sediments (Le Mer and Roger,
348 2001) since methanogenic and methanotrophic bacteria can be correlated in terms of population
349 in sediments subject to flooding (Joulian et al., 1997) and the ratio between methanogens to
350 methanotrophs is correlated to methane transfer velocity (Rey-Sanchez et al., 2019). Bednářík et
351 al. (2015) demonstrated that benthic methane fluxes are correlated with porewater
352 concentrations, suggesting that differences between porewater concentrations and surface
353 methane fluxes might be due to the activity of methane-oxidizing bacteria in the upper sediment
354 layers (Oremland and Culbertson, 1992) or the water column (Matoušů et al., 2017). Although
355 we did not systematically measure dissolved oxygen in the sediment-water interface and the
356 water column during our samplings, we conducted a series of surveys for dissolved oxygen
357 levels before sampling. These indicated that both the water column and the porewater at the
358 water-sediment interface were consistently supersaturated, offering optimal conditions for
359 biological methane oxidation. In deeper systems, such as estuaries and reservoirs, methane
360 fluxes are greater at low water levels because of reduced storage turnover times, which is the
361 time methane remains in the water column after being produced in the sediments (Valentine et
362 al., 2001; Zhu et al., 2010; Lei et al., 2019). Lessened turnover times, reduce the time for

363 potential oxidation while methane diffuses through the water column. Methane oxidation rate in
364 the water column of rivers has been correlated with the concentration of dissolved methane in the
365 water and with water temperature (Matoušů et al., 2018), which are proxies for the substrate and
366 the enzymatic activity of methanotrophic microorganisms. Therefore, we hypothesize that the
367 effect of storage-turnover time on methane oxidation will be effective in rivers, including near-
368 bank shallow waters as well. Future studies coupling methane fluxes, and oxidation rates with
369 simultaneous measurements of methane concentrations in the sediment and water column could
370 help test this hypothesis.

371 During the falling and low water stages when sediment temperatures were more favorable for
372 methane production, river level had a dissimilar effect on porewater concentrations and fluxes
373 across positions, although in general, methane fluxes were correlated (Spearman's $\rho = 0.62, p <$
374 0.001) and followed the dynamics of the integrated sediment-profile porewater concentrations.
375 Methane porewater concentration and fluxes decreased at the shallow position after the water
376 level transition from the falling to the low water stage, while porewater concentration and fluxes
377 remained similar at the deep position. In contrast, at the intermediate position, methane fluxes
378 increased at the low stage, when the water levels were also low, while the median porewater
379 concentration increased as well, though not at a significant level.

380 Low or near-zero fluxes accompanied by decreasing methane concentrations towards the
381 surface of the sediments in the shallow position strongly indicate the activity of methanotrophs
382 actively reducing methane emissions to the atmosphere in the upper region of the sediment
383 profile in the shallow position during the low water stage (Figure 4). However, the activity of
384 methanotrophs in the upper layers of the soil profile was not evident at the intermediate or deep
385 positions (that maintained water above the sediment surface). Even during the low water stage of

386 the intermediate position, the peak in methane concentrations occurred well below the sediment
387 elevation. It is possible that reduced downwelling of electron acceptors and oxygen during low
388 water stages not only stimulated heterotrophic production of methanogenic substrates but also
389 limited dissolved oxygen that is toxic to methanogens and reduced aerobic methanotrophic
390 respiration. However, without specific measurements of oxidation rates at our site, it is hard to
391 pinpoint the specific cause of the variability of methane fluxes across the different beach
392 positions and river water stages.

393 Different apparent conductance to methane transport through the water column between falling
394 and low water stages **suggests** that methane oxidation may occur at different rates depending on
395 the water **levels** (Figure 5A). Because we did not account for oxidation during transport in the
396 water column, our observations of higher apparent conductance to methane transport may be the
397 outcome of lower oxidation. Differences in conductance to methane transport through the water
398 column were evident **in** the intermediate position, with larger conductance during the low water
399 stage. In the sediment profile, conductance to methane was not different between falling and low
400 water stages. **Nonetheless, there were differences in the apparent conductance to methane in the**
401 **sediments among beach positions (Figure 5B), suggesting that there may be a significant spatial**
402 **variation in oxidation rates at the plot scale.**

403

404 **3.3 Methane concentrations in porewater peak along an elevation gradient**

405 Similar to surface fluxes, methane concentrations in the sediment profile are the result of a
406 balance between methane production, consumption, and transport to and from the sediment zone.
407 Previous studies at the **Hanford Reach in similar sites to ours** have shown that hydrological
408 mixing stimulates heterotrophic respiration and organic carbon turnover (Stegen et al., 2016).

409 Under anaerobic conditions, heterotrophic respiration at the HZ of organic matter would
410 stimulate methane production by producing favored substrates and depleting electron acceptors
411 (Schindler, 1998; Romeijn et al., 2019), whereas under aerobic conditions methane oxidation
412 would be favored (Conrad and Rothfuss, 1991). Complementarily, methane may be imported in
413 the upwelling groundwater as well. Inputs of methane dissolved in groundwater have been
414 observed at low order streams in peat-dominated watersheds (Hope et al. 2001), headwater
415 streams (Jones and Mulholland, 1998), streams in agricultural dominated landscapes (Comer-
416 Warner et al., 2019) and other riverine settings including the Willamette River, the main
417 tributary of the Columbia River (Anthony et al., 2012).

418 The observed methane porewater concentrations profile in the sediment showed distinct peaks
419 that varied among bank positions following the sediment surface elevation gradient during the
420 falling and low water stages (Figure 4). During the falling water stage, concentrations at the
421 shallow positions peaked at the lower sediment layers (relative sediment depth – RSD: -25 to -40
422 cm), while at the intermediate position, concentrations peaked at the upper sediment layers (top
423 20 cm from the sediment surface, RSD: -50 to -70 cm). During the low water stage,
424 concentrations peaked at the lowest depths at the shallow position (around RSD: -50 cm), mid-
425 to-lower depths from the sediment surface at intermediate position (RSD: -80 to -105 cm), and
426 upper sediment layers at the deep position (RSD: -100 to -110 cm). Overall the peaks in methane
427 concentration were observed at upper sediment layers during the falling water stage when the site
428 remained permanently inundated (thick blue line in Figure 4), and at lower sediment layers
429 during the low water stage when the water level was fluctuating around the reference elevation
430 (thick orange line in Figure 4).

431 The peaks may have resulted from a combination of heterotrophic respiration and imports
432 through groundwater into the HZ from the nearby upland area. Methane and CO₂ porewater
433 concentrations were significantly correlated (Figure 6). Based on the low concentrations of
434 acetate measured in similar sites along the Hanford Reach, with only 1/50 samples being above
435 the detection limit (>78 µM), and uncertainty of methyl compound identity and potential
436 utilization (Hou et al., 2017), we infer that the prevailing mode of methanogenesis was
437 hydrogenotrophic, requiring hydrogen and CO₂. However, we acknowledge that this correlation
438 is a function of overall microbial activity, rather than the result of the direct use of CO₂ for
439 methanogenesis alone (Moore and Dalva, 1997; Comer-Warner et al., 2019). Interestingly, we
440 found that the slope of the regression between methane and CO₂ porewater concentrations varied
441 during the three water stages and was larger during the falling water stage when the river
442 downwelling was stronger than during the low water stage when downwelling diminished and
443 groundwater upwelling was more frequent (Figure 6). The difference in the strength of microbial
444 activity between falling water and low water stages support findings by previous studies at
445 adjacent sites along the Hanford Reach that showed a shift in microbial communities as labile
446 organic carbon stimulates heterotrophic respiration during river downwelling periods (Stegen et
447 al. 2016). As water drops and the influence of groundwater upwelling increases, heterotrophic
448 processes of carbon cycling and decomposition succumb to autotrophic processes (Graham et al.,
449 2017).

450 On the other hand, as groundwater upwelling becomes more frequent during the low water
451 stage and heterotrophic respiration recede (and presumably the production of methane), imports
452 of dissolved methane in the groundwater increase, maintaining similar porewater concentrations
453 than during the falling water stage. This hypothesis is supported by the increase in conductivity

454 of methane in the sediments we observed at the deep position (Figure 5C), which indicates that
455 during groundwater upwelling, methane transport is faster. We hypothesize that while microbial
456 methane production is reduced when the water level drops and groundwater upwelling is
457 increased, methane concentrations and fluxes are maintained because allochthonous methane is
458 “pushed out” from the surrounding upland soils and river sediments.

459 We propose that the observed peaks in methane concentration through the sediment profile
460 during the falling water stage occurred at predominantly anaerobic zones, where hydrological
461 mixing of downwelling surface water from the river and upwelling groundwater from the aquifer
462 is enhanced. The predominant zone of methane production moved vertically downward within
463 the HZ as the river transitioned from falling to low water stage, coinciding with a shift from river
464 water dominated to groundwater-dominated mixing ratios.

465

466 **3.4 Nitrous oxide porewater concentrations and fluxes have different dynamics across river 467 water stages**

468 Unlike methane, N₂O porewater concentrations in the sediment profile and fluxes to the
469 atmosphere did not follow similar patterns throughout the river water stages (Spearman’s $\rho =$
470 0.29, $p = 0.14$). N₂O porewater concentrations were higher during the rising water stage than
471 during the falling water stage in all the three beach positions and during the low water stage at
472 the intermediate position (Figure 7A). Instead, N₂O fluxes increased from the rising to the low
473 water stage at the shallow position, while remained similar at the intermediate and deep positions
474 during the three water stages (Figure 7B).

475 The decoupling between the observed N₂O porewater concentrations in the sediments and the
476 fluxes is not surprising. N₂O production in large rivers might occur primarily at the water column

477 in microsites within suspended particles. There is significant evidence of substantial N₂O
478 production via denitrification in pelagic zones of estuaries (Barnes and Owens, 1999; de Wilde
479 and de Bie, 2000). Beaulieu et al. (2010) presented evidence of a similar pattern at a large river,
480 with N₂O production rates in the water column doubling that of the sediments, which could help
481 explain the lack of correlation between the porewater concentrations and fluxes. Marzadri et al.
482 (2014) and Marzadri et al. (2017) explained that in lotic systems there is a shift in the
483 predominant zones of N₂O production from the **hyporheic-benthic zone in streams to the benthic-**
484 **water column zone in rivers as the system gains size**, due mainly to the increase in suspended
485 particle loads.

486 Notably, we observed negative fluxes throughout the different river water stages and in all
487 positions, which is consistent with high rates of N₂O consumption at either the sediments or the
488 water column. Our plot acted primarily as a sink at the shallow position while the sediments
489 were fully saturated, and the water level was above the sediment surface and on the intermediate
490 position during the low water stage when the water level at this position was low as well (Figure
491 7A). N₂O is often produced as an intermediate species of microbially mediated denitrification, or
492 a byproduct of nitrification or reduction of ammonia to nitrate (Quick et al., 2019). Dissolved
493 organic carbon in the HZ plays a critical role in fueling nitrification under aerobic conditions
494 (Graham et al., 2016; Graham et al., 2017) and in addition, may lead to low oxygen and nitrate
495 conditions that ultimately favor N₂O consumption (Soued et al., 2015). Low oxygen conditions
496 may result from the low flow as well (Baulch et al., 2011b), which prevailed in the 3G
497 observatory, especially at lower water levels, explaining the dominant sinking functioning of the
498 shallow and intermediate positions partially. It may also be possible that atmospheric nitrous
499 oxide consumption occurred in the water column in the absence of other denitrification

500 processes, which has been demonstrated only for a few model microorganisms and ecosystems
501 (Jones et al., 2014; Yoon et al., 2016).

502 A more robust understanding of the nexus (or lack thereof) of the spatial heterogeneity and
503 dynamics of N_2O porewater concentrations and fluxes must build upon the synergistic effects of
504 the seasonal hydrological exchanges, inorganic nitrogen availability, and the activity of the
505 microbial community involved in cycling nitrous oxide at the HZ and the water column. For
506 instance, the nitrification and denitrification functional potential of microbial communities in the
507 HZ of the Hanford Reach (and possibly many other lotic systems) are linked with the ratio of
508 groundwater to surface water, likely due to the input of N in the groundwater (Nelson et al.,
509 2019). However, it is still not clear if or how the dynamics of groundwater N or other
510 environmental drivers are affecting the N-cycling functional potential in the water column and
511 overall how N_2O is produced and consumed in the sediment-water column continuum.

512

513 **3.5 Nitrous oxide concentrations peak at the sediment/water table interface**

514 Mathematical and conceptual models propose that N_2O production at the HZ is maximized
515 along flowlines representing intermediate travel times of downwelling surface water, which are
516 usually few cm below the sediment surface (Reeder et al., 2018; Quick et al., 2016). At
517 shallower depths, at the surface of the sediments (i.e., shortest travel times), nitrate is not
518 transformed, whereas at deeper depths (i.e., longest travel times), denitrification is completed
519 and N_2 is the predominantly released gas. The N_2O porewater concentrations we observed at the
520 3G are consistent with the modeling predictions, showing increased concentrations at the
521 proximity of the sediment/water table interface (~ up to 15 cm) (Figure 8).

522 We found significant negative correlations between N_2O and CO_2 porewater concentrations for
523 pooled data from the three water stages and the shallow and intermediate beach positions (Figure
524 9). We cannot discern whether the correlation is the result of N_2O production or consumption.
525 Partial denitrification, nitrate reduction to N_2O , is coupled to carbon oxidation to CO_2 and
526 therefore, we would expect a positive correlation (Tsuruta et al., 1997). Therefore, N_2O
527 production appeared decoupled from denitrification and more closely tied to other processes. The
528 negative correlations could be explained by the release of N_2O during nitrification coupled to
529 CO_2 assimilation or heterotrophic microorganisms utilizing N_2O as a terminal electron acceptor
530 (Hink et al., 2017; Lycus et al., 2018). This may help explain the negative correlation between
531 N_2O and CO_2 porewater concentrations, which were also seen in observations of other riverine
532 settings (Richey et al., 1988; Teodoru et al., 2015). However, we do not rule out that
533 simultaneous processes of production and consumption are co-occurring and that their relative
534 importance change as the river water level transitions and substrates, environmental conditions,
535 and the relative diversity and abundance of N-Cycling populations vary (Nelson et al., 2019).
536 The decoupling between N_2O and CO_2 may be explained as well at some degree by lateral
537 transport of N_2O dissolved in groundwater (Clough et al., 2006).
538 It is noteworthy that the strength of the correlation between N_2O and CO_2 porewater was
539 dictated by beach positions, indicating that different processes are occurring between locations.
540 Weaker negative correlations at the shallow position may be explained by contributions of both
541 nitrification byproducts and denitrification, N_2O consumption as an electron acceptor in the
542 absence of other denitrification processes, and labile carbon oxidation, or the increased
543 contributions from heterotrophic denitrifications. Coupling inorganic nitrogen concentrations and

544 organic carbon concentration measurements should help unveil the prevalence of these processes
545 and their influence in the observed variability between beach positions.

546

547 **4. Conclusions and outlook**

548 Hyporheic zones of rivers and streams are important hotspots of greenhouse gas emissions. The
549 interaction of river stage and biogeochemical processes govern the production, consumption, and
550 flux dynamics. This interaction of the governing factors results in high heterogeneity at the small
551 scale (m to cm) in horizontal and vertical planes. At the plot scale, methane porewater
552 concentrations have a marked vertical temporal dynamic with concentrations peaking at different
553 depths depending on the influence of the magnitude and direction of hyporheic mixing. Methane
554 fluxes followed the dynamics of porewater concentrations throughout the river water stages but
555 highlighted the potential influence of oxidation in the resulting fluxes. Hence the need for sub-
556 models capable of representing the potential effects of hydrological exchanges on methane
557 oxidation in the HZ. The effect was pronounced for the intermediate position where methane
558 fluxes increased (and the conductance to methane in the water column) from the falling water
559 stage to the low water stage. In turn, N₂O porewater concentrations rely more on the permanent
560 mixing at the HZ and occur at the upper layers just below the sediment surface. Contrary to
561 methane, fluxes of N₂O were not correlated to porewater concentrations and were reduced at low
562 water elevations, possibly because of the release of N₂O as a byproduct of aerobic nitrification or
563 the use of N₂O as an alternative terminal electron acceptor to oxygen for microbial respiration at
564 the sediment-water interface (Khalil et al., 2004; Jones et al., 2014). Overall results indicated that
565 the plot functioned as a net source of methane and could function as either a sink or source for
566 N₂O depending on both the season and position within the riparian zone. Therefore, identifying

567 the potential nexus between N_2O production and consumption and concurrency at the HZ
568 represents a critical challenge for better representation of the N_2O dynamic in biogeochemical
569 models.

570 Here we presented snapshots of detailed vertical profiles and surface fluxes of methane and
571 N_2O porewater concentrations through the different typical hydrological stages of a large-
572 regulated river. As our results indicate, river stages and consequent groundwater mixing, drive
573 the dynamics of porewater concentrations and fluxes of methane and N_2O on a seasonal scale.
574 However, coupling hydrological dynamics with methane and N_2O concentrations and fluxes at
575 small scales and parametrizing the governing processes will require longer-term and more
576 frequent assessments, especially the inclusion of measurements at a small temporal scale (days-
577 hours). Such a scale is of particular interest to assess the effects of large intra-daily water level
578 oscillations, which are characteristic of regulated rivers, on the GHG production and
579 consumption processes. This daily/sub-daily measurement scale could help to elucidate the
580 effects of preceding environmental conditions set by previous water levels (including microbial
581 populations, temperature, nutrient availability and transformations, and redox conditions) on the
582 production and consumption of GHGs. In non-regulated rivers, we would expect a similar
583 control of seasonal groundwater mixing than the one we observe here. However, in contrast to
584 regulated rivers, the shorter-term effects of preceding environmental conditions would likely be
585 less dramatic given the lower water intra-daily fluctuations.

586 Finally, as our results indicate, GHG concentration and fluxes can be significantly different
587 across small horizontal (6 m W \times 11 m L) and vertical (0.5 m) spatial scales. Moreover, water
588 level fluctuation has a significant effect on the functioning of the HZ as a sink or source of
589 methane and N_2O . The coupling of hydrology and GHGs emissions at small scales will,

590 therefore, be essential to help parametrize and calibrate predictive models in large rivers like the
591 Columbia River and other rivers and streams as well. More importantly, it is a necessary task to
592 test hypotheses discerning the microbial processes explaining the spatiotemporal heterogeneity
593 of methane and N₂O at the HZ.

594

595 **Acknowledgments**

596 This project was sponsored by the Subsurface Biogeochemical Research (SBR) program (DE-
597 SC0018170).

598

599

600

601

602

603

604

605

606

607

608

609

610

611

612

613 **References**

614 Anthony, S.E., Prahl, F.G., Peterson, T.D., 2012. Methane dynamics in the Willamette River,
615 Oregon. *Limnol. Oceanogr.* 57, 1517–1530. <https://doi.org/10.4319/lo.2012.57.5.1517>

616 Aufdenkampe, A.K., Mayorga, E., Raymond, P.A., Melack, J.M., Doney, S.C., Alin, S.R., Aalto,
617 R.E., Yoo, K., 2011. Riverine coupling of biogeochemical cycles between land, oceans,
618 and atmosphere. *Front. Ecol. Environ.* 9, 53–60. <https://doi.org/10.1890/100014>

619 Barnes, J., Owens, N.J.P., 1999. Denitrification and nitrous oxide concentrations in the Humber
620 Estuary, UK, and adjacent coastal zones. *Mar. Pollut. Bull.* 37, 247–260.
621 [https://doi.org/10.1016/S0025-326X\(99\)00079-X](https://doi.org/10.1016/S0025-326X(99)00079-X)

622 Bastviken, D., Cole, J., Pace, M., Tranvik, L., 2004. Methane emissions from lakes: Dependence
623 of lake characteristics, two regional assessments, and a global estimate. *Glob.*
624 *Biogeochem. Cycles* 18, GB4009. <https://doi.org/10.1029/2004GB002238>

625 Baulch, H.M., Dillon, P.J., Maranger, R., Schiff, S.L., 2011a. Diffusive and ebullitive transport
626 of methane and nitrous oxide from streams: Are bubble-mediated fluxes important? *J.*
627 *Geophys. Res. Biogeosciences* 116. <https://doi.org/10.1029/2011JG001656>

628 Baulch, H.M., Schiff, S.L., Maranger, R., Dillon, P.J., 2011b. Nitrogen enrichment and the
629 emission of nitrous oxide from streams. *Glob. Biogeochem. Cycles* 25, GB4013.
630 <https://doi.org/10.1029/2011GB004047>

631 Beaulieu, J.J., Shuster, W.D., Rebholz, J.A., 2010. Nitrous oxide emissions from a large,
632 impounded river: the Ohio River. *Environ. Sci. Technol.* 44, 7527–7533.
633 <https://doi.org/10.1021/es1016735>

634 Beaulieu, J.J., Tank, J.L., Hamilton, S.K., Wollheim, W.M., Hall, R.O., Mulholland, P.J.,
635 Peterson, B.J., Ashkenas, L.R., Cooper, L.W., Dahm, C.N., Dodds, W.K., Grimm, N.B.,

636 Johnson, S.L., McDowell, W.H., Poole, G.C., Valett, H.M., Arango, C.P., Bernot, M.J.,
637 Burgin, A.J., Crenshaw, C.L., Helton, A.M., Johnson, L.T., O'Brien, J.M., Potter, J.D.,
638 Sheibley, R.W., Sobota, D.J., Thomas, S.M., 2011. Nitrous oxide emission from
639 denitrification in stream and river networks. *Proc. Natl. Acad. Sci.* 108, 214.
640 <https://doi.org/10.1073/pnas.1011464108>

641 Bednářík, A., Čáp, L., Maier, V., Rulík, M., 2015. Contribution of methane benthic and
642 atmospheric fluxes of an experimental area (Sitka Stream). *CLEAN – Soil Air Water* 43,
643 1136–1142. <https://doi.org/10.1002/clen.201300982>

644 Bethke, C.M., Sanford, R.A., Kirk, M.F., Jin, Q., Flynn, T.M., 2011. The thermodynamic ladder
645 in geomicrobiology. *Am. J. Sci.* 311, 183–210. <https://doi.org/10.2475/03.2011.01>

646 Boulton, A.J., Findlay, S., Marmonier, P., Stanley, E.H., Valett, H.M., 1998. The functional
647 significance of the hyporheic zone in streams and rivers. *Annu. Rev. Ecol. Syst.* 29, 59–
648 81. <https://doi.org/10.1146/annurev.ecolsys.29.1.59>

649 Bridgham, S.D., Cadillo-Quiroz, H., Keller, J.K., Zhuang, Q., 2013. Methane emissions from
650 wetlands: biogeochemical, microbial, and modeling perspectives from local to global
651 scales. *Glob. Change Biol.* 19, 1325–1346. <https://doi.org/10.1111/gcb.12131>

652 Buchkowski, R.W., Bradford, M.A., Grandy, A.S., Schmitz, O.J., Wieder, W.R., 2017. Applying
653 population and community ecology theory to advance understanding of belowground
654 biogeochemistry. *Ecol. Lett.* 20, 231–245. <https://doi.org/10.1111/ele.12712>

655 Chistoserdova, L., Kalyuzhnaya, M.G., Lidstrom, M.E., 2009. The expanding world of
656 methylotrophic metabolism. *Annu. Rev. Microbiol.* 63, 477–499.
657 <https://doi.org/10.1146/annurev.micro.091208.073600>

658 Clough, T.J., Bertram, J.E., Sherlock, R.R., Leonard, R.L., Nowicki, B.L., 2006. Comparison of
659 measured and EF5-r-derived N₂O fluxes from a spring-fed river. *Global Change Biology*
660 12, 477–488. <https://doi.org/10.1111/j.1365-2486.2005.01092.x>

661 Cole, J., Prairie, Y., Caraco, N., McDowell, W., Tranvik, L., Striegl, R., Duarte, C., Kortelainen,
662 P., Downing, J., Middelburg, J., Melack, J., 2007. Plumbing the global carbon cycle:
663 integrating inland waters into the terrestrial carbon budget. *Ecosystems* 10, 172–185.

664 Comer-Warner, S.A., Gooddy, D.C., Ullah, S., Glover, L., Percival, A., Kettridge, N., Krause, S.,
665 2019. Seasonal variability of sediment controls of carbon cycling in an agricultural
666 stream. *Sci. Total Environ.* 688, 732–741. <https://doi.org/10.1016/j.scitotenv.2019.06.317>

667 Comer-Warner, S.A., Romeijn, P., Gooddy, D.C., Ullah, S., Kettridge, N., Marchant, B.,
668 Hannah, D.M., Krause, S., 2018. Thermal sensitivity of CO₂ and CH₄ emissions varies
669 with streambed sediment properties. *Nat. Commun.* 9, 2803.
670 <https://doi.org/10.1038/s41467-018-04756-x>

671 Conrad, R., Rothfuss, F., 1991. Methane oxidation in the soil surface layer of a flooded rice field
672 and the effect of ammonium. *Biol. Fertil. Soils* 12, 28–32.
673 <https://doi.org/10.1007/BF00369384>

674 de Wilde, H.P.J., de Bie, M.J.M., 2000. Nitrous oxide in the Schelde estuary: production by
675 nitrification and emission to the atmosphere. *Mar. Chem.* 69, 203–216.
676 [https://doi.org/10.1016/S0304-4203\(99\)00106-1](https://doi.org/10.1016/S0304-4203(99)00106-1)

677 Golaz, J., Caldwell, P.M., Van Roekel, L.P., Petersen, M.R., Tang, Q., Wolfe, J.D., Abeshu, G.,
678 Anantharaj, V., Asay- Davis, X.S., Bader, D.C., 2019. The DOE E3SM coupled model
679 version 1: overview and evaluation at standard resolution. *J. Adv. Model. Earth Syst.* 11,
680 2089–2129.

681 Graham, E.B., Crump, A.R., Resch, C.T., Fansler, S., Arntzen, E., Kennedy, D.W., Fredrickson,
682 J.K., Stegen, J.C., 2017. Deterministic influences exceed dispersal effects on
683 hydrologically-connected microbiomes. *Environ. Microbiol.* 19, 1552–1567.
684 <https://doi.org/10.1111/1462-2920.13720>

685 Graham, E.B., Crump, A.R., Resch, C.T., Fansler, S., Arntzen, E., Kennedy, D.W., Fredrickson,
686 J.K., Stegen, J.C., 2016. Coupling spatiotemporal community assembly processes to
687 changes in microbial metabolism. *Front. Microbiol.* 7, 1949.
688 <https://doi.org/10.3389/fmicb.2016.01949>

689 Graham, E.B., Stegen, J.C., Huang, M., Chen, X., Scheibe, T.D., 2019. Subsurface
690 biogeochemistry is a missing link between ecology and hydrology in dam-impacted river
691 corridors. *Sci. Total Environ.* 657, 435–445.
692 <https://doi.org/10.1016/j.scitotenv.2018.11.414>

693 Hink, L., Lycus, P., Gubry-Rangin, C., Frostegård, Å., Nicol, G.W., Prosser, J.I., Bakken, L.R.,
694 2017. Kinetics of NH₃-oxidation, NO-turnover, N₂O-production and electron flow during
695 oxygen depletion in model bacterial and archaeal ammonia oxidisers. *Environmental
696 Microbiology* 19, 4882–4896. <https://doi.org/10.1111/1462-2920.13914>

697 Holland, E.A., Robertson, G.P., Greenberg, J., Groffman, P.M., Boone, R.D., Grosz, J.R., 1999.
698 Soil CO₂, N₂O and CH₄ Exchange, in: *Standard Soil Methods for Long-Term Ecological
699 Research*. Oxford University Press, New York, pp. 185–201.

700 Hotchkiss, E.R., Hall Jr, R.O., Sponseller, R.A., Butman, D., Klaminder, J., Laudon, H., Rosvall,
701 M., Karlsson, J., 2015. Sources of and processes controlling CO₂ emissions change with
702 the size of streams and rivers. *Nat. Geosci.* 8, 696.

703 Hou, Z., Nelson, W.C., Stegen, J.C., Murray, C.J., Arntzen, E., Crump, A.R., Kennedy, D.W.,
704 Perkins, M.C., Scheibe, T.D., Fredrickson, J.K., Zachara, J.M., 2017. Geochemical and
705 microbial community attributes in relation to hyporheic zone geological facies. *Sci. Rep.*
706 7, 12006. <https://doi.org/10.1038/s41598-017-12275-w>

707 Hutchinson, G., Mosier, A., 1981. Improved soil cover method for field measurement of nitrous
708 oxide fluxes 1. *Soil Sci. Soc. Am. J.* 45, 311–316.

709 Jackson, R.B., Le Quéré, C., Andrew, R.M., Canadell, J.G., Peters, G.P., Roy, J., Wu, L., 2017.
710 Warning signs for stabilizing global CO₂ emissions. *Environ. Res. Lett.* 12, 110202.
711 <https://doi.org/10.1088/1748-9326/aa9662>

712 Jones, C.M., Spor, A., Brennan, F.P., Breuil, M.-C., Bru, D., Lemanceau, P., Griffiths, B.,
713 Hallin, S., Philippot, L., 2014. Recently identified microbial guild mediates soil N₂O sink
714 capacity. *Nat. Clim. Change* 4, 801.

715 Jones, J.B., Mulholland, P.J., 1998. Influence of drainage basin topography and elevation on
716 carbon dioxide and methane supersaturation of stream water. *Biogeochemistry* 40, 57–72.

717 Joulian, C., Escoffier, S., Le Mer, J., Neue, H., Roger, P.-A., 1997. Populations and potential
718 activities of methanogens and methanotrophs in rice fields: relations with soil properties.
719 *Eur. J. Soil Biol.* 33, 105–116.

720 Kampbell, D.H., Wilson, J.T., Vandegrift, S.A., 1989. Dissolved oxygen and methane in water
721 by a GC headspace equilibration technique. *Int. J. Environ. Anal. Chem.* 36, 249–257.
722 <https://doi.org/10.1080/03067318908026878>

723 Khalil, K., Mary, B., Renault, P., 2004. Nitrous oxide production by nitrification and
724 denitrification in soil aggregates as affected by O₂ concentration. *Soil Biology and*
725 *Biochemistry* 36, 687–699. <https://doi.org/10.1016/j.soilbio.2004.01.004>

726 Krause, S., Hannah, D.M., Fleckenstein, J.H., Heppell, C.M., Kaeser, D., Pickup, R., Pinay, G.,

727 Robertson, A.L., Wood, P.J., 2011. Inter-disciplinary perspectives on processes in the

728 hyporheic zone. *Ecohydrology* 4, 481–499. <https://doi.org/10.1002/eco.176>

729 Kutzbach, L., Scneider, J., Sachs, T., Giebels, M., Nykänen, H., Shurpali, N.J., Martikainen, P.J.,

730 Alm, J., Wilmking, M., 2007. CO₂ flux determination by closed-chamber methods can be

731 seriously biased by inappropriate application of linear regression. *Biogeosciences* 4,

732 1005–1025.

733 Le Mer, J., Roger, P., 2001. Production, oxidation, emission and consumption of methane by

734 soils: a review. *Eur. J. Soil Biol.* 37, 25–50. [https://doi.org/10.1016/S1164-5563\(01\)01067-6](https://doi.org/10.1016/S1164-5563(01)01067-6)

735

736 Lei, D., Liu, J., Zhang, J., Lorke, A., Xiao, S., Wang, Y., Wang, W., Li, Y., 2019. Methane

737 oxidation in the water column of Xiangxi Bay, Three Gorges Reservoir. *CLEAN – Soil*

738 *Air Water* 47, 1800516. <https://doi.org/10.1002/clen.201800516>

739 Lycus, P., Soriano-Laguna, M.J., Kjos, M., Richardson, D.J., Gates, A.J., Milligan, D.A.,

740 Frostegård, Å., Bergaust, L., Bakken, L.R., 2018. A bet-hedging strategy for denitrifying

741 bacteria curtails their release of N₂O. *Proc. Natl. Acad. Sci.* 115, 11820.

742 <https://doi.org/10.1073/pnas.1805000115>

743 Lyu, Z., Shao, N., Akinyemi, T., Whitman, W.B., 2018. Methanogenesis. *Curr. Biol.* 28, R727–

744 R732. <https://doi.org/10.1016/j.cub.2018.05.021>

745

746 MacDonald, L.H., Paull, J.S., Jaffé, P.R., 2013. Enhanced semipermanent dialysis samplers for

747 long-term environmental monitoring in saturated sediments. *Environ. Monit. Assess.* 185,

748 3613–3624. <https://doi.org/10.1007/s10661-012-2813-8>

749 Marzadri, A., Dee, M.M., Tonina, D., Bellin, A., Tank, J.L., 2017. Role of surface and
750 subsurface processes in scaling N₂O emissions along riverine networks. *Proc. Natl. Acad.*
751 *Sci.* 114, 4330. <https://doi.org/10.1073/pnas.1617454114>

752 Marzadri, A., Tonina, D., Bellin, A., Tank, J.L., 2014. A hydrologic model demonstrates nitrous
753 oxide emissions depend on streambed morphology. *Geophys. Res. Lett.* 41, 5484–5491.
754 <https://doi.org/10.1002/2014GL060732>

755 Matoušů, A., Osudar, R., Šimek, K., Bussmann, I., 2017. Methane distribution and methane
756 oxidation in the water column of the Elbe estuary, Germany. *Aquat. Sci.* 79, 443–458.
757 <https://doi.org/10.1007/s00027-016-0509-9>

758 Matoušů, A., Rulík, M., Tušer, M., Bednářík, A., Šimek, K., Bussmann, I., 2018. Methane
759 dynamics in a large river: a case study of the Elbe River. *Aquat. Sci.* 81, 12.
760 <https://doi.org/10.1007/s00027-018-0609-9>

761 McClain, M.E., Boyer, E.W., Dent, C.L., Gergel, S.E., Grimm, N.B., Groffman, P.M., Hart,
762 S.C., Harvey, J.W., Johnston, C.A., Mayorga, E., McDowell, W.H., Pinay, G., 2003.
763 Biogeochemical hot spots and hot moments at the interface of terrestrial and aquatic
764 ecosystems. *Ecosystems* 6, 301–312. <https://doi.org/10.1007/s10021-003-0161-9>

765 Moore, T.R., Dalva, M., 1997. Methane and carbon dioxide exchange potentials of peat soils in
766 aerobic and anaerobic laboratory incubations. *Soil Biol. Biochem.* 29, 1157–1164.
767 [https://doi.org/10.1016/S0038-0717\(97\)00037-0](https://doi.org/10.1016/S0038-0717(97)00037-0)

768 Nelson, W.C., Graham, E.B., Crump, A.R., Fansler, S.J., Arntzen, E.V., Kennedy, D.W., Stegen,
769 J.C., 2019. Temporal dynamics of nitrogen cycle gene diversity in a hyporheic
770 microbiome. *bioRxiv* 722785. <https://doi.org/10.1101/722785>

771 Neubauer, ScottC., Megonigal, J.P., 2015. Moving beyond global warming potentials to quantify
772 the climatic role of ecosystems. *Ecosystems* 18, 1000–1013.
773 <https://doi.org/10.1007/s10021-015-9879-4>

774 Oremland, R.S., Culbertson, C.W., 1992. Importance of methane-oxidizing bacteria in the
775 methane budget as revealed by the use of a specific inhibitor. *Nature* 356, 421–423.
776 <https://doi.org/10.1038/356421a0>

777 Pedersen, A.R., Petersen, S.O., Schelde, K., 2010. A comprehensive approach to soil-atmosphere
778 trace-gas flux estimation with static chambers. *Eur. J. Soil Sci.* 61, 888–902.
779 <https://doi.org/10.1111/j.1365-2389.2010.01291.x>

780 Quick, A.M., Reeder, W.J., Farrell, T.B., Tonina, D., Feris, K.P., Benner, S.G., 2019. Nitrous
781 oxide from streams and rivers: a review of primary biogeochemical pathways and
782 environmental variables. *Earth-Sci. Rev.* 191, 224–262.
783 <https://doi.org/10.1016/j.earscirev.2019.02.021>

784 Quick, A.M., Reeder, W.J., Farrell, T.B., Tonina, D., Feris, K.P., Benner, S.G., 2016. Controls
785 on nitrous oxide emissions from the hyporheic zones of streams. *Environ. Sci. Technol.*
786 50, 11491–11500. <https://doi.org/10.1021/acs.est.6b02680>

787 Raymond, P.A., Hartmann, J., Lauerwald, R., Sobek, S., McDonald, C., Hoover, M., Butman,
788 D., Striegl, R., Mayorga, E., Humborg, C., Kortelainen, P., Dürr, H., Meybeck, M., Ciais,
789 P., Guth, P., 2013. Global carbon dioxide emissions from inland waters. *Nature* 503,
790 355–359. <https://doi.org/10.1038/nature12760>

791 Reeder, W.J., Quick, A.M., Farrell, T.B., Benner, S.G., Feris, K.P., Marzadri, A., Tonina, D.,
792 2018. Hyporheic source and sink of nitrous oxide. *Water Resour. Res.* 54, 5001–5016.
793 <https://doi.org/10.1029/2018WR022564>

794 Rey-Sanchez, A.C., Morin, T.H., Stefanik, K.C., Wrighton, K., Bohrer, G., 2018. Determining
795 total emissions and environmental drivers of methane flux in a Lake Erie estuarine marsh.
796 *Ecol. Eng.* 114, 7–15. <https://doi.org/10.1016/j.ecoleng.2017.06.042>

797 Rey-Sanchez, C., Bohrer, G., Slater, J., Li, Y.-F., Grau-Andrés, R., Hao, Y., Rich, V.I., Davies,
798 G.M., 2019. The ratio of methanogens to methanotrophs and water-level dynamics drive
799 methane transfer velocity in a temperate kettle-hole peat bog. *Biogeosciences* 16, 3207–
800 3231. <https://doi.org/10.5194/bg-16-3207-2019>

801 Richey, J.E., Devol, A.H., Wofsy, S.C., Victoria, R., Riberio, M.N.G., 1988. Biogenic gases and
802 the oxidation and reduction of carbon in Amazon River and floodplain waters. *Limnol.*
803 *Oceanogr.* 33, 551–561. <https://doi.org/10.4319/lo.1988.33.4.0551>

804 Romeijn, P., Comer-Warner, S.A., Ullah, S., Hannah, D.M., Krause, S., 2019. Streambed organic
805 matter controls on carbon dioxide and methane emissions from streams. *Environ. Sci.*
806 *Technol.* 53, 2364–2374. <https://doi.org/10.1021/acs.est.8b04243>

807 Rulík, M., Čáp, L., Hlaváčová, E., 2000. Methane in the hyporheic zone of a small lowland
808 stream (Sitka, Czech Republic). *Limnologica* 30, 359–366.
809 [https://doi.org/10.1016/S0075-9511\(00\)80029-8](https://doi.org/10.1016/S0075-9511(00)80029-8)

810 Saunois, M., Bousquet, P., Poulter, B., Peregon, A., Ciais, P., Canadell, J.G., Dlugokencky, E.J.,
811 Etiope, G., Bastviken, D., Houweling, S., 2016. The global methane budget 2000–2012.
812 *Earth Syst. Sci. Data* 8, 697–751.

813 Schindler, J.E., 1998. The hyporheic zone as a source of dissolved organic carbon and carbon
814 gases to a temperate forested stream. *Biogeochemistry* 43, 157–174.

815 Segers, R., 1998. Methane production and methane consumption: a review of processes
816 underlying wetland methane fluxes. *Biogeochemistry* 41, 23–51.
817 <https://doi.org/10.1023/A:1005929032764>

818 Soued, C., del Giorgio, P.A., Maranger, R., 2015. Nitrous oxide sinks and emissions in boreal
819 aquatic networks in Québec. *Nat. Geosci.* 9, 116.

820 Stanley, E.H., Casson, N.J., Christel, S.T., Crawford, J.T., Loken, L.C., Oliver, S.K., 2016. The
821 ecology of methane in streams and rivers: patterns, controls, and global significance.
822 *Ecol. Monogr.* 86, 146–171.

823 Stegen, J.C., Fredrickson, J.K., Wilkins, M.J., Konopka, A.E., Nelson, W.C., Arntzen, E.V.,
824 Chrisler, W.B., Chu, R.K., Danczak, R.E., Fansler, S.J., Kennedy, D.W., Resch, C.T.,
825 Tfaily, M., 2016. Groundwater–surface water mixing shifts ecological assembly
826 processes and stimulates organic carbon turnover. *Nat. Commun.* 7, 11237.
827 <https://doi.org/10.1038/ncomms11237>

828 Teodoru, C.R., Nyoni, F.C., Borges, A.V., Darchambeau, F., Nyambe, I., Bouillon, S., 2015.
829 Dynamics of greenhouse gases (CO₂, CH₄, N₂O) along the Zambezi River and major
830 tributaries, and their importance in the riverine carbon budget. *Biogeosciences* 12, 2431–
831 2453. <https://doi.org/10.5194/bg-12-2431-2015>

832 Tsuruta, H., Kanda, K., Hirose, T., 1997. Nitrous oxide emission from a rice paddy field in
833 Japan. *Nutr. Cycl. Agroecosystems* 49, 51–58. <https://doi.org/10.1023/A:1009739830004>

834 Valentine, D.L., Blanton, D.C., Reeburgh, W.S., Kastner, M., 2001. Water column methane
835 oxidation adjacent to an area of active hydrate dissociation, Eel river Basin. *Geochim.
836 Cosmochim. Acta* 65, 2633–2640. [https://doi.org/10.1016/S0016-7037\(01\)00625-1](https://doi.org/10.1016/S0016-7037(01)00625-1)

837 Woessner, W.W., 2017. Chapter 8 - Hyporheic Zones, in: Hauer, F.R., Lamberti, G.A. (Eds.),
838 Methods in Stream Ecology, Volume 1 (Third Edition). Academic Press, Boston, pp.
839 129–157. <https://doi.org/10.1016/B978-0-12-416558-8.00008-1>

840 Yoon, S., Nissen, S., Park, D., Sanford, R.A., Löffler, F.E., 2016. Nitrous oxide reduction
841 kinetics distinguish bacteria harboring Clade I NosZ from those harboring Clade II NosZ.
842 Appl. Environ. Microbiol. 82, 3793–3800. <https://doi.org/10.1128/AEM.00409-16>

843 Yvon-Durocher, G., Allen, A.P., Bastviken, D., Conrad, R., Gudasz, C., St-Pierre, A., Thanh-
844 Duc, N., del Giorgio, P.A., 2014. Methane fluxes show consistent temperature
845 dependence across microbial to ecosystem scales. Nature 507, 488.

846 Zhou, T., Bao, J., Huang, M., Hou, Z., Arntzen, E., Song, X., Harding, S.F., Titzler, P.S., Ren,
847 H., Murray, C.J., Perkins, W.A., Chen, X., Stegen, J.C., Hammond, G.E., Thorne, P.D.,
848 Zachara, J.M., 2018. Riverbed hydrologic exchange dynamics in a large regulated river
849 reach. Water Resour. Res. 54, 2715–2730. <https://doi.org/10.1002/2017WR020508>

850 Zhu, C., Talbot, H.M., Wagner, T., Pan, J.M., Pancost, R.D., 2010. Intense aerobic methane
851 oxidation in the Yangtze Estuary: A record from 35-aminobacteriohopanepolyols in
852 surface sediments. Adv. Org. Geochem. 2009 41, 1056–1059.
853 <https://doi.org/10.1016/j.orggeochem.2010.03.015>

854

855

856

857

858

859

860 **Tables**

861 *Table 1. Mean water levels (m) along three beach positions at the Columbia River during*
 862 *samplings of porewater concentrations and fluxes of methane (CH_4) and N_2O under three*
 863 *different river water stages.*

Sampling	Position		
	Shallow	Intermediate	Deep
Rising water stage (porewater & fluxes)	0.46	1.00	1.44
CH_4 fluxes	0.50	1.04	1.48
N_2O fluxes	0.61	1.15	1.60
Falling water stage (porewater & fluxes)	0.78	1.32	1.76
CH_4 fluxes	0.83	1.37	1.82
N_2O fluxes	0.50	1.04	1.49
Low water stage (porewater & fluxes)	-0.28	0.26	0.70
CH_4 fluxes	0.83	1.37	1.82
N_2O fluxes	-0.81	-0.27	0.18

864

865

866

867

868

869

870

871

872

873

874

875

876

877 **List of figures**

878 *Figure 1. Experimental design. (A) Peeper array at the 3G observatory and river and*
879 *groundwater monitoring at the 300 Area, Hanford reach, Washington State. (B) Diagram*
880 *depicting the general sampling design and (C) the conventions used throughout the manuscript.*
881 **The transect marked in red in (A) denotes the transect where sediment temperatures were**
882 **measured.**

883

884 *Figure 2. Hydrological conditions during the study period (4/24 to 8/25 2018). (A) River water*
885 **levels** (dark blue), sediment temperature (red lines), and sampling periods (vertical bars with
886 different colors). (B – D) River **water levels** (dark blue) and hydraulic gradient (light blue)
887 during each **river** stage sampling, including the five preceding days of each sampling. The
888 horizontal dashed line indicates the reference elevation (sediment surface at the shallow position
889 – left axis) and the zero hydraulic gradient (right axis). Water **levels** above the horizontal line
890 represent water above the sediment surface. Hydraulic gradients above that line represent river
891 dowelling, whereas values below the line represent groundwater upwelling. At each **river** stage
892 sampling, we sampled peepers first (2 days), then methane (few hours during the next day) and
893 N_2O (few hours during the following day), as indicated by **vertical gray bars** (which are labeled
894 in (B) for clarification).

895

896 *Figure 3. (A) Integrated sediment-profile methane porewater concentrations and (B) methane*
897 *fluxes along a beach transect (plot scale) at the 3G observatory during three river water stages.*
898 *Boxes represent the 25th and 75th percentiles, the horizontal black line the median, circles mark*
899 *outliers, defined as observations that are 1.5 greater than the upper interquartile range.*

900 Whiskers extend to the furthest observation not considered **an** outlier. Letters represent
901 statistical differences calculated with non-parametric Wilcoxon paired tests for each position (α
902 $= 0.05$).

903

904 *Figure 4. Methane porewater concentrations on the sediment profile at shallow (left),*
905 *intermediate (middle), and deep (right) positions of a beach transect (plot scale) at the Columbia*
906 *River during three river water stages. Data points (circles) represent the mean concentration,*
907 *and the error bars the standard error ($n=3$). Horizontal blue areas indicate the water **level***
908 *range during the different water stages. Thick transparent color lines indicate an elevation*
909 *gradient in the peaks of methane concentrations during the rising water stage (blue) and the low*
910 *water stage (orange). The thick brown line represents the beach elevation along the gradient.*

911

912 *Figure 5. Methane conductance in the water column and sediments (A and B), and methane*
913 *conductivity (i.e., conductance per depth) in the sediments (C) along a beach transect (plot*
914 *scale) at the Columbia River during falling and low river water stages (during the rising water*
915 *stage fluxes and porewater concentrations were negligible). Boxes represent the 25th and 75th*
916 *percentiles, the horizontal black line the median and circles outliers defined as observations that*
917 *are 1.5 greater than the upper interquartile range. Whiskers extend to the furthest observation*
918 *not considered **an** outlier. Capital letters indicate **differences** between beach positions and*
919 *lowercase letters, differences between river water stages with positions.*

920

921 *Figure 6. Correlations between methane and CO₂ porewater concentrations on sediment profiles*
922 *of a beach transect (plot scale) at the Columbia River during three river water stages. Dotted*

923 lines accompanying the regression lines represent the 95% confidence intervals. The correlation
924 is stronger during the falling water stage.

925

926 *Figure 7. (A) Integrated sediment-profile methane porewater concentrations and (B) N₂O fluxes*
927 *along a beach transect (plot scale) at the Columbia River during three river water stages. Boxes*
928 *represent the 25th and 75th percentiles, the horizontal black line the median and circles outliers*
929 *defined as observations that are 1.5 greater than the upper interquartile range. Whiskers extend*
930 *to the furthest observation not considered an outlier. Letters represent statistical differences*
931 *calculated with non-parametric Wilcoxon paired tests for each position ($\alpha = 0.05$).*

932

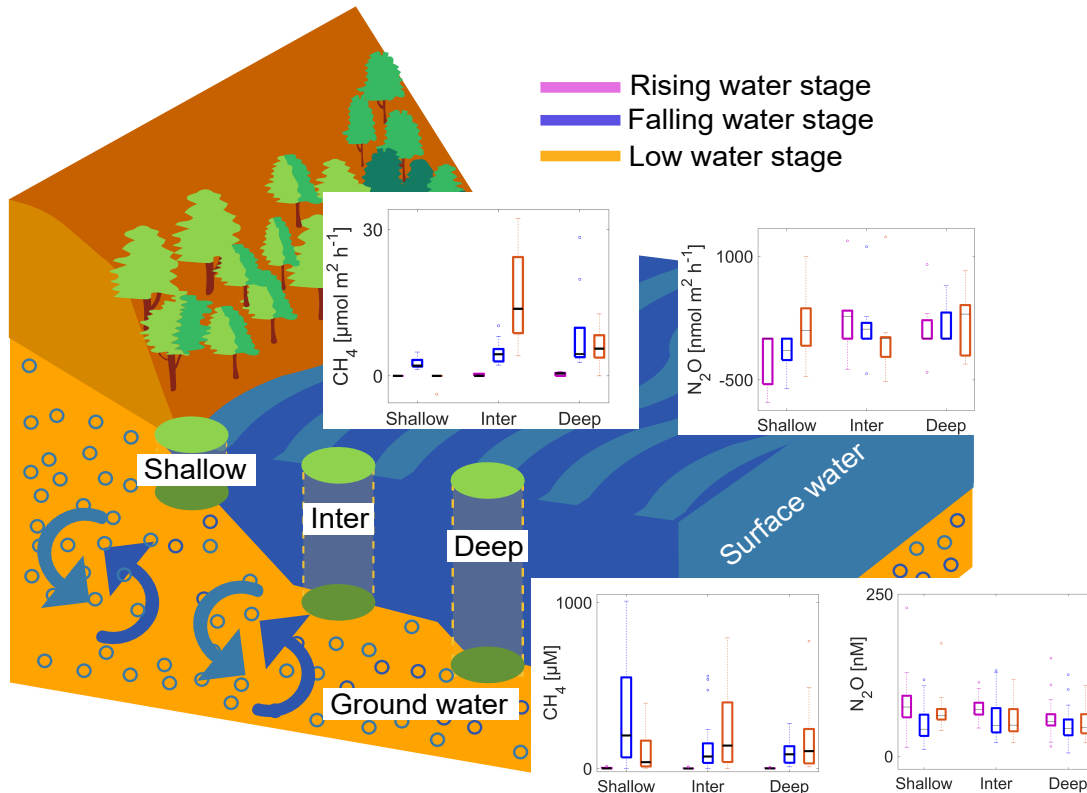
933 *Figure 8. N₂O porewater concentrations along the sediment profile at shallow (left),*
934 *intermediate (middle), and deep (right) positions of a beach transect (plot scale) at the Columbia*
935 *River during three river water stages. Data points (circles) represent the mean concentration,*
936 *and the error bars the standard error (n=3). Horizontal blue areas indicate the water level*
937 *range during the different water stages. The thick brown line represents the beach elevation*
938 *along the gradient.*

939

940 *Figure 9. Correlations between N₂O and CO₂ porewater concentrations along sediment profiles*
941 *of a beach transect (plot scale) at the Columbia River during three river water stages. Dotted*
942 *lines accompanying the regression lines represent the 95% confidence intervals. Note that the*
943 *correlation is not significant for the deep position (gray markers). The overall correlation for*
944 *data of all positions (not shown) is also significant (slope = -2.97, $r^2 = 0.065$, $p < 0.01$).*

945

*Graphical Abstract



Highlights:

A better understanding of methane and nitrous oxide emissions from rivers is needed

Porewater concentrations and fluxes were measured at three different hydrological stages

We used co-located peepers and static chambers at a beach transect in three elevations

River stage forced different gas dynamics in vertical and horizontal planes

Small-scale hydro-biogeochemical exchanges are crucial for better predictions

1 **Abstract**

2 Greenhouse gas (GHG) emissions from rivers are a critical missing component of current global
3 GHG models. Their exclusion is mainly due to a lack of in-situ measurements and a poor
4 understanding of the spatiotemporal dynamics of GHG production and emissions, which
5 prevents optimal model parametrization. We combined simultaneous observations of porewater
6 concentrations along different beach positions and depths, and surface fluxes of methane and
7 nitrous oxide at a plot scale in a large regulated river during three water stages: rising, falling,
8 and low. Our goal was to gain insights into the interactions between hydrological exchanges and
9 GHG emissions and elucidate possible hypotheses that could guide future research on the
10 mechanisms of GHG production, consumption, and transport in the hyporheic zone (HZ).
11 Results indicate that the site functioned as a net source of methane. Surface fluxes of methane
12 during river water stages at three beach positions (shallow, intermediate and deep) correlated
13 with porewater concentrations of methane. However, fluxes were significantly higher in the
14 intermediate position during the low water stage, suggesting that low residence time increased
15 methane emissions. Vertical profiles of methane peaked at different depths, indicating an
16 influence of the magnitude and direction of the hyporheic mixing during the different river water
17 stages on methane production and consumption. The site acted as either a sink or a source of
18 nitrous oxide depending on the elevation of the water column. Nitrous oxide porewater
19 concentrations peaked at the upper layers of the sediment throughout the different water stages.
20 River hydrological stages significantly influenced porewater concentrations and fluxes of GHG,
21 probably by influencing heterotrophic respiration (production and consumption processes) and
22 transport to and from the HZ. Our results highlight the importance of including dynamic

23 hydrological exchanges when studying and modeling GHG production and consumption in the
24 HZ of large rivers.

25 **Keywords:** hyporheic zone, methane conductance, porewater, methane flux, nitrous oxide flux

26

27

28

29

30

31

32

33

34

35

36

37

38

39

40

41

42

43

44

45

46 **1. Introduction**

47 Rivers and streams cover a relatively small area of the planet's terrestrial phase (0.47%).
48 Nonetheless, they play a pivotal role in greenhouse gas (GHG) emissions (Raymond et al.,
49 2013). It is estimated that they emit annually 6.6 Pg of carbon dioxide (CO₂) (Raymond et al.,
50 2013), 26.8 Tg of methane (CH₄) (Stanley et al., 2016) and 1.1 Tg of nitrous oxide (N₂O)
51 (Beaulieu et al., 2011). In other words, this is the equivalent to ~12% of CO₂ emissions from
52 fossil fuels and industry (Jackson et al., 2017), and ~5% and ~10% of global methane and N₂O
53 emissions, respectively (Beaulieu et al., 2011; Saunois et al., 2016). The disproportionate
54 contributions from rivers to GHG budgets have challenged the early assumption of rivers as
55 "passive" or "neutral" pipes in global and regional GHG budgets (Cole et al., 2007;
56 Aufdenkampe et al., 2011), placing them as active hotspots for GHG exchange.

57 Whereas the biogeochemical processes that lead to CO₂ emissions from rivers have
58 traditionally received more attention (Raymond et al., 2013; Hotchkiss et al., 2015) and are
59 relatively better represented in current models (e.g., E3SM, Golaz et al., 2019), the processes that
60 lead to methane and N₂O emissions remain poorly constrained in space and time (Bridgman et
61 al., 2013; Quick et al., 2019). Methane and N₂O emissions are low compared with those of CO₂,
62 yet on an equal mass basis, they have 45 and 270 times the potential of CO₂ to warm the
63 atmosphere over a 100-year horizon, respectively (Neubauer and Megonigal, 2015). Most of the
64 biogeochemical activity that leads to methane and N₂O production and consequent emission in
65 rivers occurs within the hyporheic zone (HZ), a transition zone in the saturated sediments
66 adjacent to the streamflow where surface water and subsurface waters are permanently mixing
67 (McClain et al., 2003; Krause et al., 2011). The mixing of downwelling oxidized surface water,
68 and upwelling of reduced subsurface water provides a unique environment of enhanced nutrient

69 and light availability, gradients of temperature and redox potentials, pH, organic matter content,
70 and microbial numbers and activity (Woessner, 2017). This environment represent
71 biogeochemical hotspots for microbial activity where aerobic and anaerobic microbial
72 metabolisms co-occur (Boulton et al., 1998). In general, the HZ is a net source of methane and
73 N₂O (Reeder et al., 2018).

74 Hydrologic exchange strongly affects the flow of organic dissolved carbon, an essential
75 microbial substrate for GHG production processes, as well as the transport of GHG themselves.
76 Methane can be produced in the anaerobic environment within the HZ from CO₂ and H₂ or
77 acetate during the degradation of organic matter (Lyu et al., 2018). Methane may also be
78 transported from the surrounding upland areas dissolved in groundwater (Jones and Mulholland,
79 1998). Once in the HZ, methane can be oxidized and transformed back into CO₂ with sufficient
80 electron acceptors, particularly oxygen, by methanotrophic microorganisms (Chistoserdova et
81 al., 2009). The remaining portion of methane that is not oxidized can be emitted via diffusion,
82 ebullition, or plant-mediated transport (Bridgham et al., 2013).

83 N₂O production in the HZ is mainly the result of four distinct processes: (1) denitrification or
84 reduction of nitrate or nitrite to dinitrogen with nitrous oxide as an intermediate, (2) by-products
85 of oxidation of ammonia to nitrate or nitrite, (3) dissimilatory reduction of nitrate to ammonia,
86 and (4) chemo-denitrification involving the abiotic reaction of nitrite with iron(II) (Quick et al.
87 2019), of which denitrification is thought as the main production pathway in lotic systems
88 (Baulch et al., 2011a; Beaulieu et al., 2011). N₂O transport from the HZ to the atmosphere occurs
89 primarily via diffusion (Baulch et al., 2011a).

90 A better understanding of the dynamics and interactions of different processes throughout the
91 HZ is needed in order to resolve the role of rivers in global GHG emissions correctly. There is a

92 need for an improved mechanistic understanding of the biogeochemical processes involved in the
93 production, consumption, and transformation of carbon and nitrogen species leading to riverine
94 GHG emissions. However, river systems are spatially complex and temporally dynamic, making
95 predictions of GHG emissions, especially challenging. The lack of observations for evaluating
96 specific parameters that describe each process often leads to simplistic representation in models,
97 and consequently, high sensitivity and uncertainty in the model results. The inclusion of sub-
98 models that can resolve transient hydrological exchanges in land-surface models is paramount to
99 more robustly represent biogeochemical processes in the terrestrial-aquatic interphases
100 (Buchkowski et al., 2017; Graham et al., 2019). With very few exceptions (e.g., Rulík et al.,
101 2000; Bednářík et al., 2015; Comer-Warner et al., 2018), field studies of GHG fluxes in rivers
102 rarely address small-scale spatial variability across the bank, and temporal variation in relation to
103 the hydrological dynamics between the groundwater and river. In addition, very few have
104 considered simultaneously methane and N₂O and how they may be linked at the site scale.

105 Here we present results from methane and N₂O porewater concentrations and chamber flux
106 measurements conducted at different river stages at a plot of the Columbia River, a large
107 regulated river. Our goal was to assess the spatio-temporal variability in porewater
108 concentrations and surface fluxes. We further utilize the results to identify the relationships
109 between HZ hydrological processes and the sources or sinks of methane and N₂O.

110

111 **2. Methods**

112 **2.1 Study site and sampling approach**

113 This study was conducted in the experimental ‘Genome to Greenhouse Gas (3G) observatory’
114 at the Columbia River on the Hanford Reach (Hanford 300 Area), Washington State, USA

115 (Figure 1). The observatory consists of an array of 3 triplicate porewater samplers (peepers)
116 deployed at a sandy beach on bank-to-river transects (6 m long) along a microtopographic
117 gradient representing three nominal beach positions: shallow, intermediate and deep (Figure 1B).
118 The sampling array encompasses a small, 11 m-long plot. The plot is located in a small cove that
119 isolates the site from the flow influences of the main river channel. Concurrent measurements of
120 methane, CO₂ and N₂O porewater concentrations and surface fluxes of methane and N₂O were
121 conducted during three distinct river stages representing the main phases of a typical
122 hydrological year at the study site, ~80 km downstream of the Priest Rapids Dam at the Hanford
123 Reach. We sampled on three occasions between 25th April and 25th August in 2018 consisting of
124 (1) a rising water stage during spring snowmelt, (2) a falling water stage during summer after the
125 annual peak in early June, and (3) a highly regulated low water stage starting late in the summer
126 that typically extends to the onset of the next spring snowmelt.

127

128 **2.2 River levels and hydraulic gradient**

129 River water and groundwater levels were recorded using pressure transducers. We conducted
130 river water measurements at the 3G observatory during August 2018 (5 min resolution) and river
131 water and groundwater measurements in a transect perpendicular to the river, 410 m downstream
132 of the 3G observatory during 2018 (15 min resolution) (Figure 1A). We generated a time series
133 for the 3G observatory during 2018 using water levels from the point of measurement
134 downstream ($r^2 = 0.99, p < 0,001$, 27 days in August), and a known discrete level at the 3G site.
135 We used as a zero-reference location for the water level the sediment surface of the shallow
136 position (Figure 1C).

137 To determine the strength of groundwater flow toward the river, we calculated the hydraulic
138 gradient (HG , m m^{-1}) between the river water and groundwater-well level as:

139
$$HG = \Delta h L^{-1} \quad (1)$$

140 Where Δh is the head difference between the river water level (m) and the groundwater level of
141 the well (m) at a given time, and L is the distance between their two points of measurement (114
142 m). Sediment temperatures (at 10 cm sediment depth) were measured at each position along one
143 transect during the study period using thermistors (marked in red in Figure 1A).

144

145 **2.3 Porewater sampling and processing**

146 Vertical profiles of methane, N_2O , and CO_2 concentration of sediment porewater were
147 determined at each gradient's position using the peepers described by MacDonald et al. (2013).
148 The peepers allowed for non-destructive consecutive sampling of the sediment profile at the
149 same depth and beach positions. The peepers feature 20 stacked cells (61.4 ml) at a 2.8 cm
150 vertical resolution. Each cell has 22.5 cm^2 windows covered with a $0.22\text{-}\mu\text{m}$ pore size
151 polyethersulfon membrane that allows water inside the cell to equilibrate with dissolved gas
152 concentrations in the sediments. Cells were fitted with two sampling ports consisting of plastic
153 tubing that allowed water extraction and refill. We used standard 4-inch PCV conduit anchored
154 to the river sediments above the peeper location with rebar to house the peeper tubing, allowing
155 for easy sampling even when water levels were high, and marking the peeper location. Peepers
156 were deployed two months before our first sampling to ensure equilibration, which usually could
157 take between 4 days and up to three weeks (MacDonald et al. 2013).

158 We sampled ten cells, starting at the top cell (at zero sediment depth) and every other after that,
159 until reaching the bottom-most cell at 50-cm sediment depth. The sampling consisted of

160 extracting 10-ml of water from the cells through one of the cell tubings while keeping the other
161 connected to a container filled with N₂ to avoid oxygen intrusion that could disturb the anaerobic
162 environment within and around the cells. After the extraction, the cell was refilled with deionized
163 water degassed with N₂. Samples were placed in 10-ml containers pre-acidified with 0.2 ml HCl
164 2M to ensure pH levels below 2.0, which prevent the post-sampling biological transformation of
165 the gases dissolved in the sample. Then, samples were refrigerated and transported to the
166 laboratory for further processing.

167

168 **2.4 Porewater concentrations**

169 Gas concentrations in porewater were determined using the gas chromatograph headspace
170 equilibration technique described by (Kampbell et al., 1989). We used a 5-ml subsample of each
171 vial to equilibrate with a 15-ml N₂ headspace. Upon equilibration, we injected 10 ml of
172 headspace into 10-ml pre-evacuated vials and analyzed them in a gas chromatograph equipped
173 with a flame ionization detector fitted with a 1.8 Poropack Q column and an electron capture Ni-
174 63 detector (Shimadzu GC-2014, Shimadzu Scientific Instruments, Kyoto, Japan). Helium (25
175 ml min⁻¹) was used as the carrier gas for methane and CO₂ analysis and ultra-pure N₂ (10 ml min⁻¹
176) was used as the carrier gas for N₂O analysis. We included methane, CO₂, and N₂O check
177 standards every 20 samples to ensure that the chromatograph maintained the calibration
178 throughout the analysis. If the deviation between the measured value and the value of the check
179 standard was greater than 10%, we recalibrated the chromatograph and re-ran the samples.

180 Molar concentrations of methane, CO₂, and N₂O (C_{molar_pore}) were calculated from the
181 measured gas concentrations as:

$$182 C_{molar_pore} = \frac{\frac{p_i}{RT} Vh + \frac{p_i}{HCP} Vl}{Vl} \quad (2)$$

183 Where p_i is the partial pressure of methane, CO₂ or N₂O, R is the universal gas constant (m³ Pa
184 mol⁻¹ K⁻¹), T is the room temperature (K), Vh is the volume of the headspace (ml), H^{cp} is
185 Henry's volatility constant (m³ Pa mol⁻¹) for methane, CO₂, and N₂O, respectively, and Vl the
186 volume of the liquid subsample used to create the headspace (ml).

187

188 **2.5 Surface flux measurements**

189 Flux measurements were conducted using non-steady-state chambers. At each sampling, we
190 conducted triplicate chamber measurements at the water surface right above the peepers when
191 they were submerged or around it when the water table was below the sediments, and the peepers
192 were surfacing. We used transparent polypropylene dome-shaped chambers (7.3×10^{-2} m²
193 surface area, 7.7×10^{-3} m³ volume), equipped with a digital thermometer to record inner
194 temperatures and a 12v fan to mix air within the chamber and polyethylene foam in the bottom
195 rim for flotation. For methane flux measurements, we used a single chamber connected to a
196 cavity ring-down spectroscopy methane analyzer (Gas Scouter G4301, Picarro, Santa Clara, CA)
197 that recirculated the air at a rate of 1L min⁻¹. The analyzer recorded methane concentrations in
198 the chamber at a 1-Hz frequency. Each chamber deployment lasted for three minutes, and
199 measurements were consecutive at each peeper location.

200 For N₂O flux measurements, the chambers included a 30-cm long, 1.6 mm ID tube for pressure
201 relief and a gray butyl rubber stopper as a sampling port as well. At each sampling, we deployed
202 three chambers simultaneously for 24-minute periods at each peeper location. Six 10-ml samples
203 were collected at 4-min frequency during each deployment, placed in pre-evacuated vials and
204 transported for chromatography analysis in the laboratory. The concentrations of the gas samples

205 were analyzed in the same chromatograph, and under the same quality control used to measure
206 N_2O concentrations in porewater.

207 Methane and N_2O chambers positioning during sampling followed an equilateral triangular
208 arrangement with two chambers positioned parallel to the shore. For methane sampling, we
209 ensured the position of the single manually during the sampling period. For the N_2O sampling,
210 we attached the chambers with polyethylene foam and then the chamber array was anchored
211 above the peeper location by surrounding the PVC conduit used to house the peeper tubing.

212

213 **2.6 Surface flux calculations**

214 For each methane chamber measurement, we fitted a 2 minute, 1-Hz time series of methane
215 concentrations, C_{HM} ($\mu\text{mol mol}^{-1}$), to the non-linear Hutchinson and Moiser one-dimension
216 diffusion model (Hutchinson and Mosier, 1981; Kutzbach et al., 2007; Pedersen et al., 2010):

217
$$C_{HM} = C_s + (C_0 - C_s) e^{-kt} \quad (3)$$

218 Where C_0 is the pre-deployment concentration of methane ($\mu\text{mol mol}^{-1}$), C_s is the constant
219 source or sink concentration ($\mu\text{mol mol}^{-1}$), and k is a curve shape parameter (h^{-1}). C_0 , C_s , and k
220 are parameters determined by fitting the observed gas concentrations in the chamber over time, t
221 (h). We then calculated the flux of methane (F_{CH_4} , $\mu\text{mol m}^{-2} \text{h}^{-1}$) at the water or sediment
222 surface as:

223
$$F_{\text{CH}_4} = k (C_0 - C_s) \frac{PV}{RTA}, \quad (4)$$

224 where P (Pa) is the atmospheric pressure, measured with a digital barometer at the site; V the
225 volume of the chamber (m^3), R the universal gas constant ($\text{m}^3 \text{Pa mol}^{-1} \text{K}^{-1}$), T the temperature
226 inside the chamber (K), and A the surface area of the chamber (m^2).

227 For N₂O chamber measurements, we calculated the molar concentrations of N₂O (C_{molar_Ch} ,
228 $\mu\text{mol m}^{-3}$), in each sample using a modified gas law, following the procedure described by
229 (Holland et al., 1999):

$$230 \quad C_{molar_Ch} = \frac{Cv \cdot P}{R \cdot T} \quad (5)$$

231 where Cv is the concentration (nmol mol⁻¹) of N₂O in the sample, P is atmospheric pressure (Pa),
232 R is the universal gas constant (m³ Pa mol⁻¹ K⁻¹), and T is the air temperature (K) of the chamber.
233 Then, the accumulation rate, C_{rate} (nmol m⁻³ h⁻¹), was determined using the slope of the linear
234 regression fitted to the time points (t , h) collected for each chamber after rejecting outliers in the
235 regressions following the procedure described by (Rey-Sanchez et al., 2018):

$$236 \quad C_{molar_Ch}(t) = C_{molar_Ch}(0) + C_{rate} \times t \quad (6)$$

237 and with the C_{rate} , we calculated the flux rate (F_{N_2O} , nmol m⁻² h⁻¹) as:

$$238 \quad F_{N_2O} = \frac{V \cdot C_{rate}}{A}, \quad (7)$$

239 where V is the volume of the chamber (m³), and A the area of the water/sediment surface covered
240 by the chamber (m²).

241 We used the coefficient of determination (r^2) of the fit between the model (linear in the case of
242 N₂O or non-linear in the case of CH₄) and concentration observations in the chamber and a
243 quality control criterion. Flux measurements with $r^2 < 0.8$ were considered of poor quality and
244 were discarded from our analyses to avoid error. Out of the 81 flux measurements for methane
245 and N₂O, 28 for methane and 29 for N₂O, were discarded due to this criterion of poor
246 observation quality.

247

248 **2.7 Methane conductance and conductivity**

249 We used the following general expression to solve for the bulk transfer velocity of methane, or
250 methane conductance (K), at the different beach positions and river water stages assuming that
251 methane is not being produced in the water column:

252 $F_CH_{4d} = K (C_{sed} - C_{air} P H^{cp})$, for $F > 0$ (8)

253 where F_CH_{4d} is methane the flux measured at each flux chamber but in units of $\mu\text{mol m}^{-2} \text{d}^{-1}$ to
254 correspond with the unit convention of conductance. C_{sed} ($\mu\text{mol m}^{-3}$) is the concentration of
255 methane in the sediments porewater at a given depth and C_{air} ($\mu\text{mol m}^{-3}$) is the aqueous
256 equivalent of the concentration of methane in the air, calculated as the product of the initial
257 concentration in the chamber ($\mu\text{mol mol}^{-1}$), P the atmospheric pressure at the moment of
258 sampling (Pa), and H^{cp} the Henry's solubility constant for methane ($\text{mol Pa}^{-1} \text{m}^{-3}$). The initial
259 concentration in the chamber, representing the concentration before enclosure, was calculated as
260 the average of the first five measurements of each chamber run.

261 We assume that the overall conductance, K , is the combined result of two transport processes –
262 K_w , the conductance to methane transport in the water from the soil surface to the air, and K_s , the
263 conductance for methane diffusion/transport in the soil from the peak concentration depth to the
264 soil surface. Adding the resistance to methane flux in a sequential process, we obtain the term
265 for the combined conductance K :

266
$$K = \frac{K_w K_s}{K_w + K_s}$$
 (9)

267 We followed the approach by Bastviken et al., (2004) to independently determine the
268 conductance to methane in the water column K_w for each flux chamber, by solving the equation:

269 $F_CH_4 = K_w (C_{ss} - C_{air})$ (10)

270 where C_{ss} ($\mu\text{mol m}^{-3}$) is the concentration of methane at the surface of the sediments assumed
271 as the concentration in the first peeper cell.

272 Substituting eq 9 into eq 8, and using the porewater concentration at the depth of peak
273 concentration in the soil, C_{ps} we obtain an equation for K_s :

274
$$F_CH_{4d} = \frac{K_w K_s}{K_w + K_s} (C_{ps} - C_{air}) \quad (11)$$

275 Equation 11 can be solved using the value we obtained for K_w , from equation (10).

276 Then we calculated the conductivity (i.e., conductance per unit length) to methane
277 transport/diffusion in the soil (k_s) as:

278
$$k_s = \frac{K_s}{D_p} \quad (12)$$

279 Where D_p (m) is the depth at which concentration peaks in the sediment profile.

280

281 **2.8 Data analysis**

282 We processed data, fit models for flux calculations, and conducted regression tests of
283 porewater concentrations using MATLAB ® 2018b. We used JMP Pro 14.0.0 for all other
284 statistical tests. All the statistical tests were conducted at a 0.05 significance level.

285 We used Spearman rank correlation to infer the significance of the relationship between
286 average porewater concentrations in the sediment profile and fluxes. We tested the significance
287 of the difference of fluxes and porewater concentrations between water stages for each beach
288 position using paired nonparametric comparisons with the Wilcoxon method. For testing the
289 significance of the differences of water and sediment conductance and sediment conductivity
290 between water stages and within beach positions, we used an ordinal logistic model with the
291 conductances or the conductivity as the response variable, position as a fixed effect and water
292 stage nested by position.

293

294 **2.9 Data availability**

295 All porewater concentrations and fluxes data will be made available through ESS-DiVE
296 (<https://ess-dive.lbl.gov/>), DOI pending. Additional ancillary data for the Hanford site is
297 available through the Phoenix – PNNL Environmental Information Exchange
298 (<https://www.hanford.gov/page.cfm/PHOENIX>).

299

300 **3. Results and discussion**

301 **3.1 Water level and sediment temperature**

302 The water level at the shallow bank position was low (near the sediment surface) during the
303 first part of the year until April when water levels started rising after the spring thaw (Figure
304 2A). The maximum water levels (> 3 m above the reference elevation, set at the shallow peeper
305 position) were observed in mid-May and were followed by a steadily falling water stage until the
306 beginning of July and remained low during the rest of the year. A brief rising limb in the second
307 half of June was driven by dam water release during the falling stage and coincided with the
308 moment we conducted our sampling. Water levels below the reference elevation were observed
309 during the low stages before the rising stage and after the falling stage. The water level during
310 the low water stage was more variable than during previous stages. The operation of the dam
311 upstream can cause up to 0.5 m variations in water levels within a daily period (Zhou et al.,
312 2018).

313 Positive hydraulic gradients (downwelling) occurred through the hydrological year, including
314 the time during the rising and falling water stages (Figure 2B, C). However, reversals to the
315 negative hydraulic gradient (upwelling) were frequent during the low water stage. Hydraulic
316 gradient reversal represents groundwater upwelling or moments when the river receives water

317 from the aquifer. Reversals were also frequent on the days preceding the low water stage
318 sampling (Figure 2D).

319 Sediment temperature increased throughout the sampling period. In general, mean positions'
320 temperatures had a 10 °C increase between the beginning of the study during the rising water
321 stage in April and the study end in August (Figure 2). Temperatures were similar throughout the
322 different beach positions during the rising and falling stages but differed and were more variable
323 at the low water stage when the water level dropped below the soil surface at the reference level.

324

325 **3.2 Methane porewater concentration and fluxes respond similarly to river stage variation**

326 Methane flux to the atmosphere is the result of a balance between methane production and
327 consumption and is influenced by the relative importance of the transport pathways, including
328 diffusion, bubbling, and plant transport (Bridgman et al. 2013). At our site, we regard diffusion
329 as the main transport pathway. We did not observe evidence of bubbling in our peeper chamber
330 measurements (i.e., sudden spikes in methane concentration in the time series during chamber
331 deployments). We also neglected the influence of plant transport because macrophyte vegetation
332 was not present near the sampling locations, although a negligible fraction could have been
333 transported from the shallow bank position through the vascular system of some shrubs present
334 on the riverbank. Methane porewater concentrations and fluxes at the 3G site were negligible
335 during the rising water stage when the sediment temperatures were low (~10 °C, Figure 3A),
336 which is not surprising given the high sensitivity of methane production to temperature (Yvon-
337 Durocher et al., 2014). Methane flux was low at the shallow position during the low water stage
338 as well, when the water level was below the sediment surface (Table 1). Despite relatively higher
339 concentrations in the sediment profile (Figure 3B), the water level dropdown during the low

340 water stage may have resulted in unsaturated or oxygenated sediments and as a result, a
341 predominantly aerobic environment that would have increased methane oxidation above the
342 water table in the sediment column (Segers, 1998). Indeed, the porewater concentration profile at
343 the shallow position during the low water stage showed very low concentrations throughout the
344 sediment above the water table (Figure 4), consistent with increased methane oxidation coupled
345 to aerobic respiration (Conrad and Rothfuss, 1991) or low methane production due to
346 thermodynamic exclusion (Bethke et al., 2011).

347 Both methane production and consumption can co-occur in sediments (Le Mer and Roger,
348 2001) since methanogenic and methanotrophic bacteria can be correlated in terms of population
349 in sediments subject to flooding (Joulian et al., 1997) and the ratio between methanogens to
350 methanotrophs is correlated to methane transfer velocity (Rey-Sanchez et al., 2019). Bednářík et
351 al. (2015) demonstrated that benthic methane fluxes are correlated with porewater
352 concentrations, suggesting that differences between porewater concentrations and surface
353 methane fluxes might be due to the activity of methane-oxidizing bacteria in the upper sediment
354 layers (Oremland and Culbertson, 1992) or the water column (Matoušů et al., 2017). Although
355 we did not systematically measure dissolved oxygen in the sediment-water interface and the
356 water column during our samplings, we conducted a series of surveys for dissolved oxygen
357 levels before sampling. These indicated that both the water column and the porewater at the
358 water-sediment interface were consistently supersaturated, offering optimal conditions for
359 biological methane oxidation. In deeper systems, such as estuaries and reservoirs, methane
360 fluxes are greater at low water levels because of reduced storage turnover times, which is the
361 time methane remains in the water column after being produced in the sediments (Valentine et
362 al., 2001; Zhu et al., 2010; Lei et al., 2019). Lessened turnover times, reduce the time for

363 potential oxidation while methane diffuses through the water column. Methane oxidation rate in
364 the water column of rivers has been correlated with the concentration of dissolved methane in the
365 water and with water temperature (Matoušů et al., 2018), which are proxies for the substrate and
366 the enzymatic activity of methanotrophic microorganisms. Therefore, we hypothesize that the
367 effect of storage-turnover time on methane oxidation will be effective in rivers, including near-
368 bank shallow waters as well. Future studies coupling methane fluxes, and oxidation rates with
369 simultaneous measurements of methane concentrations in the sediment and water column could
370 help test this hypothesis.

371 During the falling and low water stages when sediment temperatures were more favorable for
372 methane production, river level had a dissimilar effect on porewater concentrations and fluxes
373 across positions, although in general, methane fluxes were correlated (Spearman's $\rho = 0.62, p <$
374 0.001) and followed the dynamics of the integrated sediment-profile porewater concentrations.
375 Methane porewater concentration and fluxes decreased at the shallow position after the water
376 level transition from the falling to the low water stage, while porewater concentration and fluxes
377 remained similar at the deep position. In contrast, at the intermediate position, methane fluxes
378 increased at the low stage, when the water levels were also low, while the median porewater
379 concentration increased as well, though not at a significant level.

380 Low or near-zero fluxes accompanied by decreasing methane concentrations towards the
381 surface of the sediments in the shallow position strongly indicate the activity of methanotrophs
382 actively reducing methane emissions to the atmosphere in the upper region of the sediment
383 profile in the shallow position during the low water stage (Figure 4). However, the activity of
384 methanotrophs in the upper layers of the soil profile was not evident at the intermediate or deep
385 positions (that maintained water above the sediment surface). Even during the low water stage of

386 the intermediate position, the peak in methane concentrations occurred well below the sediment
387 elevation. It is possible that reduced downwelling of electron acceptors and oxygen during low
388 water stages not only stimulated heterotrophic production of methanogenic substrates but also
389 limited dissolved oxygen that is toxic to methanogens and reduced aerobic methanotrophic
390 respiration. However, without specific measurements of oxidation rates at our site, it is hard to
391 pinpoint the specific cause of the variability of methane fluxes across the different beach
392 positions and river water stages.

393 Different apparent conductance to methane transport through the water column between falling
394 and low water stages suggests that methane oxidation may occur at different rates depending on
395 the water levels (Figure 5A). Because we did not account for oxidation during transport in the
396 water column, our observations of higher apparent conductance to methane transport may be the
397 outcome of lower oxidation. Differences in conductance to methane transport through the water
398 column were evident in the intermediate position, with larger conductance during the low water
399 stage. In the sediment profile, conductance to methane was not different between falling and low
400 water stages. Nonetheless, there were differences in the apparent conductance to methane in the
401 sediments among beach positions (Figure 5B), suggesting that there may be a significant spatial
402 variation in oxidation rates at the plot scale.

403

404 **3.3 Methane concentrations in porewater peak along an elevation gradient**

405 Similar to surface fluxes, methane concentrations in the sediment profile are the result of a
406 balance between methane production, consumption, and transport to and from the sediment zone.
407 Previous studies at the Hanford Reach in similar sites to ours have shown that hydrological
408 mixing stimulates heterotrophic respiration and organic carbon turnover (Stegen et al., 2016).

409 Under anaerobic conditions, heterotrophic respiration at the HZ of organic matter would
410 stimulate methane production by producing favored substrates and depleting electron acceptors
411 (Schindler, 1998; Romeijn et al., 2019), whereas under aerobic conditions methane oxidation
412 would be favored (Conrad and Rothfuss, 1991). Complementarily, methane may be imported in
413 the upwelling groundwater as well. Inputs of methane dissolved in groundwater have been
414 observed at low order streams in peat-dominated watersheds (Hope et al. 2001), headwater
415 streams (Jones and Mulholland, 1998), streams in agricultural dominated landscapes (Comer-
416 Warner et al., 2019) and other riverine settings including the Willamette River, the main
417 tributary of the Columbia River (Anthony et al., 2012).

418 The observed methane porewater concentrations profile in the sediment showed distinct peaks
419 that varied among bank positions following the sediment surface elevation gradient during the
420 falling and low water stages (Figure 4). During the falling water stage, concentrations at the
421 shallow positions peaked at the lower sediment layers (relative sediment depth – RSD: -25 to -40
422 cm), while at the intermediate position, concentrations peaked at the upper sediment layers (top
423 20 cm from the sediment surface, RSD: -50 to -70 cm). During the low water stage,
424 concentrations peaked at the lowest depths at the shallow position (around RSD: -50 cm), mid-
425 to-lower depths from the sediment surface at intermediate position (RSD: -80 to -105 cm), and
426 upper sediment layers at the deep position (RSD: -100 to -110 cm). Overall the peaks in methane
427 concentration were observed at upper sediment layers during the falling water stage when the site
428 remained permanently inundated (thick blue line in Figure 4), and at lower sediment layers
429 during the low water stage when the water level was fluctuating around the reference elevation
430 (thick orange line in Figure 4).

431 The peaks may have resulted from a combination of heterotrophic respiration and imports
432 through groundwater into the HZ from the nearby upland area. Methane and CO₂ porewater
433 concentrations were significantly correlated (Figure 6). Based on the low concentrations of
434 acetate measured in similar sites along the Hanford Reach, with only 1/50 samples being above
435 the detection limit (>78 µM), and uncertainty of methyl compound identity and potential
436 utilization (Hou et al., 2017), we infer that the prevailing mode of methanogenesis was
437 hydrogenotrophic, requiring hydrogen and CO₂. However, we acknowledge that this correlation
438 is a function of overall microbial activity, rather than the result of the direct use of CO₂ for
439 methanogenesis alone (Moore and Dalva, 1997; Comer-Warner et al., 2019). Interestingly, we
440 found that the slope of the regression between methane and CO₂ porewater concentrations varied
441 during the three water stages and was larger during the falling water stage when the river
442 downwelling was stronger than during the low water stage when downwelling diminished and
443 groundwater upwelling was more frequent (Figure 6). The difference in the strength of microbial
444 activity between falling water and low water stages support findings by previous studies at
445 adjacent sites along the Hanford Reach that showed a shift in microbial communities as labile
446 organic carbon stimulates heterotrophic respiration during river downwelling periods (Stegen et
447 al. 2016). As water drops and the influence of groundwater upwelling increases, heterotrophic
448 processes of carbon cycling and decomposition succumb to autotrophic processes (Graham et al.,
449 2017).

450 On the other hand, as groundwater upwelling becomes more frequent during the low water
451 stage and heterotrophic respiration recede (and presumably the production of methane), imports
452 of dissolved methane in the groundwater increase, maintaining similar porewater concentrations
453 than during the falling water stage. This hypothesis is supported by the increase in conductivity

454 of methane in the sediments we observed at the deep position (Figure 5C), which indicates that
455 during groundwater upwelling, methane transport is faster. We hypothesize that while microbial
456 methane production is reduced when the water level drops and groundwater upwelling is
457 increased, methane concentrations and fluxes are maintained because allochthonous methane is
458 “pushed out” from the surrounding upland soils and river sediments.

459 We propose that the observed peaks in methane concentration through the sediment profile
460 during the falling water stage occurred at predominantly anaerobic zones, where hydrological
461 mixing of downwelling surface water from the river and upwelling groundwater from the aquifer
462 is enhanced. The predominant zone of methane production moved vertically downward within
463 the HZ as the river transitioned from falling to low water stage, coinciding with a shift from river
464 water dominated to groundwater-dominated mixing ratios.

465

466 **3.4 Nitrous oxide porewater concentrations and fluxes have different dynamics across river
467 water stages**

468 Unlike methane, N_2O porewater concentrations in the sediment profile and fluxes to the
469 atmosphere did not follow similar patterns throughout the river water stages (Spearman’s $\rho =$
470 $0.29, p = 0.14$). N_2O porewater concentrations were higher during the rising water stage than
471 during the falling water stage in all the three beach positions and during the low water stage at
472 the intermediate position (Figure 7A). Instead, N_2O fluxes increased from the rising to the low
473 water stage at the shallow position, while remained similar at the intermediate and deep positions
474 during the three water stages (Figure 7B).

475 The decoupling between the observed N_2O porewater concentrations in the sediments and the
476 fluxes is not surprising. N_2O production in large rivers might occur primarily at the water column

477 in microsites within suspended particles. There is significant evidence of substantial N₂O
478 production via denitrification in pelagic zones of estuaries (Barnes and Owens, 1999; de Wilde
479 and de Bie, 2000). Beaulieu et al. (2010) presented evidence of a similar pattern at a large river,
480 with N₂O production rates in the water column doubling that of the sediments, which could help
481 explain the lack of correlation between the porewater concentrations and fluxes. Marzadri et al.
482 (2014) and Marzadri et al. (2017) explained that in lotic systems there is a shift in the
483 predominant zones of N₂O production from the hyporheic-benthic zone in streams to the benthic-
484 water column zone in rivers as the system gains size, due mainly to the increase in suspended
485 particle loads.

486 Notably, we observed negative fluxes throughout the different river water stages and in all
487 positions, which is consistent with high rates of N₂O consumption at either the sediments or the
488 water column. Our plot acted primarily as a sink at the shallow position while the sediments
489 were fully saturated, and the water level was above the sediment surface and on the intermediate
490 position during the low water stage when the water level at this position was low as well (Figure
491 7A). N₂O is often produced as an intermediate species of microbially mediated denitrification, or
492 a byproduct of nitrification or reduction of ammonia to nitrate (Quick et al., 2019). Dissolved
493 organic carbon in the HZ plays a critical role in fueling nitrification under aerobic conditions
494 (Graham et al., 2016; Graham et al., 2017) and in addition, may lead to low oxygen and nitrate
495 conditions that ultimately favor N₂O consumption (Soued et al., 2015). Low oxygen conditions
496 may result from the low flow as well (Baulch et al., 2011b), which prevailed in the 3G
497 observatory, especially at lower water levels, explaining the dominant sinking functioning of the
498 shallow and intermediate positions partially. It may also be possible that atmospheric nitrous
499 oxide consumption occurred in the water column in the absence of other denitrification

500 processes, which has been demonstrated only for a few model microorganisms and ecosystems
501 (Jones et al., 2014; Yoon et al., 2016).

502 A more robust understanding of the nexus (or lack thereof) of the spatial heterogeneity and
503 dynamics of N_2O porewater concentrations and fluxes must build upon the synergistic effects of
504 the seasonal hydrological exchanges, inorganic nitrogen availability, and the activity of the
505 microbial community involved in cycling nitrous oxide at the HZ and the water column. For
506 instance, the nitrification and denitrification functional potential of microbial communities in the
507 HZ of the Hanford Reach (and possibly many other lotic systems) are linked with the ratio of
508 groundwater to surface water, likely due to the input of N in the groundwater (Nelson et al.,
509 2019). However, it is still not clear if or how the dynamics of groundwater N or other
510 environmental drivers are affecting the N-cycling functional potential in the water column and
511 overall how N_2O is produced and consumed in the sediment-water column continuum.

512

513 **3.5 Nitrous oxide concentrations peak at the sediment/water table interface**

514 Mathematical and conceptual models propose that N_2O production at the HZ is maximized
515 along flowlines representing intermediate travel times of downwelling surface water, which are
516 usually few cm below the sediment surface (Reeder et al., 2018; Quick et al., 2016). At
517 shallower depths, at the surface of the sediments (i.e., shortest travel times), nitrate is not
518 transformed, whereas at deeper depths (i.e., longest travel times), denitrification is completed
519 and N_2 is the predominantly released gas. The N_2O porewater concentrations we observed at the
520 3G are consistent with the modeling predictions, showing increased concentrations at the
521 proximity of the sediment/water table interface (~ up to 15 cm) (Figure 8).

522 We found significant negative correlations between N₂O and CO₂ porewater concentrations for
523 pooled data from the three water stages and the shallow and intermediate beach positions (Figure
524 9). We cannot discern whether the correlation is the result of N₂O production or consumption.
525 Partial denitrification, nitrate reduction to N₂O, is coupled to carbon oxidation to CO₂ and
526 therefore, we would expect a positive correlation (Tsuruta et al., 1997). Therefore, N₂O
527 production appeared decoupled from denitrification and more closely tied to other processes. The
528 negative correlations could be explained by the release of N₂O during nitrification coupled to
529 CO₂ assimilation or heterotrophic microorganisms utilizing N₂O as a terminal electron acceptor
530 (Hink et al., 2017; Lycus et al., 2018). This may help explain the negative correlation between
531 N₂O and CO₂ porewater concentrations, which were also seen in observations of other riverine
532 settings (Richey et al., 1988; Teodoru et al., 2015). However, we do not rule out that
533 simultaneous processes of production and consumption are co-occurring and that their relative
534 importance change as the river water level transitions and substrates, environmental conditions,
535 and the relative diversity and abundance of N-Cycling populations vary (Nelson et al., 2019).
536 The decoupling between N₂O and CO₂ may be explained as well at some degree by lateral
537 transport of N₂O dissolved in groundwater (Clough et al., 2006).
538 It is noteworthy that the strength of the correlation between N₂O and CO₂ porewater was
539 dictated by beach positions, indicating that different processes are occurring between locations.
540 Weaker negative correlations at the shallow position may be explained by contributions of both
541 nitrification byproducts and denitrification, N₂O consumption as an electron acceptor in the
542 absence of other denitrification processes, and labile carbon oxidation, or the increased
543 contributions from heterotrophic denitrifications. Coupling inorganic nitrogen concentrations and

544 organic carbon concentration measurements should help unveil the prevalence of these processes
545 and their influence in the observed variability between beach positions.

546

547 **4. Conclusions and outlook**

548 Hyporheic zones of rivers and streams are important hotspots of greenhouse gas emissions. The
549 interaction of river stage and biogeochemical processes govern the production, consumption, and
550 flux dynamics. This interaction of the governing factors results in high heterogeneity at the small
551 scale (m to cm) in horizontal and vertical planes. At the plot scale, methane porewater
552 concentrations have a marked vertical temporal dynamic with concentrations peaking at different
553 depths depending on the influence of the magnitude and direction of hyporheic mixing. Methane
554 fluxes followed the dynamics of porewater concentrations throughout the river water stages but
555 highlighted the potential influence of oxidation in the resulting fluxes. Hence the need for sub-
556 models capable of representing the potential effects of hydrological exchanges on methane
557 oxidation in the HZ. The effect was pronounced for the intermediate position where methane
558 fluxes increased (and the conductance to methane in the water column) from the falling water
559 stage to the low water stage. In turn, N₂O porewater concentrations rely more on the permanent
560 mixing at the HZ and occur at the upper layers just below the sediment surface. Contrary to
561 methane, fluxes of N₂O were not correlated to porewater concentrations and were reduced at low
562 water elevations, possibly because of the release of N₂O as a byproduct of aerobic nitrification or
563 the use of N₂O as an alternative terminal electron acceptor to oxygen for microbial respiration at
564 the sediment-water interface (Khalil et al., 2004; Jones et al., 2014). Overall results indicated that
565 the plot functioned as a net source of methane and could function as either a sink or source for
566 N₂O depending on both the season and position within the riparian zone. Therefore, identifying

567 the potential nexus between N_2O production and consumption and concurrency at the HZ
568 represents a critical challenge for better representation of the N_2O dynamic in biogeochemical
569 models.

570 Here we presented snapshots of detailed vertical profiles and surface fluxes of methane and
571 N_2O porewater concentrations through the different typical hydrological stages of a large-
572 regulated river. As our results indicate, river stages and consequent groundwater mixing, drive
573 the dynamics of porewater concentrations and fluxes of methane and N_2O on a seasonal scale.
574 However, coupling hydrological dynamics with methane and N_2O concentrations and fluxes at
575 small scales and parametrizing the governing processes will require longer-term and more
576 frequent assessments, especially the inclusion of measurements at a small temporal scale (days-
577 hours). Such a scale is of particular interest to assess the effects of large intra-daily water level
578 oscillations, which are characteristic of regulated rivers, on the GHG production and
579 consumption processes. This daily/sub-daily measurement scale could help to elucidate the
580 effects of preceding environmental conditions set by previous water levels (including microbial
581 populations, temperature, nutrient availability and transformations, and redox conditions) on the
582 production and consumption of GHGs. In non-regulated rivers, we would expect a similar
583 control of seasonal groundwater mixing than the one we observe here. However, in contrast to
584 regulated rivers, the shorter-term effects of preceding environmental conditions would likely be
585 less dramatic given the lower water intra-daily fluctuations.

586 Finally, as our results indicate, GHG concentration and fluxes can be significantly different
587 across small horizontal (6 m W \times 11 m L) and vertical (0.5 m) spatial scales. Moreover, water
588 level fluctuation has a significant effect on the functioning of the HZ as a sink or source of
589 methane and N_2O . The coupling of hydrology and GHGs emissions at small scales will,

590 therefore, be essential to help parametrize and calibrate predictive models in large rivers like the
591 Columbia River and other rivers and streams as well. More importantly, it is a necessary task to
592 test hypotheses discerning the microbial processes explaining the spatiotemporal heterogeneity
593 of methane and N₂O at the HZ.

594

595 **Acknowledgments**

596 This project was sponsored by the Subsurface Biogeochemical Research (SBR) program (DE-
597 SC0018170).

598

599

600

601

602

603

604

605

606

607

608

609

610

611

612

613 **References**

614 Anthony, S.E., Prahl, F.G., Peterson, T.D., 2012. Methane dynamics in the Willamette River,
615 Oregon. *Limnol. Oceanogr.* 57, 1517–1530. <https://doi.org/10.4319/lo.2012.57.5.1517>

616 Aufdenkampe, A.K., Mayorga, E., Raymond, P.A., Melack, J.M., Doney, S.C., Alin, S.R., Aalto,
617 R.E., Yoo, K., 2011. Riverine coupling of biogeochemical cycles between land, oceans,
618 and atmosphere. *Front. Ecol. Environ.* 9, 53–60. <https://doi.org/10.1890/100014>

619 Barnes, J., Owens, N.J.P., 1999. Denitrification and nitrous oxide concentrations in the Humber
620 Estuary, UK, and adjacent coastal zones. *Mar. Pollut. Bull.* 37, 247–260.
621 [https://doi.org/10.1016/S0025-326X\(99\)00079-X](https://doi.org/10.1016/S0025-326X(99)00079-X)

622 Bastviken, D., Cole, J., Pace, M., Tranvik, L., 2004. Methane emissions from lakes: Dependence
623 of lake characteristics, two regional assessments, and a global estimate. *Glob.*
624 *Biogeochem. Cycles* 18, GB4009. <https://doi.org/10.1029/2004GB002238>

625 Baulch, H.M., Dillon, P.J., Maranger, R., Schiff, S.L., 2011a. Diffusive and ebullitive transport
626 of methane and nitrous oxide from streams: Are bubble-mediated fluxes important? *J.*
627 *Geophys. Res. Biogeosciences* 116. <https://doi.org/10.1029/2011JG001656>

628 Baulch, H.M., Schiff, S.L., Maranger, R., Dillon, P.J., 2011b. Nitrogen enrichment and the
629 emission of nitrous oxide from streams. *Glob. Biogeochem. Cycles* 25, GB4013.
630 <https://doi.org/10.1029/2011GB004047>

631 Beaulieu, J.J., Shuster, W.D., Rebholz, J.A., 2010. Nitrous oxide emissions from a large,
632 impounded river: the Ohio River. *Environ. Sci. Technol.* 44, 7527–7533.
633 <https://doi.org/10.1021/es1016735>

634 Beaulieu, J.J., Tank, J.L., Hamilton, S.K., Wollheim, W.M., Hall, R.O., Mulholland, P.J.,
635 Peterson, B.J., Ashkenas, L.R., Cooper, L.W., Dahm, C.N., Dodds, W.K., Grimm, N.B.,

636 Johnson, S.L., McDowell, W.H., Poole, G.C., Valett, H.M., Arango, C.P., Bernot, M.J.,
637 Burgin, A.J., Crenshaw, C.L., Helton, A.M., Johnson, L.T., O'Brien, J.M., Potter, J.D.,
638 Sheibley, R.W., Sobota, D.J., Thomas, S.M., 2011. Nitrous oxide emission from
639 denitrification in stream and river networks. *Proc. Natl. Acad. Sci.* 108, 214.
640 <https://doi.org/10.1073/pnas.1011464108>

641 Bednářík, A., Čáp, L., Maier, V., Rulík, M., 2015. Contribution of methane benthic and
642 atmospheric fluxes of an experimental area (Sitka Stream). *CLEAN – Soil Air Water* 43,
643 1136–1142. <https://doi.org/10.1002/clen.201300982>

644 Bethke, C.M., Sanford, R.A., Kirk, M.F., Jin, Q., Flynn, T.M., 2011. The thermodynamic ladder
645 in geomicrobiology. *Am. J. Sci.* 311, 183–210. <https://doi.org/10.2475/03.2011.01>

646 Boulton, A.J., Findlay, S., Marmonier, P., Stanley, E.H., Valett, H.M., 1998. The functional
647 significance of the hyporheic zone in streams and rivers. *Annu. Rev. Ecol. Syst.* 29, 59–
648 81. <https://doi.org/10.1146/annurev.ecolsys.29.1.59>

649 Bridgham, S.D., Cadillo-Quiroz, H., Keller, J.K., Zhuang, Q., 2013. Methane emissions from
650 wetlands: biogeochemical, microbial, and modeling perspectives from local to global
651 scales. *Glob. Change Biol.* 19, 1325–1346. <https://doi.org/10.1111/gcb.12131>

652 Buchkowski, R.W., Bradford, M.A., Grandy, A.S., Schmitz, O.J., Wieder, W.R., 2017. Applying
653 population and community ecology theory to advance understanding of belowground
654 biogeochemistry. *Ecol. Lett.* 20, 231–245. <https://doi.org/10.1111/ele.12712>

655 Chistoserdova, L., Kalyuzhnaya, M.G., Lidstrom, M.E., 2009. The expanding world of
656 methylotrophic metabolism. *Annu. Rev. Microbiol.* 63, 477–499.
657 <https://doi.org/10.1146/annurev.micro.091208.073600>

658 Clough, T.J., Bertram, J.E., Sherlock, R.R., Leonard, R.L., Nowicki, B.L., 2006. Comparison of
659 measured and EF5-r-derived N₂O fluxes from a spring-fed river. *Global Change Biology*
660 12, 477–488. <https://doi.org/10.1111/j.1365-2486.2005.01092.x>

661 Cole, J., Prairie, Y., Caraco, N., McDowell, W., Tranvik, L., Striegl, R., Duarte, C., Kortelainen,
662 P., Downing, J., Middelburg, J., Melack, J., 2007. Plumbing the global carbon cycle:
663 integrating inland waters into the terrestrial carbon budget. *Ecosystems* 10, 172–185.

664 Comer-Warner, S.A., Gooddy, D.C., Ullah, S., Glover, L., Percival, A., Kettridge, N., Krause, S.,
665 2019. Seasonal variability of sediment controls of carbon cycling in an agricultural
666 stream. *Sci. Total Environ.* 688, 732–741. <https://doi.org/10.1016/j.scitotenv.2019.06.317>

667 Comer-Warner, S.A., Romeijn, P., Gooddy, D.C., Ullah, S., Kettridge, N., Marchant, B.,
668 Hannah, D.M., Krause, S., 2018. Thermal sensitivity of CO₂ and CH₄ emissions varies
669 with streambed sediment properties. *Nat. Commun.* 9, 2803.
670 <https://doi.org/10.1038/s41467-018-04756-x>

671 Conrad, R., Rothfuss, F., 1991. Methane oxidation in the soil surface layer of a flooded rice field
672 and the effect of ammonium. *Biol. Fertil. Soils* 12, 28–32.
673 <https://doi.org/10.1007/BF00369384>

674 de Wilde, H.P.J., de Bie, M.J.M., 2000. Nitrous oxide in the Schelde estuary: production by
675 nitrification and emission to the atmosphere. *Mar. Chem.* 69, 203–216.
676 [https://doi.org/10.1016/S0304-4203\(99\)00106-1](https://doi.org/10.1016/S0304-4203(99)00106-1)

677 Golaz, J., Caldwell, P.M., Van Roekel, L.P., Petersen, M.R., Tang, Q., Wolfe, J.D., Abeshu, G.,
678 Anantharaj, V., Asay- Davis, X.S., Bader, D.C., 2019. The DOE E3SM coupled model
679 version 1: overview and evaluation at standard resolution. *J. Adv. Model. Earth Syst.* 11,
680 2089–2129.

681 Graham, E.B., Crump, A.R., Resch, C.T., Fansler, S., Arntzen, E., Kennedy, D.W., Fredrickson,
682 J.K., Stegen, J.C., 2017. Deterministic influences exceed dispersal effects on
683 hydrologically-connected microbiomes. *Environ. Microbiol.* 19, 1552–1567.
684 <https://doi.org/10.1111/1462-2920.13720>

685 Graham, E.B., Crump, A.R., Resch, C.T., Fansler, S., Arntzen, E., Kennedy, D.W., Fredrickson,
686 J.K., Stegen, J.C., 2016. Coupling spatiotemporal community assembly processes to
687 changes in microbial metabolism. *Front. Microbiol.* 7, 1949.
688 <https://doi.org/10.3389/fmicb.2016.01949>

689 Graham, E.B., Stegen, J.C., Huang, M., Chen, X., Scheibe, T.D., 2019. Subsurface
690 biogeochemistry is a missing link between ecology and hydrology in dam-impacted river
691 corridors. *Sci. Total Environ.* 657, 435–445.
692 <https://doi.org/10.1016/j.scitotenv.2018.11.414>

693 Hink, L., Lycus, P., Gubry-Rangin, C., Frostegård, Å., Nicol, G.W., Prosser, J.I., Bakken, L.R.,
694 2017. Kinetics of NH₃-oxidation, NO-turnover, N₂O-production and electron flow during
695 oxygen depletion in model bacterial and archaeal ammonia oxidisers. *Environmental
696 Microbiology* 19, 4882–4896. <https://doi.org/10.1111/1462-2920.13914>

697 Holland, E.A., Robertson, G.P., Greenberg, J., Groffman, P.M., Boone, R.D., Grosz, J.R., 1999.
698 Soil CO₂, N₂O and CH₄ Exchange, in: *Standard Soil Methods for Long-Term Ecological
699 Research*. Oxford University Press, New York, pp. 185–201.

700 Hotchkiss, E.R., Hall Jr, R.O., Sponseller, R.A., Butman, D., Klaminder, J., Laudon, H., Rosvall,
701 M., Karlsson, J., 2015. Sources of and processes controlling CO₂ emissions change with
702 the size of streams and rivers. *Nat. Geosci.* 8, 696.

703 Hou, Z., Nelson, W.C., Stegen, J.C., Murray, C.J., Arntzen, E., Crump, A.R., Kennedy, D.W.,
704 Perkins, M.C., Scheibe, T.D., Fredrickson, J.K., Zachara, J.M., 2017. Geochemical and
705 microbial community attributes in relation to hyporheic zone geological facies. *Sci. Rep.*
706 7, 12006. <https://doi.org/10.1038/s41598-017-12275-w>

707 Hutchinson, G., Mosier, A., 1981. Improved soil cover method for field measurement of nitrous
708 oxide fluxes 1. *Soil Sci. Soc. Am. J.* 45, 311–316.

709 Jackson, R.B., Le Quéré, C., Andrew, R.M., Canadell, J.G., Peters, G.P., Roy, J., Wu, L., 2017.
710 Warning signs for stabilizing global CO₂ emissions. *Environ. Res. Lett.* 12, 110202.
711 <https://doi.org/10.1088/1748-9326/aa9662>

712 Jones, C.M., Spor, A., Brennan, F.P., Breuil, M.-C., Bru, D., Lemanceau, P., Griffiths, B.,
713 Hallin, S., Philippot, L., 2014. Recently identified microbial guild mediates soil N₂O sink
714 capacity. *Nat. Clim. Change* 4, 801.

715 Jones, J.B., Mulholland, P.J., 1998. Influence of drainage basin topography and elevation on
716 carbon dioxide and methane supersaturation of stream water. *Biogeochemistry* 40, 57–72.

717 Joulian, C., Escoffier, S., Le Mer, J., Neue, H., Roger, P.-A., 1997. Populations and potential
718 activities of methanogens and methanotrophs in rice fields: relations with soil properties.
719 *Eur. J. Soil Biol.* 33, 105–116.

720 Kampbell, D.H., Wilson, J.T., Vandegrift, S.A., 1989. Dissolved oxygen and methane in water
721 by a GC headspace equilibration technique. *Int. J. Environ. Anal. Chem.* 36, 249–257.
722 <https://doi.org/10.1080/03067318908026878>

723 Khalil, K., Mary, B., Renault, P., 2004. Nitrous oxide production by nitrification and
724 denitrification in soil aggregates as affected by O₂ concentration. *Soil Biology and
725 Biochemistry* 36, 687–699. <https://doi.org/10.1016/j.soilbio.2004.01.004>

726 Krause, S., Hannah, D.M., Fleckenstein, J.H., Heppell, C.M., Kaeser, D., Pickup, R., Pinay, G.,

727 Robertson, A.L., Wood, P.J., 2011. Inter-disciplinary perspectives on processes in the

728 hyporheic zone. *Ecohydrology* 4, 481–499. <https://doi.org/10.1002/eco.176>

729 Kutzbach, L., Scneider, J., Sachs, T., Giebels, M., Nykänen, H., Shurpali, N.J., Martikainen, P.J.,

730 Alm, J., Wilmking, M., 2007. CO₂ flux determination by closed-chamber methods can be

731 seriously biased by inappropriate application of linear regression. *Biogeosciences* 4,

732 1005–1025.

733 Le Mer, J., Roger, P., 2001. Production, oxidation, emission and consumption of methane by

734 soils: a review. *Eur. J. Soil Biol.* 37, 25–50. [https://doi.org/10.1016/S1164-5563\(01\)01067-6](https://doi.org/10.1016/S1164-5563(01)01067-6)

735

736 Lei, D., Liu, J., Zhang, J., Lorke, A., Xiao, S., Wang, Y., Wang, W., Li, Y., 2019. Methane

737 oxidation in the water column of Xiangxi Bay, Three Gorges Reservoir. *CLEAN – Soil*

738 *Air Water* 47, 1800516. <https://doi.org/10.1002/clen.201800516>

739 Lycus, P., Soriano-Laguna, M.J., Kjos, M., Richardson, D.J., Gates, A.J., Milligan, D.A.,

740 Frostegård, Å., Bergaust, L., Bakken, L.R., 2018. A bet-hedging strategy for denitrifying

741 bacteria curtails their release of N₂O. *Proc. Natl. Acad. Sci.* 115, 11820.

742 <https://doi.org/10.1073/pnas.1805000115>

743 Lyu, Z., Shao, N., Akinyemi, T., Whitman, W.B., 2018. Methanogenesis. *Curr. Biol.* 28, R727–

744 R732. <https://doi.org/10.1016/j.cub.2018.05.021>

745

746 MacDonald, L.H., Paull, J.S., Jaffé, P.R., 2013. Enhanced semipermanent dialysis samplers for

747 long-term environmental monitoring in saturated sediments. *Environ. Monit. Assess.* 185,

748 3613–3624. <https://doi.org/10.1007/s10661-012-2813-8>

749 Marzadri, A., Dee, M.M., Tonina, D., Bellin, A., Tank, J.L., 2017. Role of surface and
750 subsurface processes in scaling N₂O emissions along riverine networks. *Proc. Natl. Acad.*
751 *Sci.* 114, 4330. <https://doi.org/10.1073/pnas.1617454114>

752 Marzadri, A., Tonina, D., Bellin, A., Tank, J.L., 2014. A hydrologic model demonstrates nitrous
753 oxide emissions depend on streambed morphology. *Geophys. Res. Lett.* 41, 5484–5491.
754 <https://doi.org/10.1002/2014GL060732>

755 Matoušů, A., Osudar, R., Šimek, K., Bussmann, I., 2017. Methane distribution and methane
756 oxidation in the water column of the Elbe estuary, Germany. *Aquat. Sci.* 79, 443–458.
757 <https://doi.org/10.1007/s00027-016-0509-9>

758 Matoušů, A., Rulík, M., Tušer, M., Bednářík, A., Šimek, K., Bussmann, I., 2018. Methane
759 dynamics in a large river: a case study of the Elbe River. *Aquat. Sci.* 81, 12.
760 <https://doi.org/10.1007/s00027-018-0609-9>

761 McClain, M.E., Boyer, E.W., Dent, C.L., Gergel, S.E., Grimm, N.B., Groffman, P.M., Hart,
762 S.C., Harvey, J.W., Johnston, C.A., Mayorga, E., McDowell, W.H., Pinay, G., 2003.
763 Biogeochemical hot spots and hot moments at the interface of terrestrial and aquatic
764 ecosystems. *Ecosystems* 6, 301–312. <https://doi.org/10.1007/s10021-003-0161-9>

765 Moore, T.R., Dalva, M., 1997. Methane and carbon dioxide exchange potentials of peat soils in
766 aerobic and anaerobic laboratory incubations. *Soil Biol. Biochem.* 29, 1157–1164.
767 [https://doi.org/10.1016/S0038-0717\(97\)00037-0](https://doi.org/10.1016/S0038-0717(97)00037-0)

768 Nelson, W.C., Graham, E.B., Crump, A.R., Fansler, S.J., Arntzen, E.V., Kennedy, D.W., Stegen,
769 J.C., 2019. Temporal dynamics of nitrogen cycle gene diversity in a hyporheic
770 microbiome. *bioRxiv* 722785. <https://doi.org/10.1101/722785>

771 Neubauer, ScottC., Megonigal, J.P., 2015. Moving beyond global warming potentials to quantify
772 the climatic role of ecosystems. *Ecosystems* 18, 1000–1013.
773 <https://doi.org/10.1007/s10021-015-9879-4>

774 Oremland, R.S., Culbertson, C.W., 1992. Importance of methane-oxidizing bacteria in the
775 methane budget as revealed by the use of a specific inhibitor. *Nature* 356, 421–423.
776 <https://doi.org/10.1038/356421a0>

777 Pedersen, A.R., Petersen, S.O., Schelde, K., 2010. A comprehensive approach to soil-atmosphere
778 trace-gas flux estimation with static chambers. *Eur. J. Soil Sci.* 61, 888–902.
779 <https://doi.org/10.1111/j.1365-2389.2010.01291.x>

780 Quick, A.M., Reeder, W.J., Farrell, T.B., Tonina, D., Feris, K.P., Benner, S.G., 2019. Nitrous
781 oxide from streams and rivers: a review of primary biogeochemical pathways and
782 environmental variables. *Earth-Sci. Rev.* 191, 224–262.
783 <https://doi.org/10.1016/j.earscirev.2019.02.021>

784 Quick, A.M., Reeder, W.J., Farrell, T.B., Tonina, D., Feris, K.P., Benner, S.G., 2016. Controls
785 on nitrous oxide emissions from the hyporheic zones of streams. *Environ. Sci. Technol.*
786 50, 11491–11500. <https://doi.org/10.1021/acs.est.6b02680>

787 Raymond, P.A., Hartmann, J., Lauerwald, R., Sobek, S., McDonald, C., Hoover, M., Butman,
788 D., Striegl, R., Mayorga, E., Humborg, C., Kortelainen, P., Dürr, H., Meybeck, M., Ciais,
789 P., Guth, P., 2013. Global carbon dioxide emissions from inland waters. *Nature* 503,
790 355–359. <https://doi.org/10.1038/nature12760>

791 Reeder, W.J., Quick, A.M., Farrell, T.B., Benner, S.G., Feris, K.P., Marzadri, A., Tonina, D.,
792 2018. Hyporheic source and sink of nitrous oxide. *Water Resour. Res.* 54, 5001–5016.
793 <https://doi.org/10.1029/2018WR022564>

794 Rey-Sanchez, A.C., Morin, T.H., Stefanik, K.C., Wrighton, K., Bohrer, G., 2018. Determining
795 total emissions and environmental drivers of methane flux in a Lake Erie estuarine marsh.
796 *Ecol. Eng.* 114, 7–15. <https://doi.org/10.1016/j.ecoleng.2017.06.042>

797 Rey-Sanchez, C., Bohrer, G., Slater, J., Li, Y.-F., Grau-Andrés, R., Hao, Y., Rich, V.I., Davies,
798 G.M., 2019. The ratio of methanogens to methanotrophs and water-level dynamics drive
799 methane transfer velocity in a temperate kettle-hole peat bog. *Biogeosciences* 16, 3207–
800 3231. <https://doi.org/10.5194/bg-16-3207-2019>

801 Richey, J.E., Devol, A.H., Wofsy, S.C., Victoria, R., Riberio, M.N.G., 1988. Biogenic gases and
802 the oxidation and reduction of carbon in Amazon River and floodplain waters. *Limnol.*
803 *Oceanogr.* 33, 551–561. <https://doi.org/10.4319/lo.1988.33.4.0551>

804 Romeijn, P., Comer-Warner, S.A., Ullah, S., Hannah, D.M., Krause, S., 2019. Streambed organic
805 matter controls on carbon dioxide and methane emissions from streams. *Environ. Sci.*
806 *Technol.* 53, 2364–2374. <https://doi.org/10.1021/acs.est.8b04243>

807 Rulík, M., Čáp, L., Hlaváčová, E., 2000. Methane in the hyporheic zone of a small lowland
808 stream (Sitka, Czech Republic). *Limnologica* 30, 359–366.
809 [https://doi.org/10.1016/S0075-9511\(00\)80029-8](https://doi.org/10.1016/S0075-9511(00)80029-8)

810 Saunois, M., Bousquet, P., Poulter, B., Peregon, A., Ciais, P., Canadell, J.G., Dlugokencky, E.J.,
811 Etiope, G., Bastviken, D., Houweling, S., 2016. The global methane budget 2000–2012.
812 *Earth Syst. Sci. Data* 8, 697–751.

813 Schindler, J.E., 1998. The hyporheic zone as a source of dissolved organic carbon and carbon
814 gases to a temperate forested stream. *Biogeochemistry* 43, 157–174.

815 Segers, R., 1998. Methane production and methane consumption: a review of processes
816 underlying wetland methane fluxes. *Biogeochemistry* 41, 23–51.
817 <https://doi.org/10.1023/A:1005929032764>

818 Soued, C., del Giorgio, P.A., Maranger, R., 2015. Nitrous oxide sinks and emissions in boreal
819 aquatic networks in Québec. *Nat. Geosci.* 9, 116.

820 Stanley, E.H., Casson, N.J., Christel, S.T., Crawford, J.T., Loken, L.C., Oliver, S.K., 2016. The
821 ecology of methane in streams and rivers: patterns, controls, and global significance.
822 *Ecol. Monogr.* 86, 146–171.

823 Stegen, J.C., Fredrickson, J.K., Wilkins, M.J., Konopka, A.E., Nelson, W.C., Arntzen, E.V.,
824 Chrisler, W.B., Chu, R.K., Danczak, R.E., Fansler, S.J., Kennedy, D.W., Resch, C.T.,
825 Tfaily, M., 2016. Groundwater–surface water mixing shifts ecological assembly
826 processes and stimulates organic carbon turnover. *Nat. Commun.* 7, 11237.
827 <https://doi.org/10.1038/ncomms11237>

828 Teodoru, C.R., Nyoni, F.C., Borges, A.V., Darchambeau, F., Nyambe, I., Bouillon, S., 2015.
829 Dynamics of greenhouse gases (CO₂, CH₄, N₂O) along the Zambezi River and major
830 tributaries, and their importance in the riverine carbon budget. *Biogeosciences* 12, 2431–
831 2453. <https://doi.org/10.5194/bg-12-2431-2015>

832 Tsuruta, H., Kanda, K., Hirose, T., 1997. Nitrous oxide emission from a rice paddy field in
833 Japan. *Nutr. Cycl. Agroecosystems* 49, 51–58. <https://doi.org/10.1023/A:1009739830004>

834 Valentine, D.L., Blanton, D.C., Reeburgh, W.S., Kastner, M., 2001. Water column methane
835 oxidation adjacent to an area of active hydrate dissociation, Eel river Basin. *Geochim.
836 Cosmochim. Acta* 65, 2633–2640. [https://doi.org/10.1016/S0016-7037\(01\)00625-1](https://doi.org/10.1016/S0016-7037(01)00625-1)

837 Woessner, W.W., 2017. Chapter 8 - Hyporheic Zones, in: Hauer, F.R., Lamberti, G.A. (Eds.),
838 Methods in Stream Ecology, Volume 1 (Third Edition). Academic Press, Boston, pp.
839 129–157. <https://doi.org/10.1016/B978-0-12-416558-8.00008-1>

840 Yoon, S., Nissen, S., Park, D., Sanford, R.A., Löffler, F.E., 2016. Nitrous oxide reduction
841 kinetics distinguish bacteria harboring Clade I NosZ from those harboring Clade II NosZ.
842 Appl. Environ. Microbiol. 82, 3793–3800. <https://doi.org/10.1128/AEM.00409-16>

843 Yvon-Durocher, G., Allen, A.P., Bastviken, D., Conrad, R., Gudasz, C., St-Pierre, A., Thanh-
844 Duc, N., del Giorgio, P.A., 2014. Methane fluxes show consistent temperature
845 dependence across microbial to ecosystem scales. Nature 507, 488.

846 Zhou, T., Bao, J., Huang, M., Hou, Z., Arntzen, E., Song, X., Harding, S.F., Titzler, P.S., Ren,
847 H., Murray, C.J., Perkins, W.A., Chen, X., Stegen, J.C., Hammond, G.E., Thorne, P.D.,
848 Zachara, J.M., 2018. Riverbed hydrologic exchange dynamics in a large regulated river
849 reach. Water Resour. Res. 54, 2715–2730. <https://doi.org/10.1002/2017WR020508>

850 Zhu, C., Talbot, H.M., Wagner, T., Pan, J.M., Pancost, R.D., 2010. Intense aerobic methane
851 oxidation in the Yangtze Estuary: A record from 35-aminobacteriohopanepolyols in
852 surface sediments. Adv. Org. Geochem. 2009 41, 1056–1059.
853 <https://doi.org/10.1016/j.orggeochem.2010.03.015>

854

855

856

857

858

859

860 **Tables**

861 *Table 1. Mean water levels (m) along three beach positions at the Columbia River during*
 862 *samplings of porewater concentrations and fluxes of methane (CH_4) and N_2O under three*
 863 *different river water stages.*

Sampling	Position		
	Shallow	Intermediate	Deep
Rising water stage (porewater & fluxes)	0.46	1.00	1.44
CH_4 fluxes	0.50	1.04	1.48
N_2O fluxes	0.61	1.15	1.60
Falling water stage (porewater & fluxes)	0.78	1.32	1.76
CH_4 fluxes	0.83	1.37	1.82
N_2O fluxes	0.50	1.04	1.49
Low water stage (porewater & fluxes)	-0.28	0.26	0.70
CH_4 fluxes	0.83	1.37	1.82
N_2O fluxes	-0.81	-0.27	0.18

864

865

866

867

868

869

870

871

872

873

874

875

876

877 **List of figures**

878 *Figure 1. Experimental design. (A) Peeper array at the 3G observatory and river and*
879 *groundwater monitoring at the 300 Area, Hanford reach, Washington State. (B) Diagram*
880 *depicting the general sampling design and (C) the conventions used throughout the manuscript.*
881 *The transect marked in red in (A) denotes the transect where sediment temperatures were*
882 *measured.*

883

884 *Figure 2. Hydrological conditions during the study period (4/24 to 8/25 2018). (A) River water*
885 *levels (dark blue), sediment temperature (red lines), and sampling periods (vertical bars with*
886 *different colors). (B – D) River water levels (dark blue) and hydraulic gradient (light blue)*
887 *during each river stage sampling, including the five preceding days of each sampling. The*
888 *horizontal dashed line indicates the reference elevation (sediment surface at the shallow position*
889 *– left axis) and the zero hydraulic gradient (right axis). Water levels above the horizontal line*
890 *represent water above the sediment surface. Hydraulic gradients above that line represent river*
891 *dowelling, whereas values below the line represent groundwater upwelling. At each river stage*
892 *sampling, we sampled peepers first (2 days), then methane (few hours during the next day) and*
893 *N_2O (few hours during the following day), as indicated by vertical gray bars (which are labeled*
894 *in (B) for clarification).*

895

896 *Figure 3. (A) Integrated sediment-profile methane porewater concentrations and (B) methane*
897 *fluxes along a beach transect (plot scale) at the 3G observatory during three river water stages.*
898 *Boxes represent the 25th and 75th percentiles, the horizontal black line the median, circles mark*
899 *outliers, defined as observations that are 1.5 greater than the upper interquartile range.*

900 Whiskers extend to the furthest observation not considered an outlier. Letters represent
901 statistical differences calculated with non-parametric Wilcoxon paired tests for each position (α
902 $= 0.05$).

903

904 *Figure 4. Methane porewater concentrations on the sediment profile at shallow (left),*
905 *intermediate (middle), and deep (right) positions of a beach transect (plot scale) at the Columbia*
906 *River during three river water stages. Data points (circles) represent the mean concentration,*
907 *and the error bars the standard error ($n=3$). Horizontal blue areas indicate the water level*
908 *range during the different water stages. Thick transparent color lines indicate an elevation*
909 *gradient in the peaks of methane concentrations during the rising water stage (blue) and the low*
910 *water stage (orange). The thick brown line represents the beach elevation along the gradient.*

911

912 *Figure 5. Methane conductance in the water column and sediments (A and B), and methane*
913 *conductivity (i.e., conductance per depth) in the sediments (C) along a beach transect (plot*
914 *scale) at the Columbia River during falling and low river water stages (during the rising water*
915 *stage fluxes and porewater concentrations were negligible). Boxes represent the 25th and 75th*
916 *percentiles, the horizontal black line the median and circles outliers defined as observations that*
917 *are 1.5 greater than the upper interquartile range. Whiskers extend to the furthest observation*
918 *not considered an outlier. Capital letters indicate differences between beach positions and*
919 *lowercase letters, differences between river water stages with positions.*

920

921 *Figure 6. Correlations between methane and CO₂ porewater concentrations on sediment profiles*
922 *of a beach transect (plot scale) at the Columbia River during three river water stages. Dotted*

923 lines accompanying the regression lines represent the 95% confidence intervals. The correlation
924 is stronger during the falling water stage.

925

926 *Figure 7. (A) Integrated sediment-profile methane porewater concentrations and (B) N₂O fluxes*
927 *along a beach transect (plot scale) at the Columbia River during three river water stages. Boxes*
928 *represent the 25th and 75th percentiles, the horizontal black line the median and circles outliers*
929 *defined as observations that are 1.5 greater than the upper interquartile range. Whiskers extend*
930 *to the furthest observation not considered an outlier. Letters represent statistical differences*
931 *calculated with non-parametric Wilcoxon paired tests for each position ($\alpha = 0.05$).*

932

933 *Figure 8. N₂O porewater concentrations along the sediment profile at shallow (left),*
934 *intermediate (middle), and deep (right) positions of a beach transect (plot scale) at the Columbia*
935 *River during three river water stages. Data points (circles) represent the mean concentration,*
936 *and the error bars the standard error (n=3). Horizontal blue areas indicate the water level*
937 *range during the different water stages. The thick brown line represents the beach elevation*
938 *along the gradient.*

939

940 *Figure 9. Correlations between N₂O and CO₂ porewater concentrations along sediment profiles*
941 *of a beach transect (plot scale) at the Columbia River during three river water stages. Dotted*
942 *lines accompanying the regression lines represent the 95% confidence intervals. Note that the*
943 *correlation is not significant for the deep position (gray markers). The overall correlation for*
944 *data of all positions (not shown) is also significant (slope = -2.97, $r^2 = 0.065$, $p < 0.01$).*

945

Table 1[Click here to download Table: Table1.docx](#)

Table 1. Mean water levels (m) along three beach positions at the Columbia River during samplings of porewater concentrations and fluxes of methane (CH_4) and N_2O under three different river water stages.

Sampling	Position		
	Shallow	Intermediate	Deep
Rising water stage (porewater & fluxes)	0.46	1.00	1.44
CH_4 fluxes	0.50	1.04	1.48
N_2O fluxes	0.61	1.15	1.60
Falling water stage (porewater & fluxes)	0.78	1.32	1.76
CH_4 fluxes	0.83	1.37	1.82
N_2O fluxes	0.50	1.04	1.49
Low water stage (porewater & fluxes)	-0.28	0.26	0.70
CH_4 fluxes	0.83	1.37	1.82
N_2O fluxes	-0.81	-0.27	0.18

Figure 1

[Click here to download Figure: Fig1.eps](#)

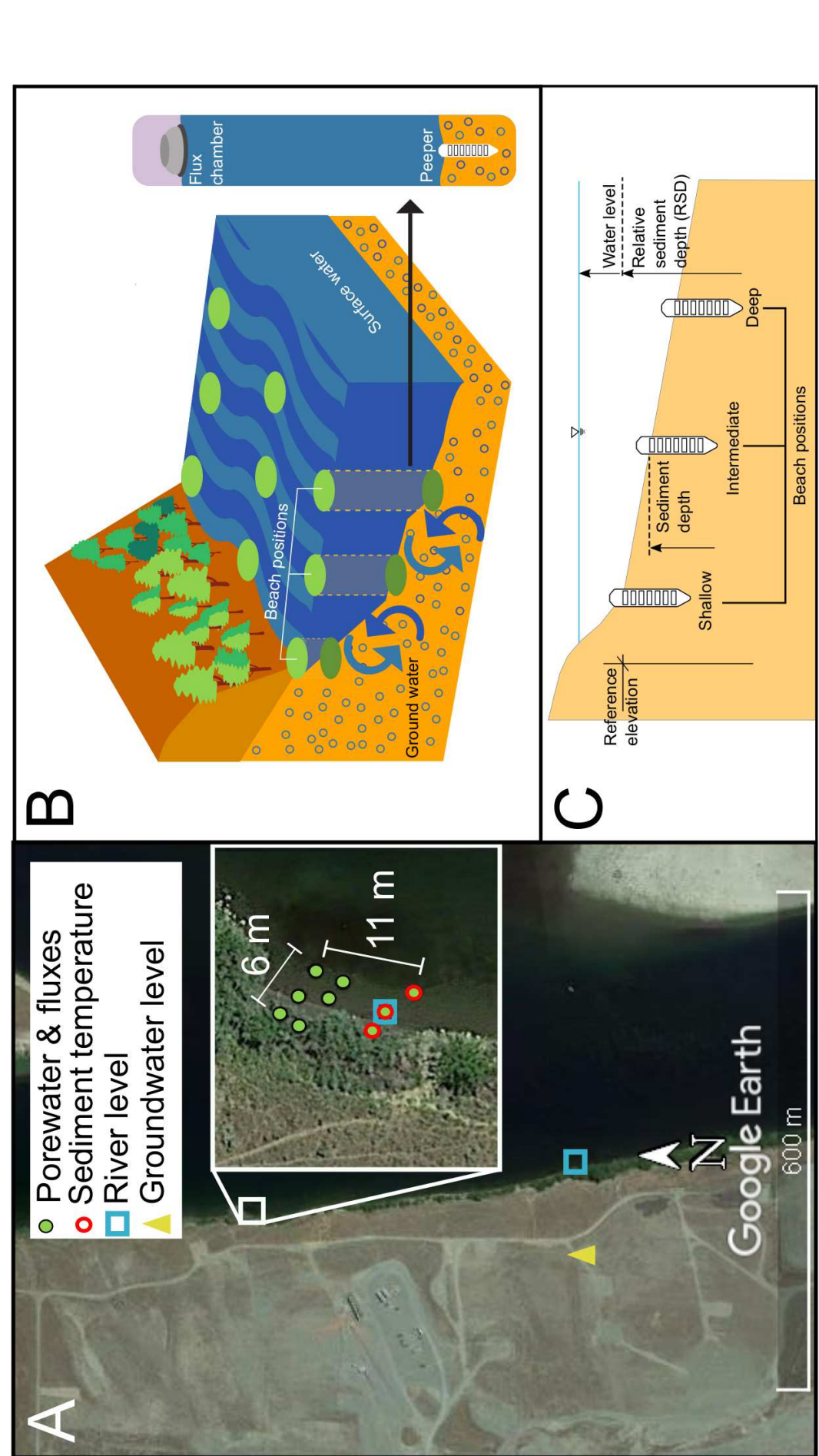
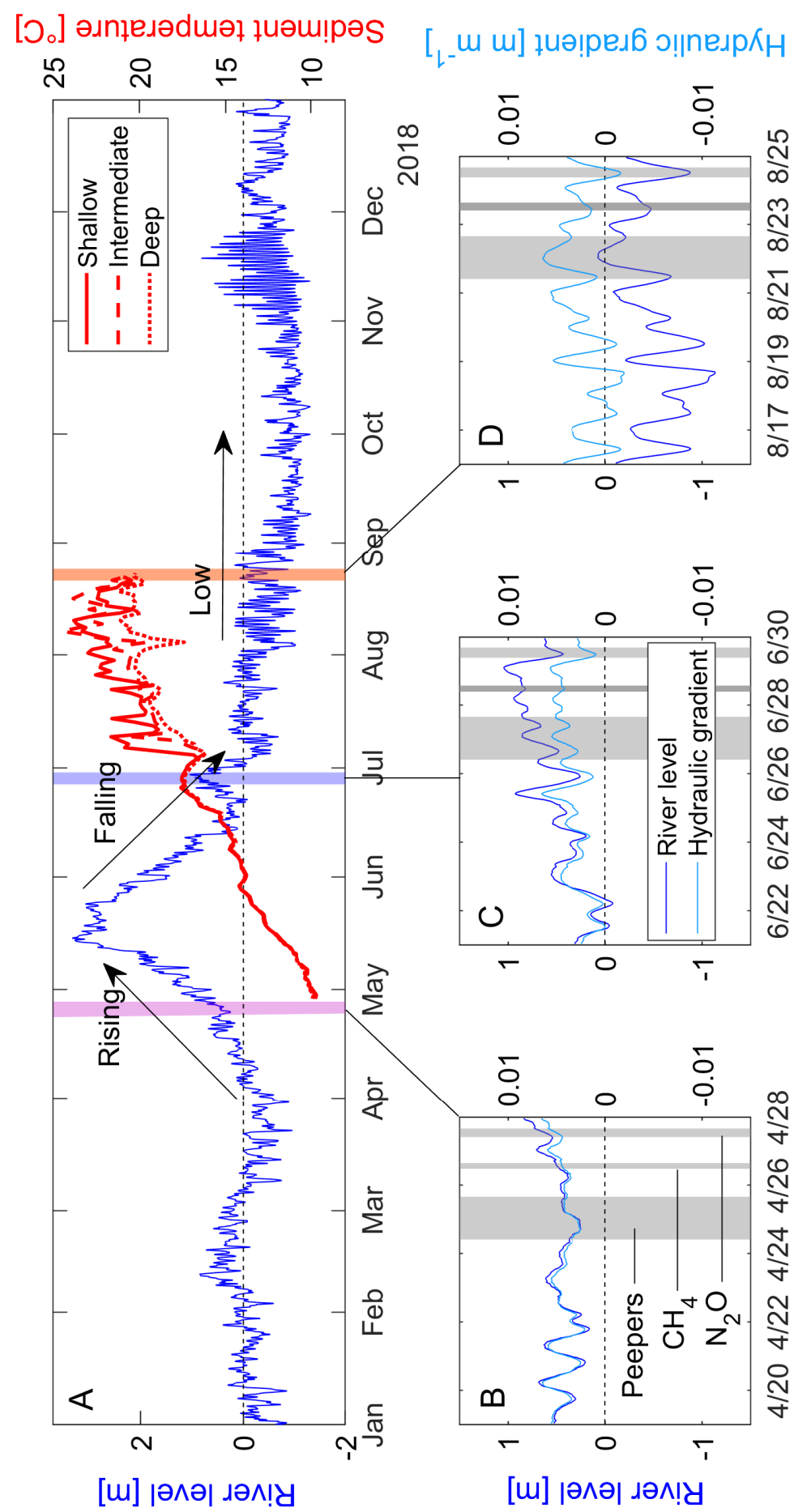


Figure 2[Click here to download Figure: Fig 2.eps](#)

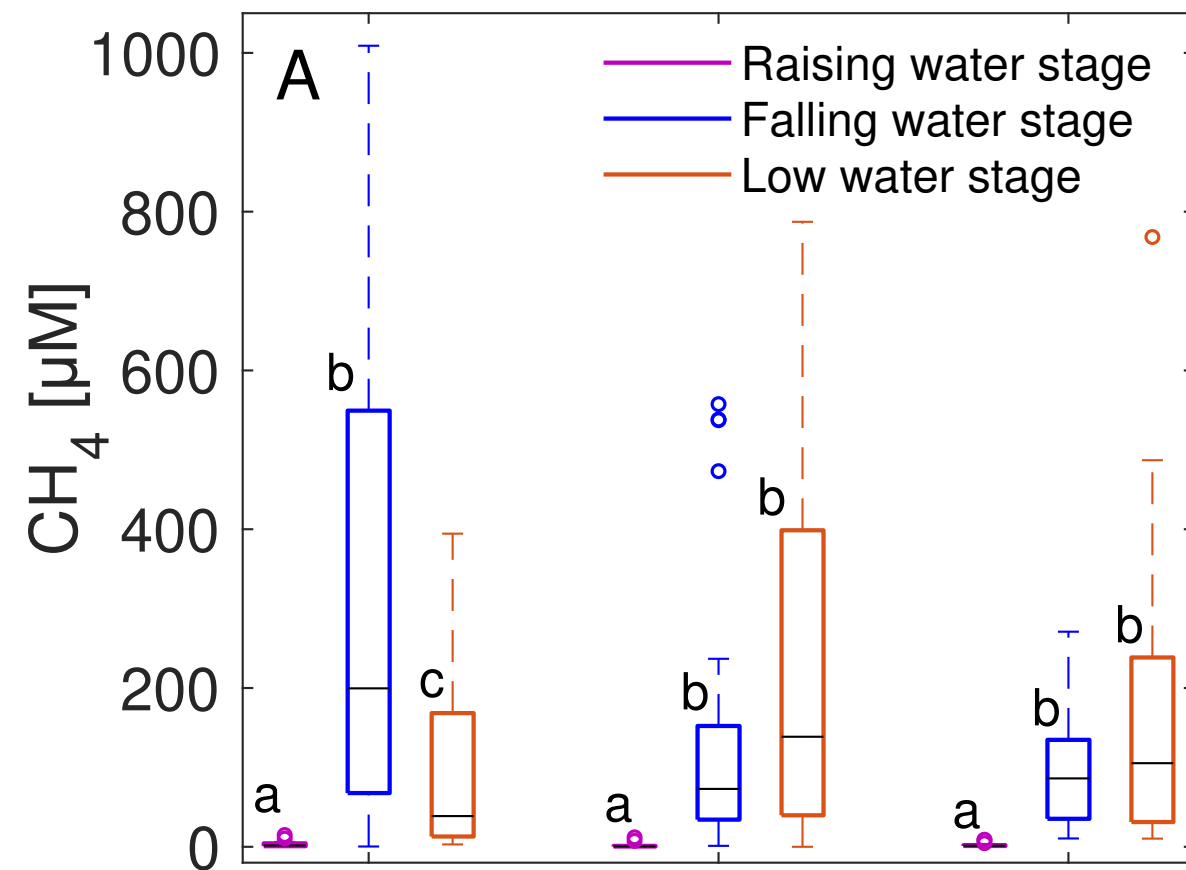
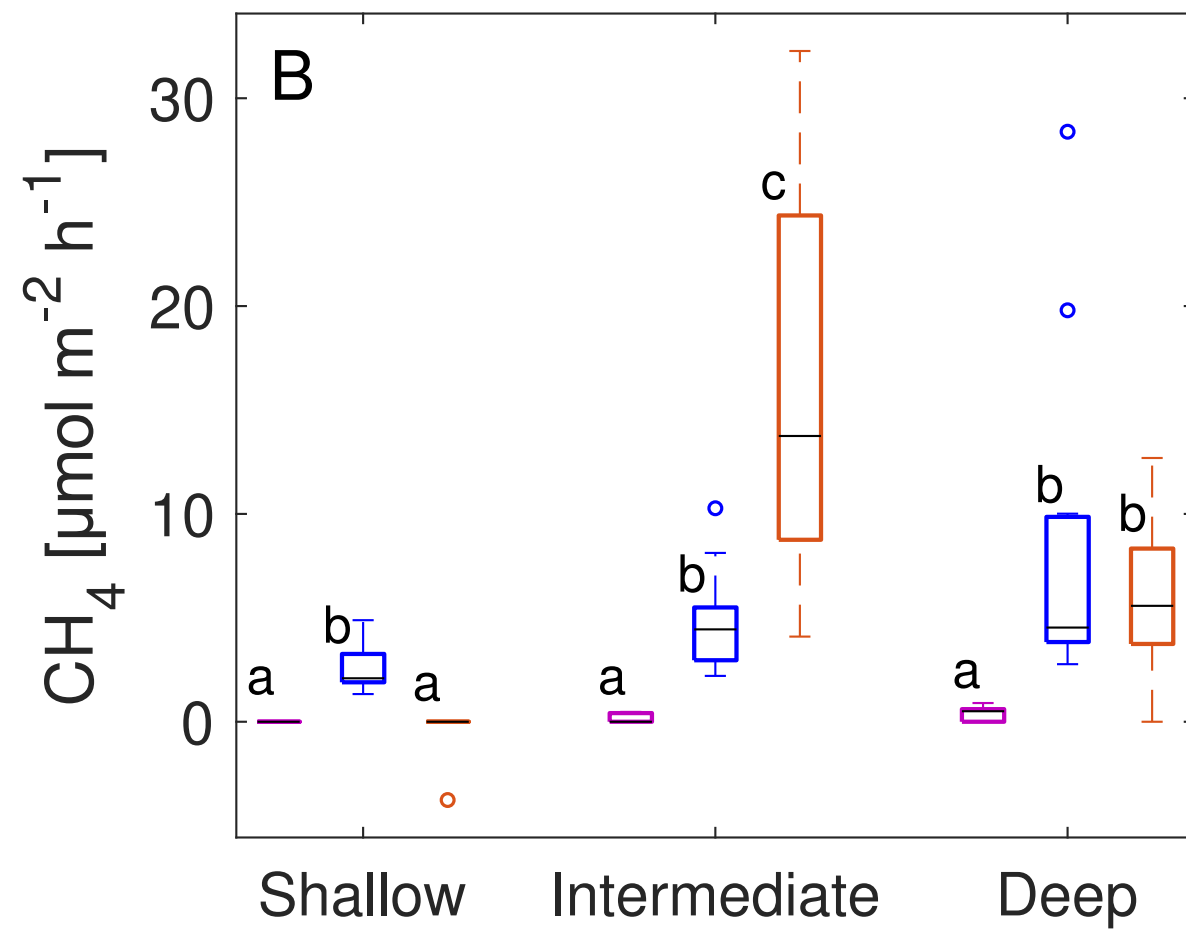
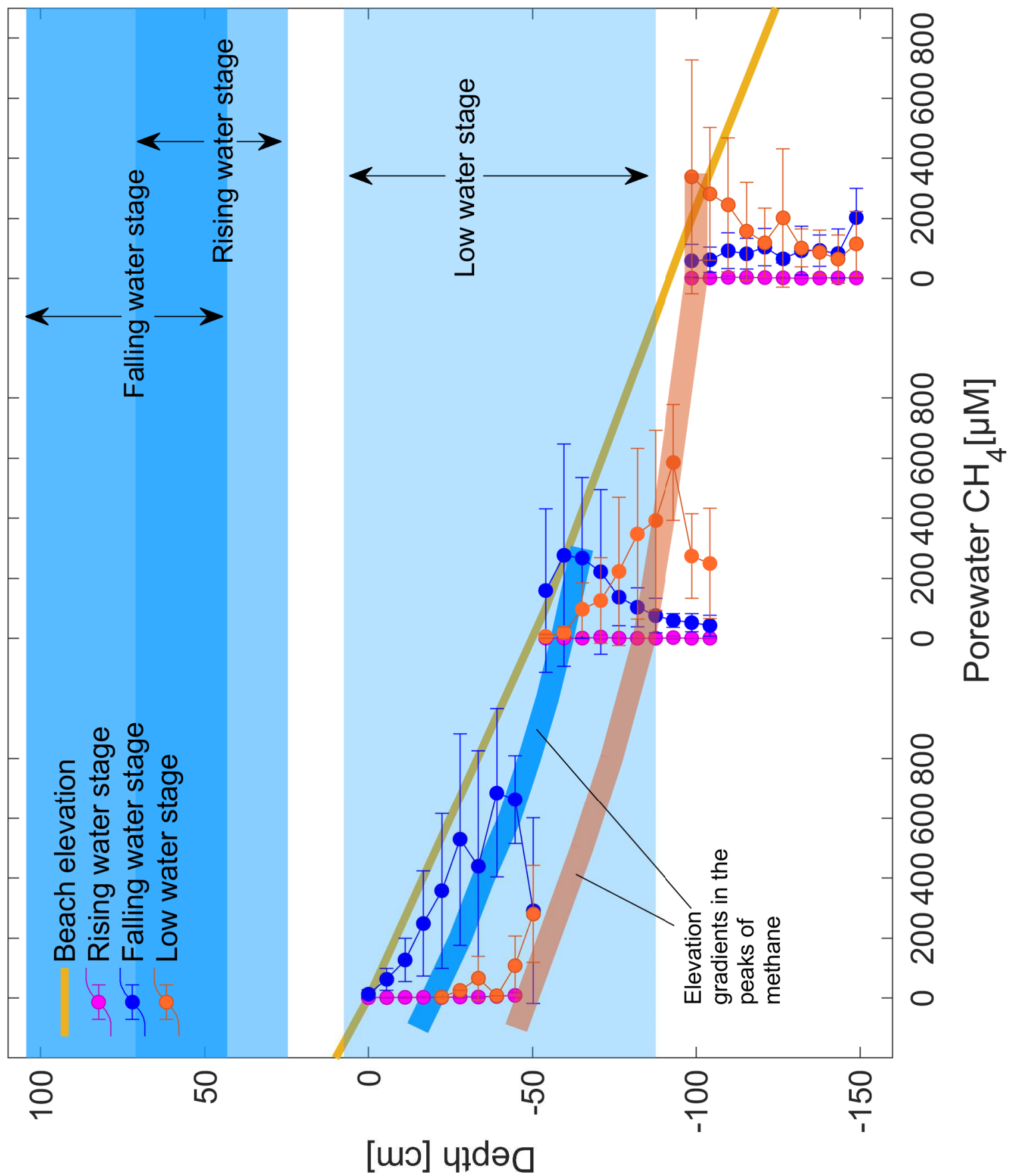
Porewater*Surface flux*

Figure 4

[Click here to download Figure: Fig 4.eps](#)



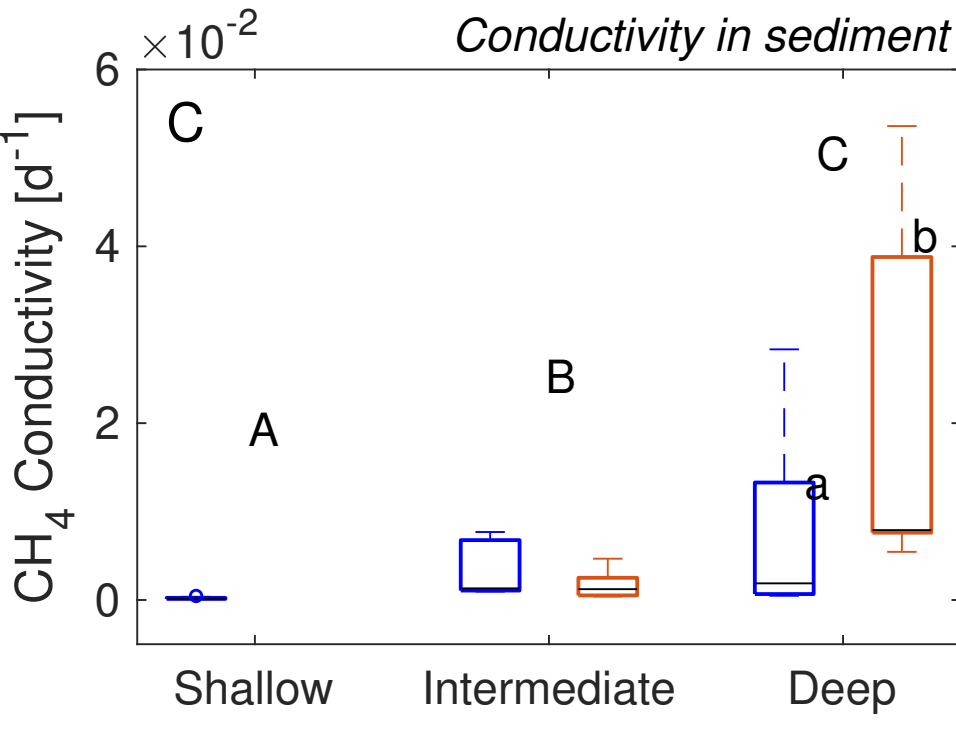
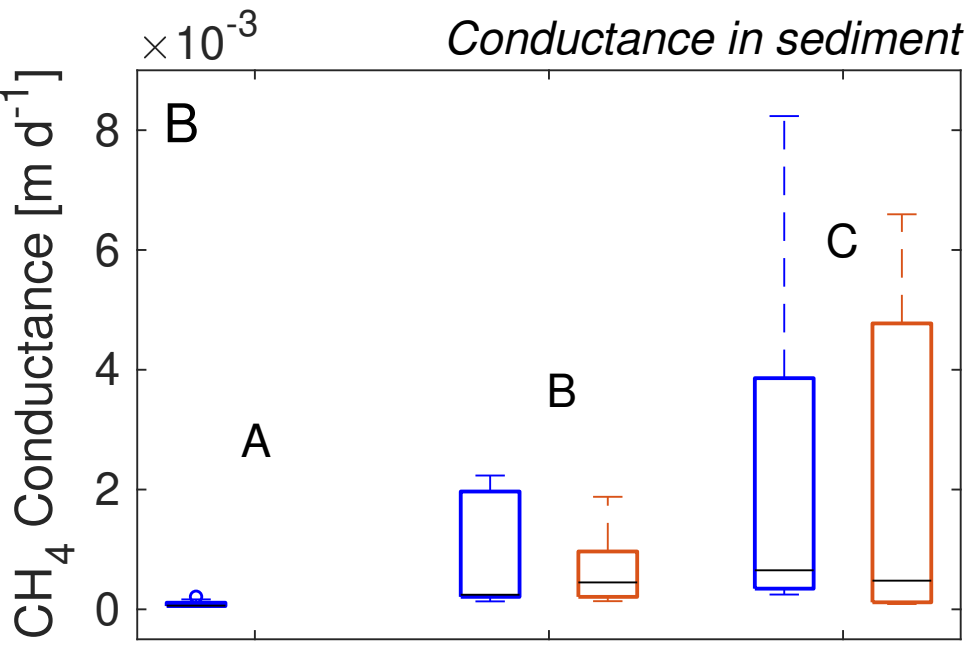
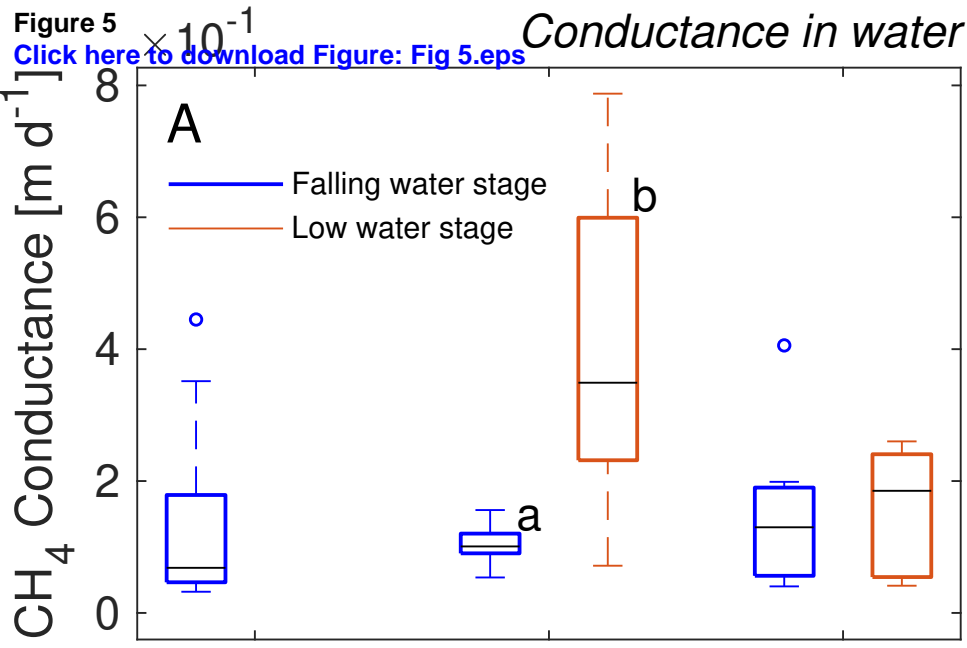


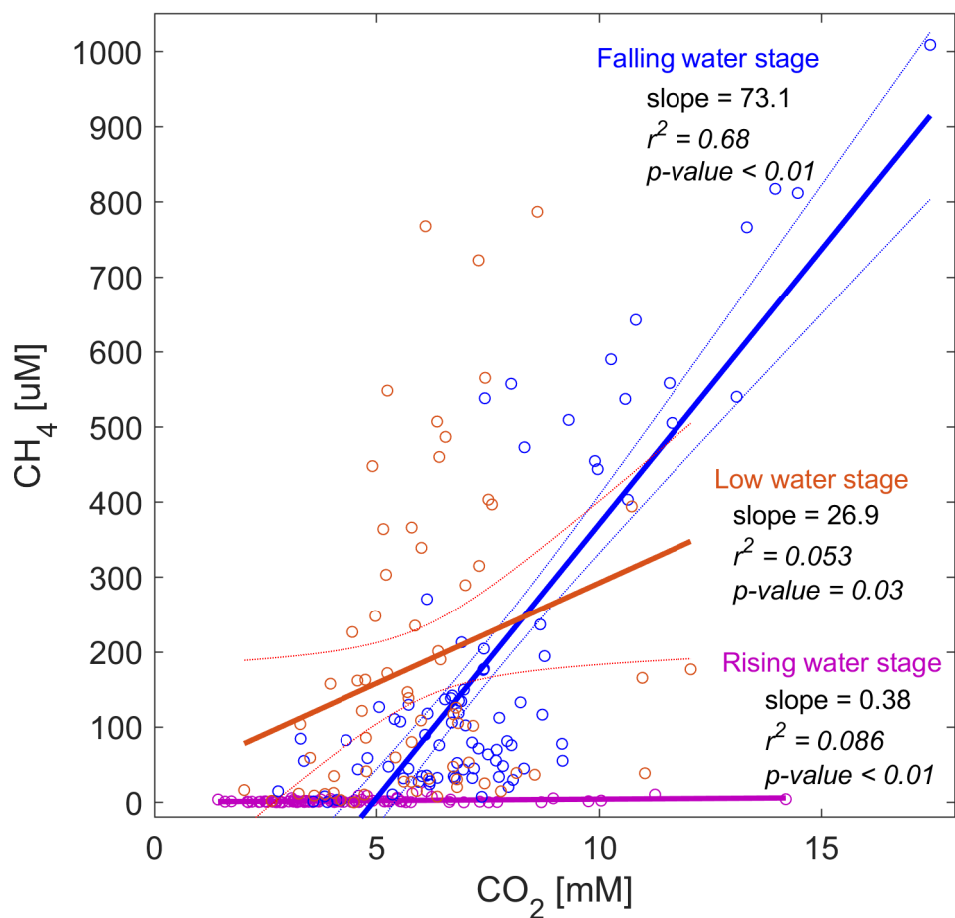
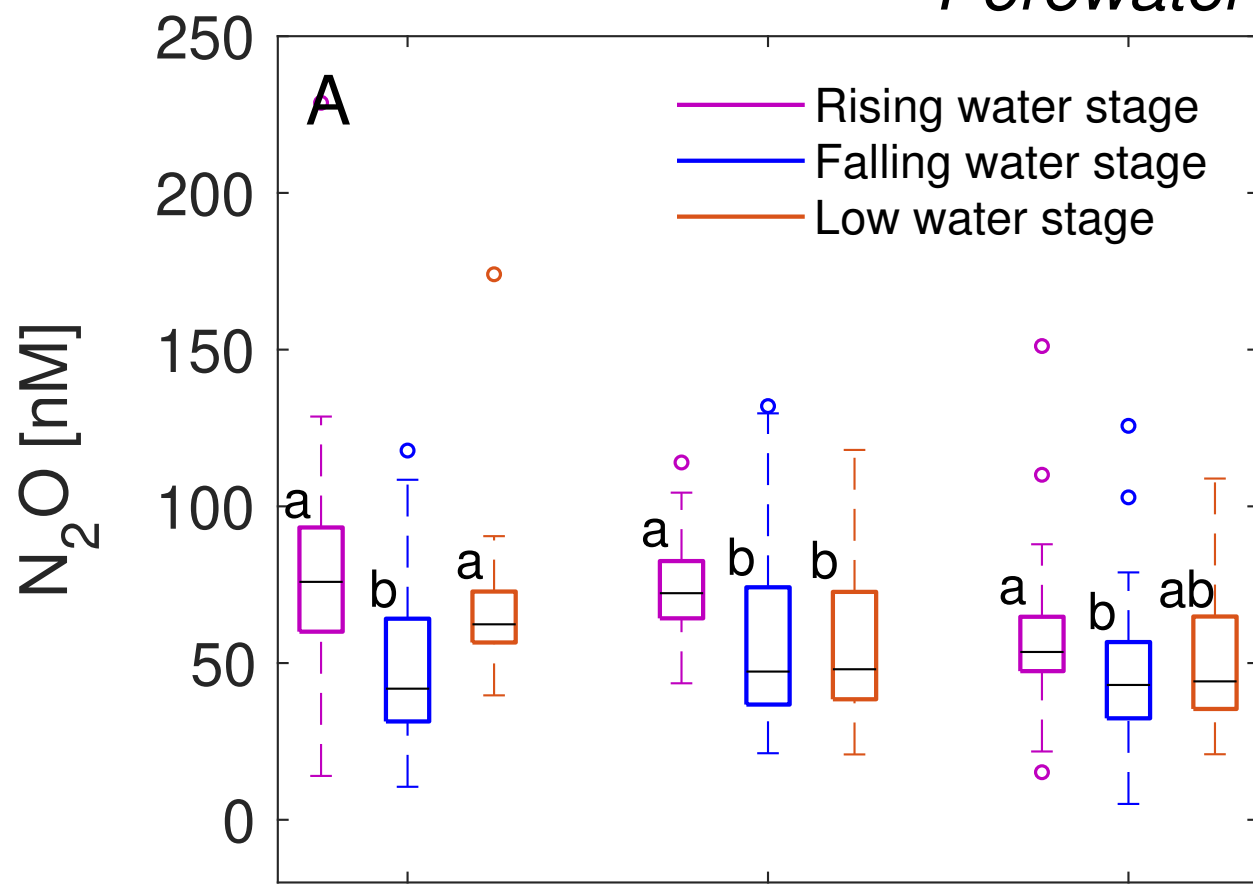
Figure 6[Click here to download Figure: Fig 6.pdf](#)

Figure 7

[Click here to download Figure: Fig 7.eps](#)

Porewater



Surface flux

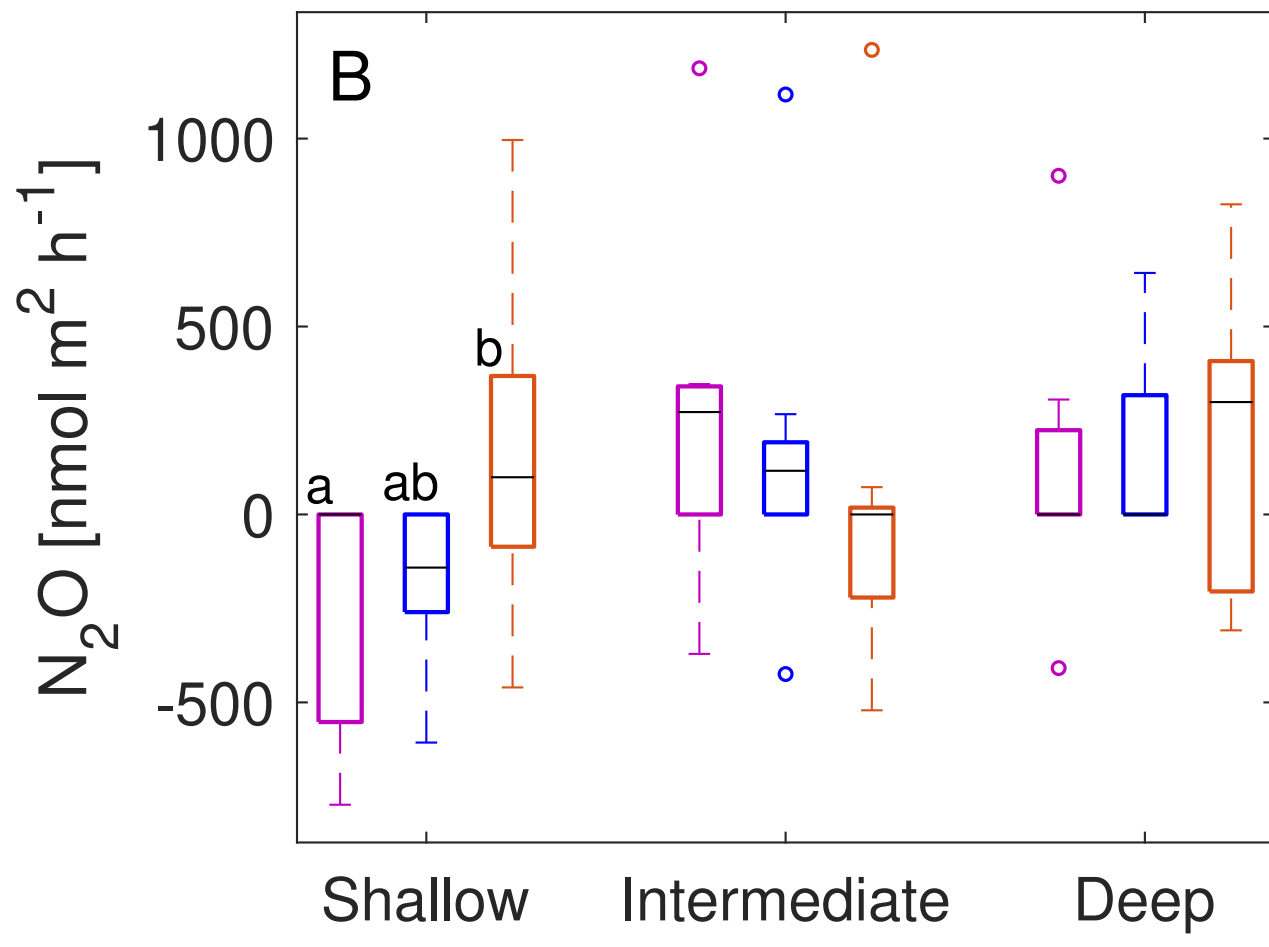


Figure 8

[Click here to download Figure: Fig 8.eps](#)

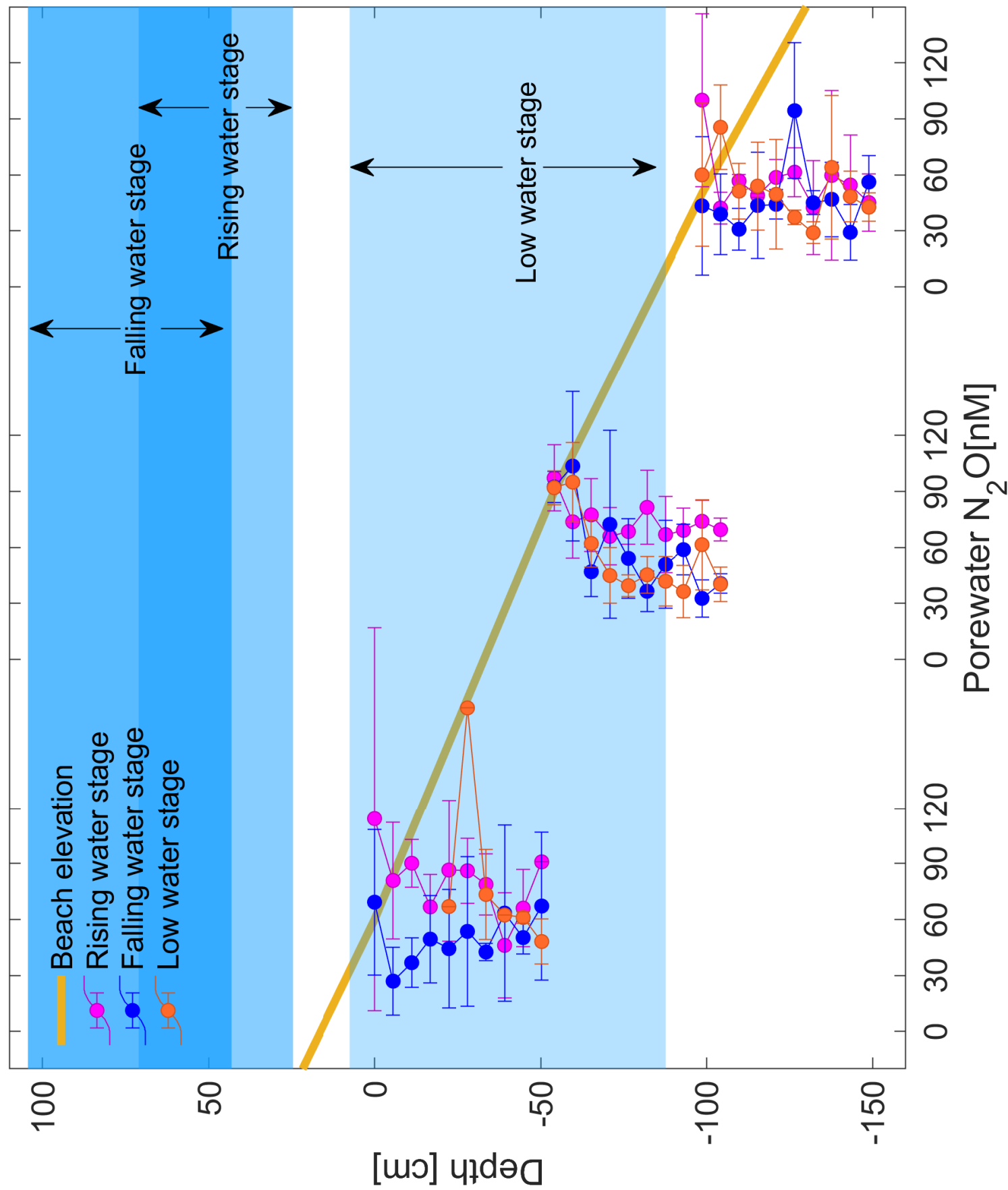
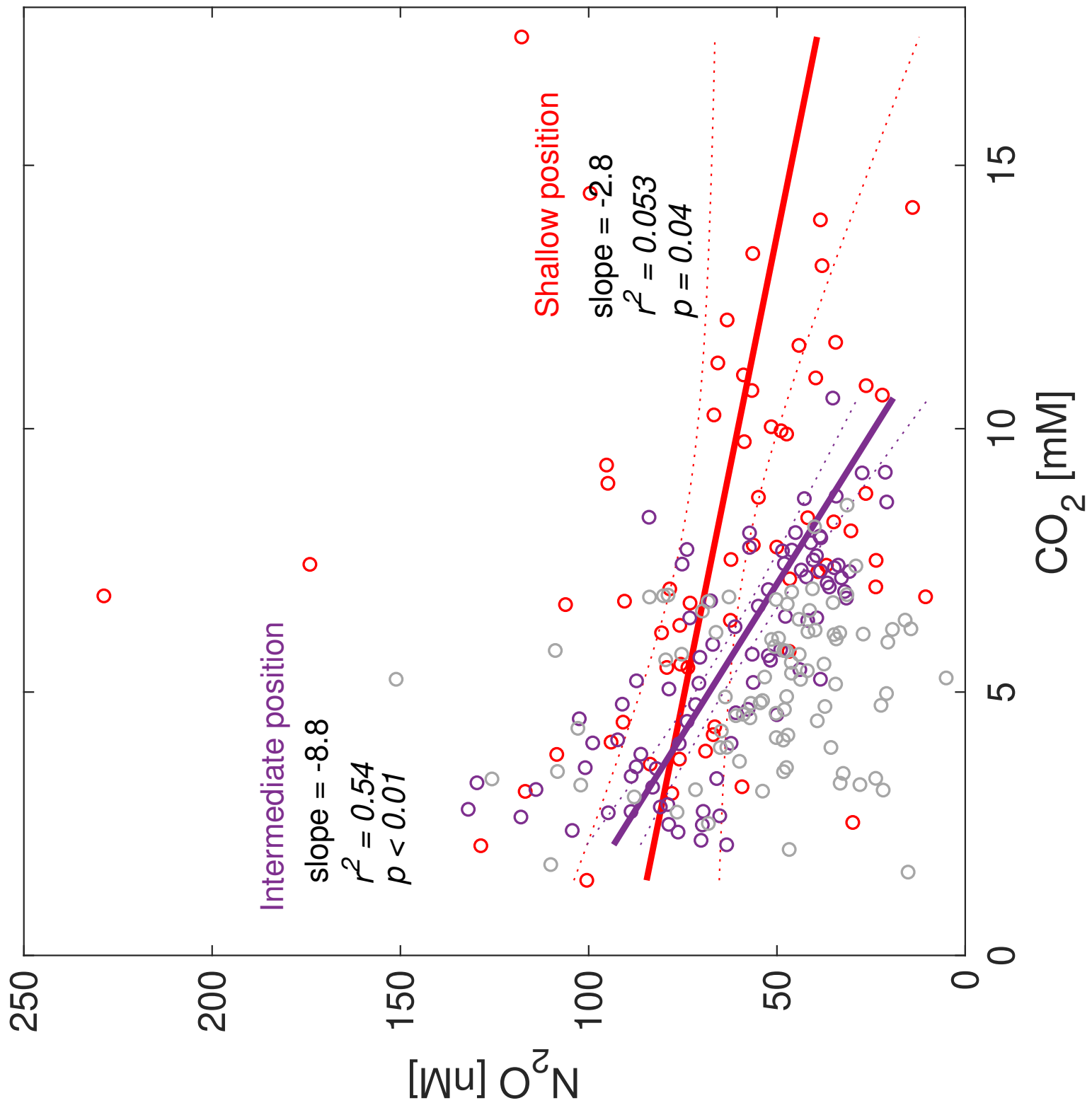


Figure 9

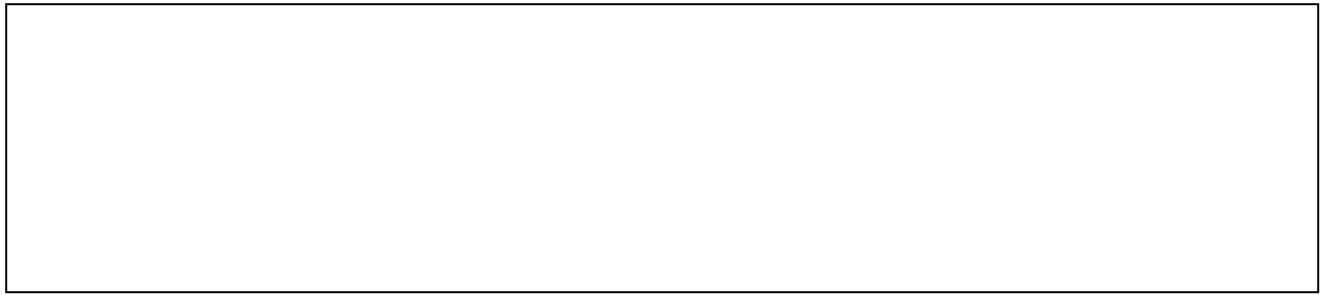
[Click here to download Figure: Fig 9.eps](#)



Declaration of interests

The authors declare that they have no known competing financial interests or personal relationships that could have appeared to influence the work reported in this paper.

The authors declare the following financial interests/personal relationships which may be considered as potential competing interests:

A large, empty rectangular box with a thin black border, occupying the lower half of the page. It is intended for authors to declare any potential competing interests.